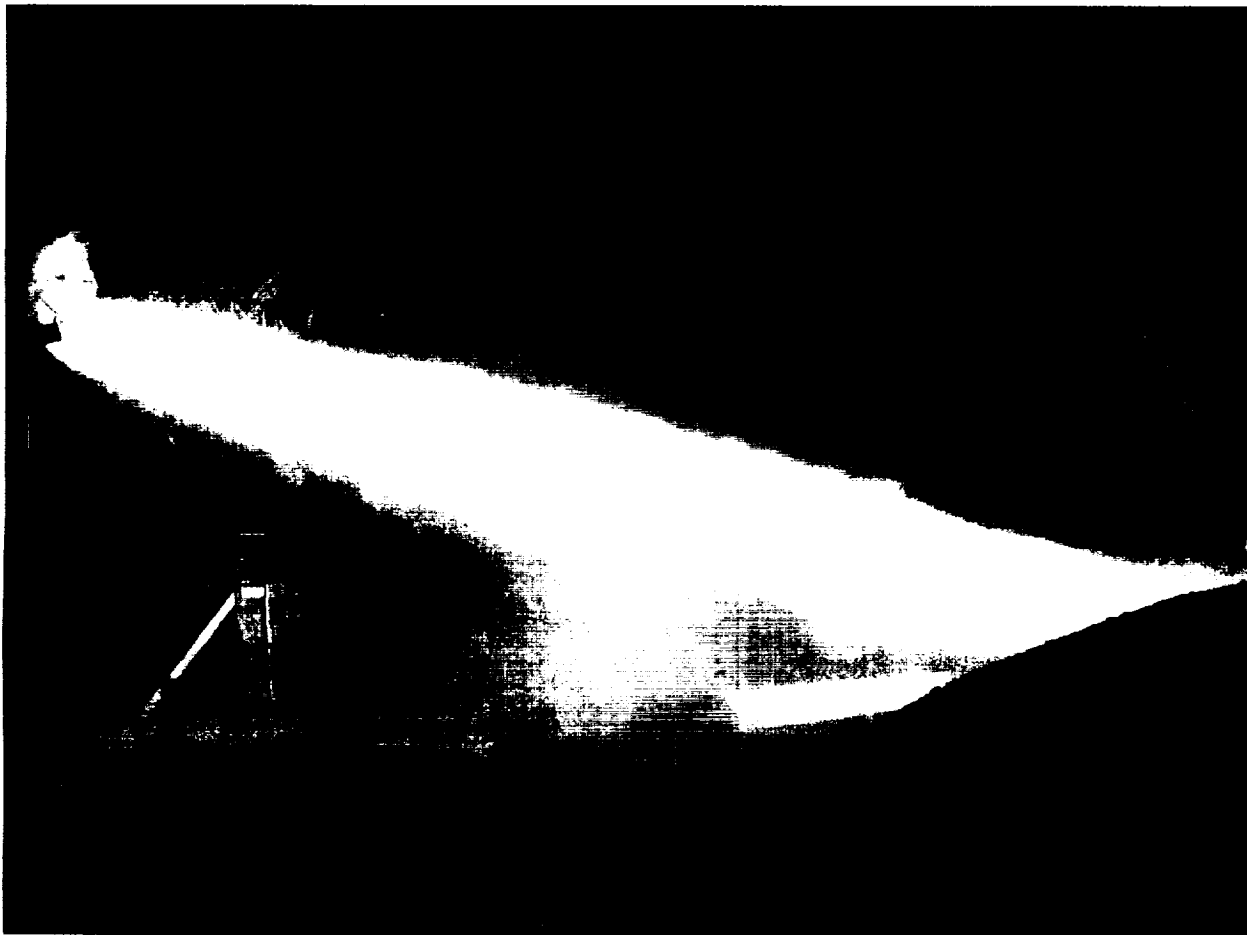


4/3/92
p-126

Pressure Fed Thrust Chamber Technology Program

Contract NAS 8-37365
Final Report
July 1992



N92-31550

Unclas

(NASA-CR-190666) PRESSURE FED
THRUST CHAMBER TECHNOLOGY PROGRAM
Final Report (GenCorp Aerojet)
126 p

Prepared For:
National Aeronautics and Space Administration
George C. Marshall Space Flight Center
Marshall Space Flight Center, AL 35812

"Developing Tomorrow's Low Cost LOX/RP-1 Engines"

Propulsion Division

ORIGINAL PAGE
COLOR PHOTOGRAPH

July 1992

ORIGINAL CONTENT
COLOR ILLUSTRATIONS

PRESSURE FED THRUST CHAMBER
TECHNOLOGY PROGRAM

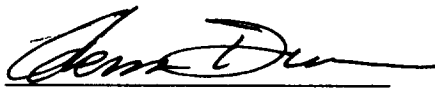
Contract NAS 8-37365

Final Report

Prepared For

National Aeronautics and Space Administration
George C. Marshall Space Flight Center
Marshall Space Flight Center, AL 35812

Prepared By



G. M. Dunn
Project Engineer

Approved By



C. Faulkner
Program Manager

Aerojet Propulsion Division
P.O. Box 13222
Sacramento, California 95813-6000

ACKNOWLEDGMENTS

The overwhelming success of this program was the result of the efforts of many people who should be congratulated for a job well done. The program was completed with excellent results and within the prescribed budget.

The very successful and innovative design was created in Lee Femlings' design group by Ed Higgins and Brian Carothers.

The Engineering Analysis group provided design parameters for the design and operation of the unique hardware, and their predictions were proven by test results. Combustion analysis and test data reduction was performed under the leadership of Jack Ito by Bill Anderson, Yuriko Jones, Karen Niiya, Thong Nguyen, and Cherie Cotter. Thermal analysis was done by Brian Scott. Stress analysis was performed by John Canders and Larry Bush. Materials evaluation was handled by Paul Marchol for the composites and George Janser for metallics.

Fabrication of the hardware was organized and monitored by Lynn Graham, who spent many hours making sure the hardware was completed correctly and on time. Dave Sutherland provided Quality Assurance support.

The Test Area "E" crew had a great deal to do with the success of the subscale testing. Their diligent handling of the hardware and assistance in test planning was invaluable. Special thanks are due Test Engineers Cliff Crossman and Jack Standen, and their managers Dave Eccli and Paul Hill. Efficient testing was a result of the efforts of the test crew, Louie DeGroot, Jim Fradenburg, Carl Vickers, Pat Leeds and Bert Watford.

Glenn Dunn
22 July 1992

TABLE OF CONTENTS

	<u>Page</u>
1.0 INTRODUCTION	1
1.1 Program Summary	1
1.2 Background	2
1.3 Methodology	3
1.4 Budget and Schedule	6
2.0 RESULTS AND CONCLUSIONS	10
2.1 Methodology Confirmed	10
2.2 Large Scale Applicability	10
2.3 Recommendations	15
3.0 HARDWARE DESIGN	16
3.1 Requirements and Concept Selection	16
3.2 Injector Design	19
3.3 Chamber Design	28
3.4 Instrumentation	30
3.5 Ancillary Hardware	32
4.0 FABRICATION	35
4.1 Injector	35
4.2 Chamber	46
4.3 Engine Assembly	50
5.0 TEST PREDICTIONS AND RESULTS	54
5.1 Testing Plan	54
5.2 Test Results	55
5.3 Performance Predictions and Results	58
5.4 Stability Predictions and Results	73
5.5 Thermal Predictions and Results	95
5.6 Hardware Durability	106

TABLE OF CONTENTS (cont.)

	<u>Page</u>
6.0 APPLICABILITY TO FULLSCALE	113
6.1 Subscale Testing Results and Conclusions	113
6.2 Full-Scale Design Features	114
6.3 Development Requirements	115
References	117

LIST OF FIGURES

<u>Figure No.</u>		<u>Page</u>
1.4.1	Program Expenditures Remained Within Budget	8
1.4.2	Master Schedule Shows Program Changes and Performance	9
2.2.1	Modular Design Facilitates Engine Sizing	11
3.1.1	Subscale Hardware Utilizes Low Cost Simple Components	18
3.2.1	The O-F-O Triplet is the Best Element for LOX/RP	20
3.2.2	LOX Inlet Design is Simplified for Subscale Testing	23
3.2.3	Face-Mounted Thermocouples Measure Face Heat Flux	25
3.2.4	FFC Ring Injects Coolant to Injector Face	27
3.2.5	Extensive Instrumentation Monitors Engine Performance	31
4.1.1	Inlet Plate and Screen After Brazing	36
4.1.2	Completed LOX Inlet Assembly	37
4.1.3	Core Assembly Weldment	38
4.1.4	Injector Modules Can Be Mass Produced for Economy	40
4.1.5	Modules are Inserted into Core for Brazing	41
4.1.6	Module Thermocouples are Staked Directly to Modules	43
4.1.7	Face Thermocouples are Mounted in Stands	43
4.1.8	Distribution Plate (top circuit) and Filter (lower circuit) Condition Fuel Flow	44
4.1.9	Concentric Rings Form FFC Injection Ring	45
4.1.10	Faceplate is Compression Molded from Silica Phenolic Chips	47
4.1.11	Faceplate Bores are Machined Using Special Tooling	48
4.1.12	Completed Ablative Faceplate	49
4.3.1	Rolling Stand Facilities Assembly	51
4.3.2	Completed Subscale Hardware	53
5.2.1	Test Program Met All Test Objectives	57
5.3.1	Measured Injector Admittance Closely Matches Predicted Values	60
5.3.2	Combustion Pressure Profile Matches Predictions	61
5.3.3	Combustion Efficiency is Greatest Around Core $MR = 2.5$	63
5.3.4	Injector Efficiencies Combine to Give Greatest Isp at About $MR = 2.4$	64
5.3.5	Performance Testing Summary	65

LIST OF FIGURES

<u>Figure No.</u>		<u>Page</u>
5.3.6	Specific Impulse Varies with Percent FFC	67
5.3.7	Specific Impulse Varies with P_c	68
5.3.8	Fuel Film Cooling (FFC) Efficiency Changes with MR	70
5.3.9	Injector Efficiency Decreases with MR Increases	71
5.3.10	Core Efficiency Changes as MR Increases	72
5.3.11	Injector Efficiency Increases with Chamber Pressure and Injector ΔP	74
5.4.1	Stability Predictions for Chamber with No Cavities	77
5.4.2	Stability Testing Summary	78
5.4.3	A Typical Induced Instability which was Damped Quickly (Test 15)	82
5.4.4	This Induced Instability Damped Almost Instantly (Test 25)	83
5.4.5	A Typical Induced Instability which Remained Unstable (Test 22)	84
5.4.6	"Waterfall" Plot of Test 22 Shows the Evolution of the Instability	85
5.4.7	Power Spectral Density (PSD) Plot Shows Unstable Frequencies	86
5.4.8	PSD Plots of Manifold Pressures and Chamber Accelerations Confirm Instabilities	87
5.4.9	Acoustic Cavity Gas Temperature Can Infer Gas Composition and Cavity Sound Speed for Cavity Damping Optimization	89
5.4.10	Stability Map for Series 1, 4 inch Cavity	90
5.4.11	Stability Map for Series 2, No Cavity	90
5.4.12	Stability Map for Series 3, 2 inch Cavity	92
5.4.13	Stability Map for Series 4, Bituned Cavity	92
5.4.14	Cavity Damping Ability Varies with Gas Temperature	93
5.5.1	Module Temperatures Were Predicted Using Thermal Models	98
5.5.2	Module Temperatures Were Less Than Expected (Test 4)	99
5.5.3	Face Temperatures Were Less Than Expected (TJ4 Data)	100
5.5.4	Face Temperature Measurements Show Cool Face Environment	101

LIST OF FIGURES

<u>Figure No.</u>		<u>Page</u>
5.5.5	Chamber Wall Temperatures Vary With Module Position	103
5.5.6	Temperature Profile Inline with Modules	104
5.5.7	Temperature Profile Between Modules	105
5.6.1	Some Module Erosion Occurred After High Pc Tests	108
5.6.2	The Chamber was Modified to Correct FFC Impingement Point	110
5.6.3	Chamber Indicated Erosion Areas at the Completion of Tests	112
6.2.1	This Low Cost Concept Can be Sized to Many Applications	116

1.0 INTRODUCTION

1.1 PROGRAM SUMMARY

The program was initiated in June, 1989 with the issuance of an Authorization to Proceed (ATP). The NASA-MSFC contract, NAS 8-37365, Phase 1 period of performance was through September, 1991.

Full-scale concept design began at ATP with the first concept review held in September 1989. This review solidified the injector and chamber concept and allowed subscale design to proceed. Design work continued on the fullscale configuration until, in March 1990, NASA-MSFC officially put fullscale activities on hold due to budget restraints.

Subscale design began after the fullscale concept review. The design task required approximately seven months to complete, and culminated in a Critical Design Review (CDR) in June 1990.

Fabrication of subscale hardware was initiated by ordering long-lead components and materials in January 1990. At the conclusion of the design phase in June, most long-lead items had been received. Fabrication began on schedule. Very few fabrication problems were encountered, and the hardware was completed in December 1990.

The assembly and cleaning of the components was more difficult than expected due to their large size and weight. The components were ready for the test stand in March, 1991. Delays encountered in assembly and cleaning caused the program to miss its testing window in the test area, which resulted in a 6 month delay.

Test installation and instrumentation began in mid-September 1991. This included test readiness reviews and coordination meetings. Calibration and propellant loading followed. The first hot-fire occurred on 16 October 1991. The testing program progressed remarkably well for new and unique hardware. A total of 32 tests were accomplished, satisfying all goals for test data and hardware durability. The test components were still very serviceable on December 11, the last day of testing. Data analysis and the writing of the final report were accomplished in mid 1992. Test data and

results from this subscale testing will be applicable to low-cost pressure-fed and pump-fed LOX / RP engines.

1.2 BACKGROUND

1.2.1 LRB Study Results

In 1987, Martin Marietta Manned Space Systems Division , Aerojet Propulsion Division and others, embarked on a study to evaluate the feasibility of a Liquid Rocket Booster (LRB) system to replace the Solid Rocket Boosters (SRB's) of the current Space Shuttle configuration. This study was performed for NASA- MSFC (NAS8-37136), to evaluate a system that would have operational advantages over the present system;

- Increase Space Transportation System (STS) Safety and Reliability (Abort Capability, Throttleability)
- STS Integration with Minimum Impact (No ET or Launch Pad Mods)
- Increase STS Performance (Eliminate SSME Boost Phase)

The study concluded that **LRB's are a viable alternative** to the SRB's for the space shuttle system. The following recommendations and conclusions were drawn:

- **LOX/RP-1** is the recommended fuel for both Pump and Pressure Fed Systems
- Both pump and pressure-fed versions would be **expendable**
- Both versions can be flown within present STS constraints
- Technology requirements for the pressure fed version include Large Propellant tank Pressurization Systems and **Large, Low Pc Thrust Chamber Characterization**

1.2.2 Pressure Fed Technology Program

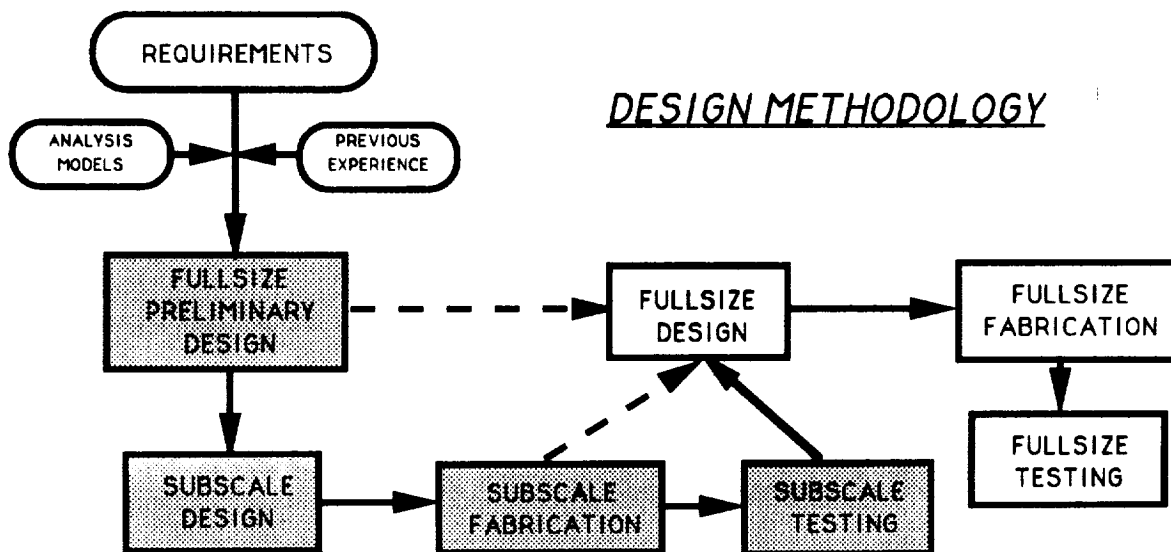
In late 1988, Aerojet responded to an RFP from NASA-Marshall Space Flight Center for the development of pressure fed technology. The program was awarded to Aerojet in June 1989 and consisted of the following Tasks:

- (1) Perform large scale preliminary analysis to determine operating parameters and configuration requirements
- (2) Design , build, and test subscale hardware to obtain technology for full scale design
- (3) Design and build a full size test article (750 k thrust) for testing at MSFC

The program was modified in 1991 to change the full size task to an option that could be exercised as late as December 1992.

1.3 METHODOLOGY

The methodology used to develop this new technology is similar to the methods Aerojet has been using successfully for over 20 years for earth storable propellants engines and for the last several years to develop LOX / RP engines. It combines the use of state-of-the-art combustion models and subscale testing to successfully develop full scale engine designs with minimum development cost. Our design methodology is shown in the following chart. This methodology has been used successfully with the Injector Characterization Program, AFAL contract F04611-85-C-0100 (referred to as the -0100 program) as well as the just-completed LOX/Hydrocarbon Rocket Engine Analytical Design Methodology Development and Validation program (NAS 3-25556).



For this program, we were fortunate to have a new analysis tool available. Aerojet has developed, along with NASA-Lewis Research Center, a powerful analysis model, the **ROCKET Combustor Interactive Design (ROCCID)**, which combines several of the existing models into a single interactive design methodology. ROCCID predicts performance as well as combustion stability characteristics for the liquid engine combustors.

Aerojet has been successful in developing large scale engines using subscale testing as a design database. The subscale engine is sized so that the 1T instability mode frequency corresponds to the fullscale 3T mode frequency. The 3T fullscale instability mode represents the practical upper limit of stability development risk. This sizing results in a subscale diameter which is 43% of the fullscale diameter. In addition, fullsize injection elements were used for the subscale injector to duplicate the mixing and performance response of the fullsize injector.

The fullsize combustion chamber was proposed as an ablative design to minimize cost and maximize performance for an expendable engine. Silica phenolic was the chosen material as it has shown superior performance up to 3500 °F in past programs.

Steady-state heat loads and adiabatic gas temperatures were determined during subscale testing to assist in the design of the fullscale ablative components. Since ablative chambers make high frequency stability data acquisition difficult, a steel "heat-sink" chamber was chosen for subscale testing. The steel chamber allows

more accurate instrumentation to measure both high frequency pressures as well as static pressures and temperatures at the gas wall. Fuel film cooling (FFC) of the chamber wall served two purposes; cooling of the steel wall for longer test duration and determination of FFC effectiveness for use in the fullscale design which uses FFC to lower wall temperature and therefore extend ablative life.

Testing of subscale hardware sought to obtain several types of operational data. Data on combustion stability, modular injector durability, film cooling effectiveness and face temperatures were equal in importance to the engine performance data. Measurement of acoustic cavity gas temperatures allows determination of cavity sound speed and predictions of fullscale stability. Heat flux measurements provide data on film cooling efficiency as well as provide data for chamber design. Testing was divided into discrete blocks to prioritize tests according to the testing objectives. After initial start-up, stability data was most important, followed by film cooling and performance at other operating points. Test logic is discussed in more detail in the Test Prediction and Results section. The following table lists the expected outputs for each of the engine parameters measured.

<u>Parameter Measured</u>	<u>Desired Output</u>
High frequency chamber pressure	Instability mode, magnitude
Acoustic cavity temperature	Instability damping characteristics
Chamber wall heat flux	Film cooling effectiveness Prediction of fullscale film cooling req'mts Ablative liner performance predictions
Chamber pressure profile	Combustion performance profile
Module temperature	Module durability predictions
Faceplate temperature	Ablative faceplate durability
Thrust, Propellant flowrates	Injector performance

The primary goal of this program was to develop the technology for a low-cost LOX/RP engine. To measure program success, the following goals were set:

- Establish a low-cost LOX/RP engine design which, through analysis and study, is shown to provide the required reliability, performance and producibility.

- Fabricate subscale hardware to demonstrate producibility and conduct testing to demonstrate reliability and performance.
- Design and fabricate fullscale hardware, utilizing subscale test results, which can be tested to verify readiness for flight engine development.

In addition to the design, fabrication and test tasks, two other tasks were designed to supplement the development of low-cost pressure fed technology.

Ablative Versus Regen Analysis - This study evaluated the benefits of an ablative approach versus a regeneratively cooled approach to a low cost engine. The study predicted coolant pressure drops in a regeneratively cooled (tube bundle) chamber with and without the effects of coking. The study was suspended in favor of concurrent ALS studies on regen cooled chambers and the Ablative Materials Study described below. The study results are reported in the March 1990 Technical Progress Report-7.

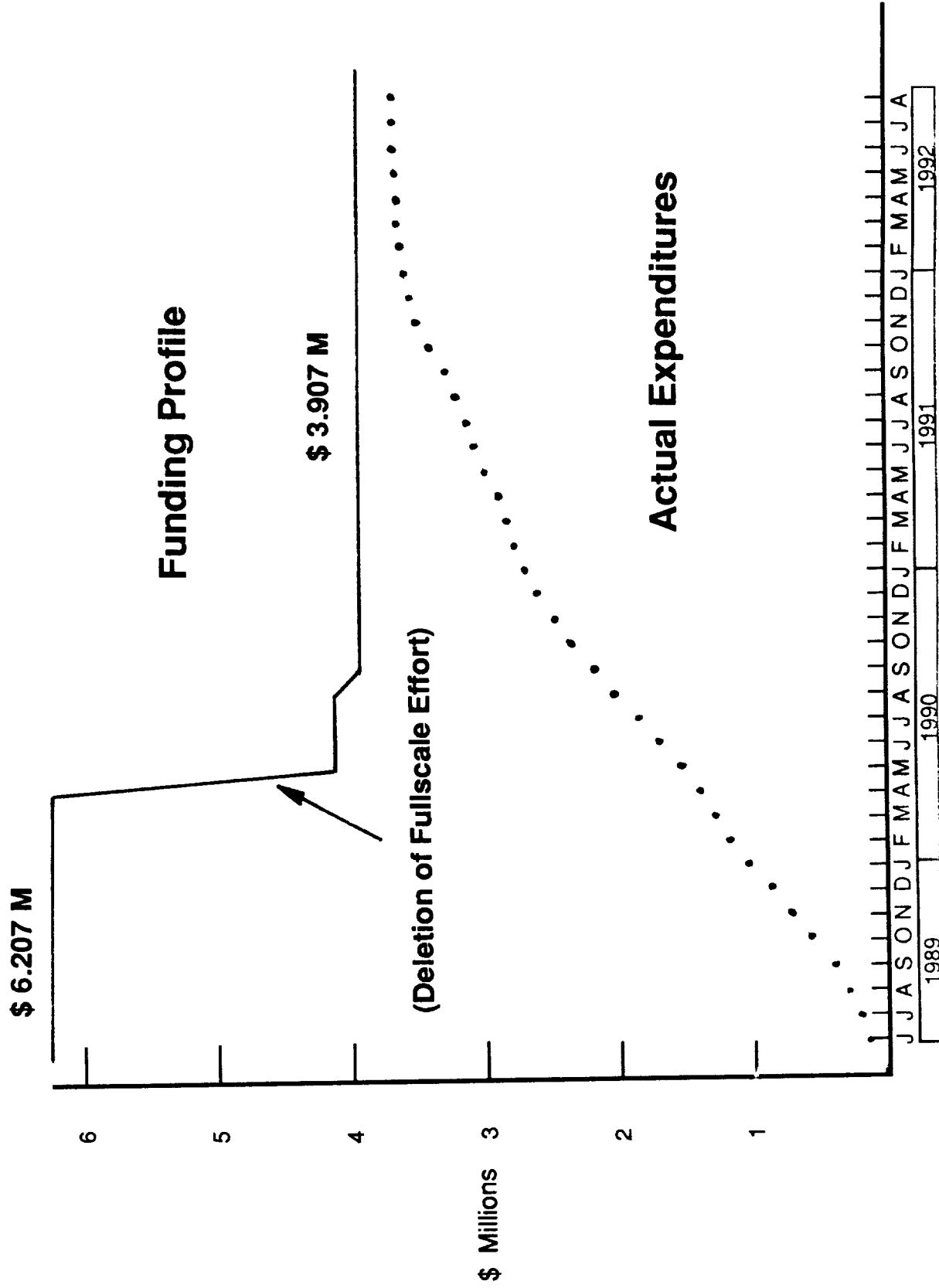
Ablative Materials Study - A thorough study of available ablative materials and fabrication techniques was performed to determine the low-cost alternatives to a regen chamber. A new approach using quartz phenolic materials and a 3D braiding method was identified as a weight and cost saving chamber fabrication technique. Numerous material tests were conducted to establish a firm database for future development. The complete results are reported in the June 1990 Technical Progress Report-10.

1.4 BUDGET AND SCHEDULE

The program was initiated as a \$6.2 M program which included both subscale and fullscale design and fabrication. In late 1990, scope was changed to delete the remaining fullscale design and fabrication, as well as a test stand dynamic analysis task. The remaining program value was approximately \$3.8M.

Monthly budget reports and evaluations were made to NASA-MSFC to present program status. Figure 1.4.1 shows project cost performance relative to budget. All required tasks were completed within budget.

The program was originally scheduled as a 24 months but was modified by directive in 1989 to a 28 month program. The final schedule and progress is documented in Figure 1.4.2.



PRESSURE FED THRUST CHAMBER TECHNOLOGY PROGRAM **MASTER SCHEDULE** **CONTRACT NUMBER : NAS8-37365**

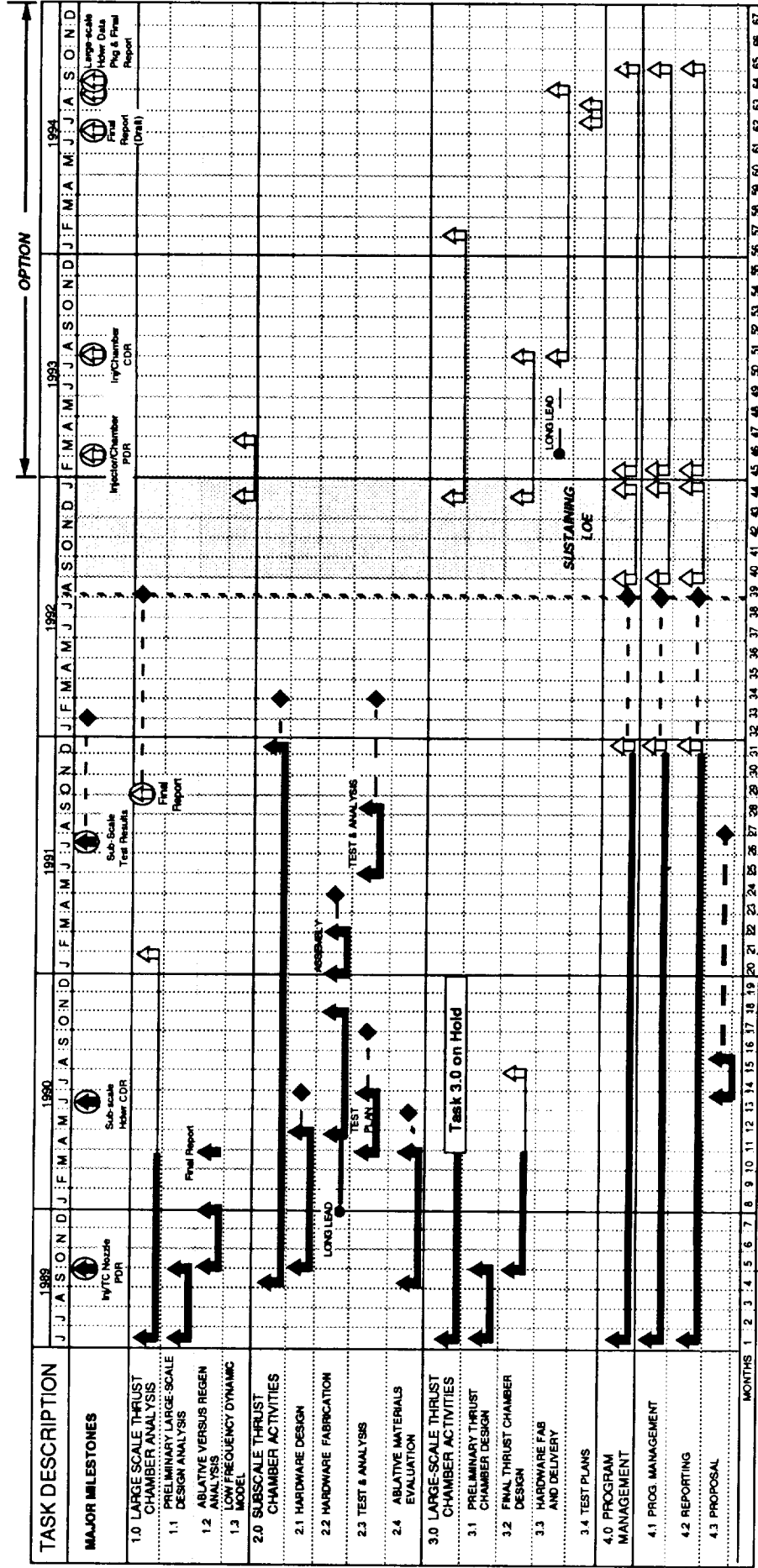


Figure 1.4.2 Master Schedule Shows Program Changes and Performance

2.0 RESULTS, CONCLUSIONS AND RECOMMENDATIONS

The overall program was very successful from definition of the fullscale design through the subscale test conclusions. Technology for the development of a fullscale low cost, pressure fed engine is now in place. The innovative low-cost modular injector/ablative faceplate design demonstrated expected performance and was very durable. The quality and quantity of test data obtained exceeded expectations and has laid a firm foundation for future low-cost LOX/RP engine development.

2.1 METHODOLOGY CONFIRMED

A new computer model was used to predict engine performance and high-frequency stability. The **ROCKET Combustor Interactive Design (ROCCID)** program was used to analyze instability operating modes and was also used to modify the chamber acoustics to eliminate instabilities. Confirmation of this methodology is a significant step forward for the development of LOX/RP engines.

2.2 LARGE SCALE APPLICABILITY

Success in analyzing, measuring and correcting instability modes in this development program allows the program to move forward into fullscale design with confidence. Test data obtained enables us to confidently predict fullscale engine performance, requirements for acoustic damping devices, chamber wall cooling requirements and materials selection. Knowledge of acoustic cavity effects allows us to begin sizing the injector depth and calculating component weights for the fullscale engine. As shown in figure 2.2.1, the modular concept facilitates engine sizing for a range of thrust levels. The modular concept can also reduce production costs significantly through the use of mass-production techniques. All these factors combine to indicate a promising application for reliable, low cost and efficient first stage/booster propulsion.

2.2.1 Subscale Testing Results and Conclusions

The goal of this program was to develop the technology for pressure fed engines by resolving design issues through subscale testing. This testing was very successful in resolving many of these design issues with test data. The most critical issues and their resolutions are described below.

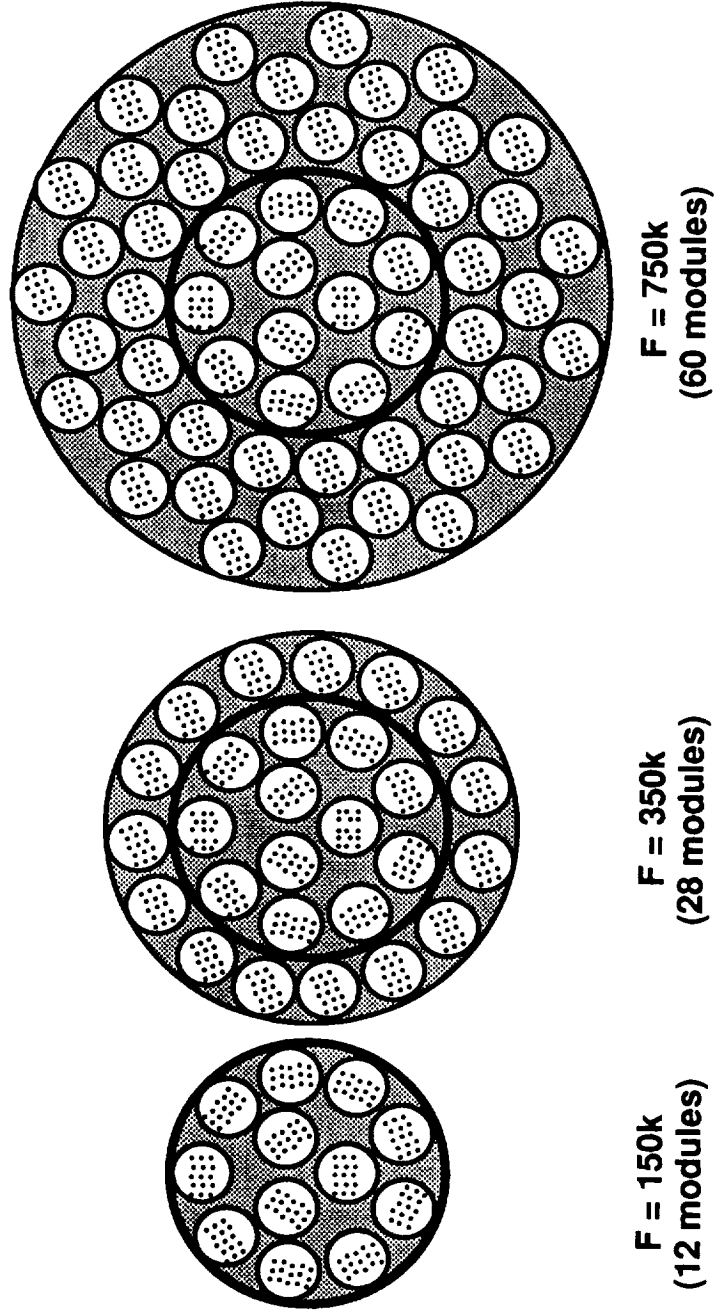


Figure 2.2.1 Modular Design Facilitates Engine Sizing

2.2.1.1 Fullscale Design will Require Only Simple Damping Devices for Stable Operation

The most important issue requiring resolution was the stability of LOX / RP engines, which have a reputation for being difficult to throttle and unstable using fine injection patterns. Demonstrated stability is an essential step in the development of a new engine technology. The plan was to demonstrate stability on a subscale level which could be correlated to the full-scale engine using proven scaling techniques.

The subscale engine was stable at all operating points tested. Artificial perturbation of the combustion drove some instabilities, all in the 1T (first tangential) mode. A bituned acoustic cavity successfully damped the instabilities, and the engine was dynamically stable at the conclusion of testing.

This result indicates that stable operation in the fullscale configuration will be achievable and will require only acoustic cavity damping for the 1T mode. This elimination of the need for higher-order mode damping (baffles, etc.) will significantly reduce complexity and cost of the fullscale design.

2.2.1.2 Ablative Chamber / Nozzle will Meet Design Requirements

The full-scale design employs an ablative lined chamber and nozzle for economy and performance. The ablative material chosen was silica phenolic due to its low cost and past success in LOX/RP engines in short duration applications. Verification of its suitability for flight application (approximately 150 seconds duration) was required.

Measurement of gas-side temperatures during subscale testing was performed to predict full-scale temperatures during a long duration burn. Temperatures were measured with varying chamber pressure, mixture ratio and film coolant rate to establish the effect of each on ablative performance. Although tests were of short duration, thermal data indicated that steady-state temperatures had been achieved.

Maximum gas-side temperatures measured were 2200-2300 °F as discussed in Section 5.6. Silica phenolic is capable of sustained temperatures in the 3500-4000 °F range while exhibiting negligible erosion. Test results indicate that silica phenolic will withstand chamber conditions for the full scale design. Test data has indicated that the silica phenolic lined chamber/nozzle will perform well for the full scale engine. However, thorough testing of an ablative assembly, either subscale or full scale, is required to confirm design predictions

2.2.1.3 Copper Module / Ablative Face Injector Design is Suitable for LOX/RP Application

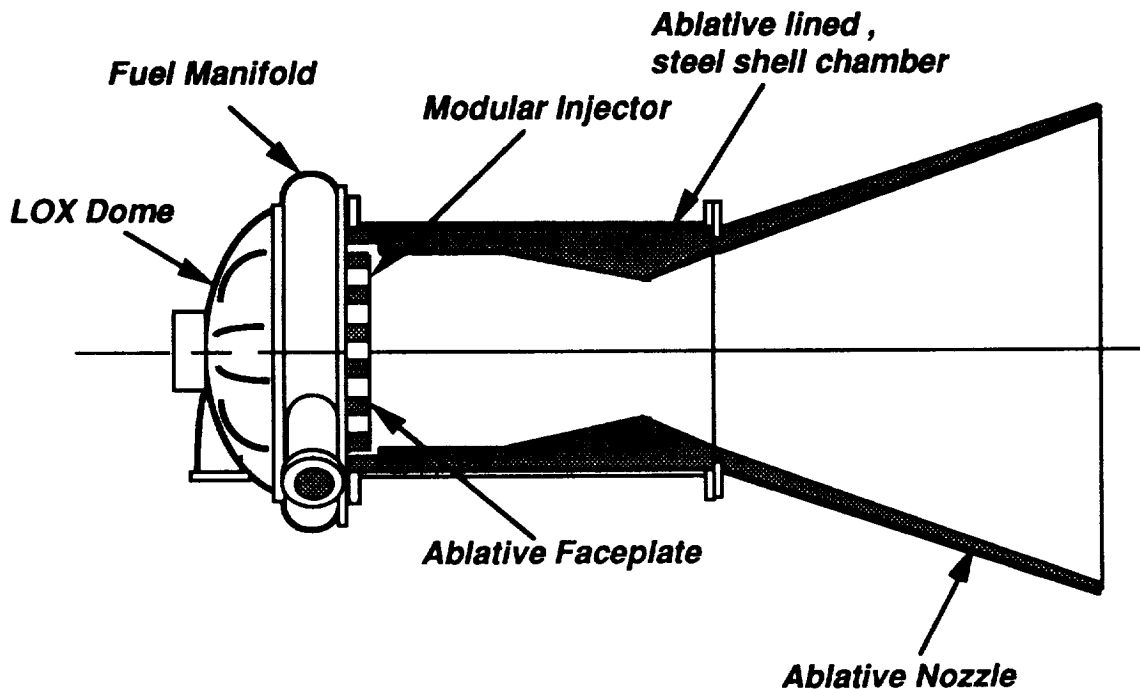
The use of an ablative material on the injector face is an unusual approach for a liquid engine. Face heat flux can vary widely depending on the injection element geometry, spacing, injection velocities, recirculation of propellants and other factors. Verification of face heat flux was required to confirm the ablative faceplate design.

Direct measurement of the face heat flux was accomplished with face mounted thermocouples, both on the modules and by surface temperature measurements in the ablative area. Test data indicated maximum module/surface temperatures, for the nominal operating condition, in the 700-800 °F range. These temperatures are below the maximum 1100°F copper maximum temperature and far below ablative maximums. These measurements are confirmed by visual effects on the injector face, which showed negligible erosion after nominal tests. Nearly all module/faceplate erosion occurred during high Pc (1000 psia) tests where heat flux is considerably higher than at the nominal Pc of 720 psia.

2.2.2 Full-scale Design Concept

The successful subscale testing resulted in very few changes in the full-scale preliminary design generated at the beginning of the program. The modular concept for the injector was a proven success. The ablative chamber/nozzle design is predicted sound by test results, as is the ablative faceplate. The inherent stability of the engine will result in a shorter acoustic cavity requirement, which will shorten the injector and significantly reduce weight. The demonstrated low chug point (≤ 350 psia) indicates that this engine will be highly throttleable. A preliminary flight configuration is shown

below without regard to engine size. It is expected that this low-cost concept could be adapted to any reasonable engine size.



2.2.3 Development Requirements

This engine will require limited development work when it is scaled up to its full-scale configuration. The following characteristics have either been predicted with high confidence or have a demonstrated database. All are considered to be low risk development items.

- (1) Verification of ablative performance under long duration testing. Ablative liners and faceplates must be tested long duration to measure and verify ablation rates.
- (2) Demonstrate injector characteristics at full scale. Full scale testing must be performed to size acoustic damping devices and to confirm stability and performance.
- (3) Demonstrate fuel film cooling performance at the full-scale size. Confirm that film cooling can be tailored to match injector mixing patterns.

2.3 RECOMMENDATIONS

This NASA-MSFC sponsored program has successfully developed the technology for a low-cost LOX/ RP engine. Using the design and production approaches developed in this program, very simple and low cost LOX/RP thrust chamber assemblies (TCAs) can be developed at minimum risk.

By minimizing pressures across the injector face, this TCA design is not only suitable for pressure-fed applications (as originally intended) but is also attractive for pump-fed engines where it's low pressure requirements will reduce demands on the turbomachinery.

The modular injector is readily adapted to a range of engine sizes. For example, by adding one additional module row, and retaining the present module configuration and density, an engine in the 300 to 400,000 lb thrust class is feasible (as shown in Figure 2.2.1). This engine would be directly applicable for upgrading the existing U.S. expendable launch vehicle (ELV) fleet, offering substantially lower propulsion costs, a throttleable propulsion system, and performance improvements. It is understood that ELV upgrade is becoming a national priority.

It is recommended that serious consideration be given to exercising the existing contract option to proceed with the design and fabrication of a large scale TCA which would be tested at NASA-MSFC. Depending on NASA priorities, this TCA could be sized for a large shuttle-compatible liquid rocket booster (750,000 lb thrust) as originally planned, or be matched to the requirement for upgrading the U.S. ELV fleet (300-400,000 lb thrust). The low cost technology developed in this program is ready to meet either requirement.

3.0 HARDWARE DESIGN

3.1 REQUIREMENTS AND CONCEPT SELECTION

The groundrules for this hardware specified that it must be capable of obtaining the data necessary to support development of a pressure fed engine. The hardware was required to simulate, at a subscale level, the approach to be used in the fullscale design.

Selection of a design concept began immediately with the establishment of program requirements. These requirements , in the order of importance, were as follows:

- Stability and Compatibility (Reliability)
- Low Cost
- Medium Performance (~95% C* efficiency)
- Minimum Injector Pressure Drop (1000 psia Inlet Pressure Goal)
- Throttle Capability (to 65%)
- Low Weight

Element selection was the first task in determining the engine configuration. Previous LOX / RP-1 programs performed by Aerojet (ref 1) have indicated that the Oxygen-Fuel-Oxygen (OFO) triplet element is the highest performing and one of the lower cost elements . It also provides a good stability margin when used with large orifice diameters. These facts, along with a well documented history, led to the selection of the large orifice O-F-O triplet element.

The next task was to size the full scale engine. With thrust and C* efficiency specified as requirements, a trade study between performance and stability margin was performed which established the chamber diameter at 44 inches. Injection mixing performance dictated an L' (face to throat) distance of 40 inches. Element quantity and spacing were determined from the thrust and element design ready determined. The very coarse element spacing resulted in large uncooled face areas. These areas could have been cooled using several common face cooling techniques, but this approach did not satisfy the requirement for low cost. We chose to group the elements in discrete

modules and to fill the areas between the modules with a heat resistant material. Using this approach, the modules would be self-cooling and the remainder of the face would be protected.

Chamber requirements for low cost and expandability led to the selection of an ablative design. Ablative liners are much less expensive than cooled designs and meet the requirements for an expendable engine. The chamber would be either a steel shell with ablative liner or an entirely composite structure utilizing the latest tape-wrapping techniques. In either case, film cooling of the wall would be required to extend the life of the liner to match the mission profile. The subscale chamber would be required to measure film cooling effectiveness with extensive instrumentation. Temperature measurement at the chamber wall is difficult with ablative chambers due to the flow of ablating material along the wall. High frequency pressure measurements are also difficult due to the necessity of mounting the transducer sensing element close to the wall. A steel "heat sink" chamber was proposed for the subscale testing to achieve more reliable data at a lower cost.

Combustion stability was the primary operational goal of the engine design. The hardware had to be capable of modification to adjust to yet to be determined combustion characteristics. The acoustic cavity, placed near the injector face, is a reliable method of changing chamber acoustics to coincide with combustion response. Several different size resonator blocks allowed for change in the cavity depth, and therefore its damping characteristics. This enabled "tuning" the chamber during testing.

Full-scale requirements for fuel film cooling (FFC) of the chamber wall required that extensive data be obtained on FFC effectiveness during subscale testing. The heat sink chamber facilitated the measurements. The ability to change to rate of FFC at a constant core combustion MR was required to properly characterize the FFC effects. The FFC circuit was manifolded separately from the fuel injection circuit to achieve independent control of FFC flow. A schematic of the hardware concept is shown in Figure 3.1.1.

3.1.1 Design Parameters

The subscale design was based on the following parameters to ensure design integrity and performance :

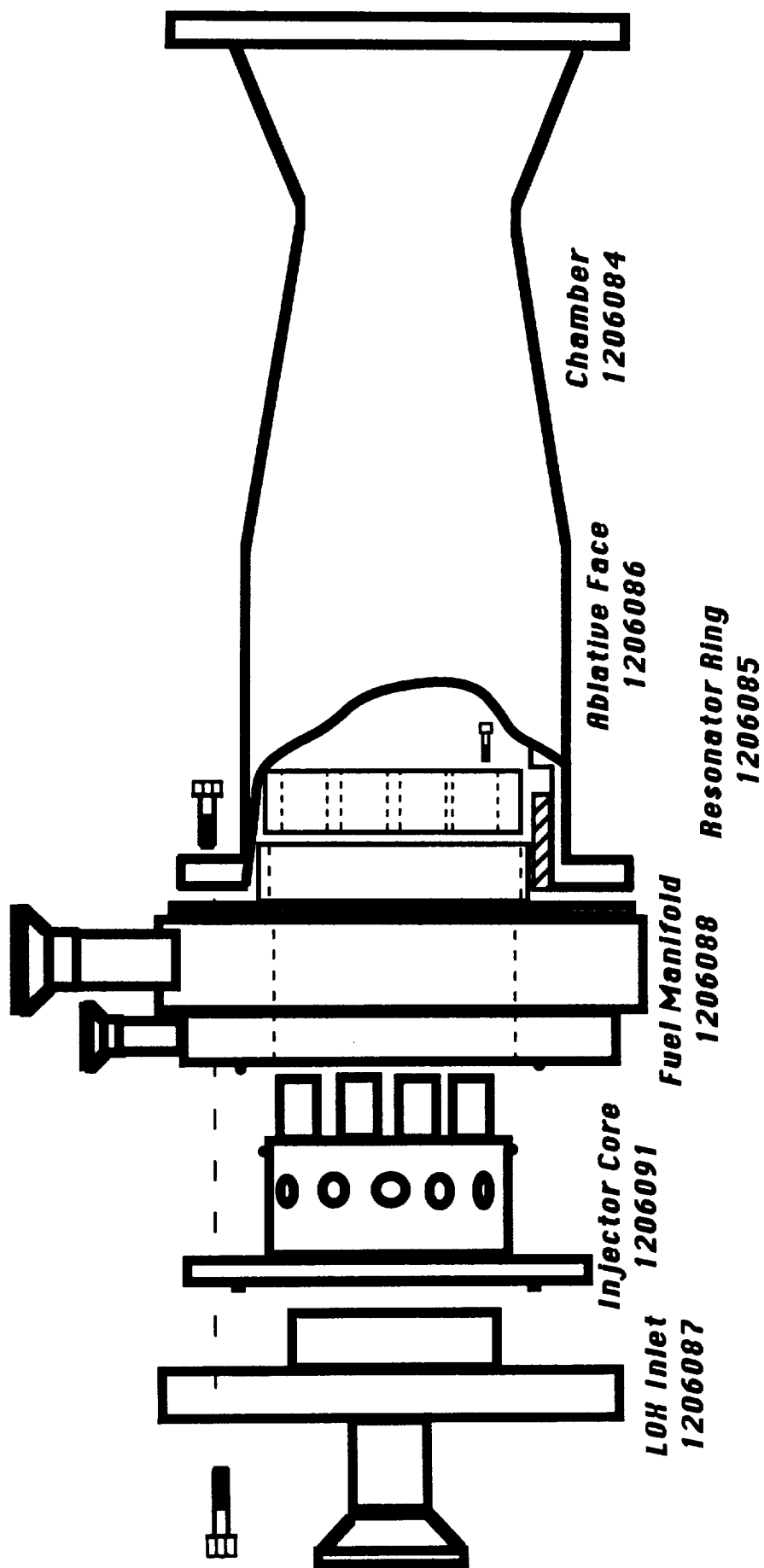


Figure 3.1.1 Subscale Hardware Utilizes Low Cost Simple Components

- Simulate full-scale characteristics wherever possible except that the chamber diameter will be subscale to reduce testing costs.
- Utilize conventional materials and machining techniques wherever possible to minimize costs.
- Follow established stress and cycle life safety factors for low risk testing.

3.2 INJECTOR DESIGN

The pressure fed concept is designed to be a reliable and low cost engine. Another requirement is to minimize pressure drop across the injector to minimize tank pressures and weights. Reliability translates into stable operation with adequate stability safety margins.

For LOX/RP-1, the O-F-O triplet injection element is one of the highest performing elements (ref 1) . A coarse O-F-O element also has a low combustion response frequency as shown in Figure 3.2.1, which simplifies damping devices. In addition, for LOX/RP -1 combustion, the optimum oxidizer-to-fuel ratio is near 3:1 which, when combined with a density ratio of 1.4:1, results in an injection area ratio of 2:1, ideal for the O-F-O triplet with equal orifice diameters.

As a comparison, the like doublet element, used in the F-1 engine, can achieve high performance only with fine injection patterns. The fine injection pattern has a high frequency sensitivity that requires elaborate damping devices . In the F-1 engine development, persistent stability problems resulted in an enlargement of the injection orifices and a subsequent loss in performance, to about 91% combustion efficiency.

The challenge of this design was to design an injector with a 19-inch diameter utilizing the O-F-O triplet element for performance, a coarse pattern for stability, and low cost features. These requirements presented a design conflict. The large face area and coarse pattern dictated a very low element density. Typical injector element densities are on the order of 2 to 3 elements per sq-in. The pressure fed design requires a density of 0.5 elements per sq-in. This low density results in a large distance between elements which must be cooled to prevent face erosion problems. Cooling of the injector face is

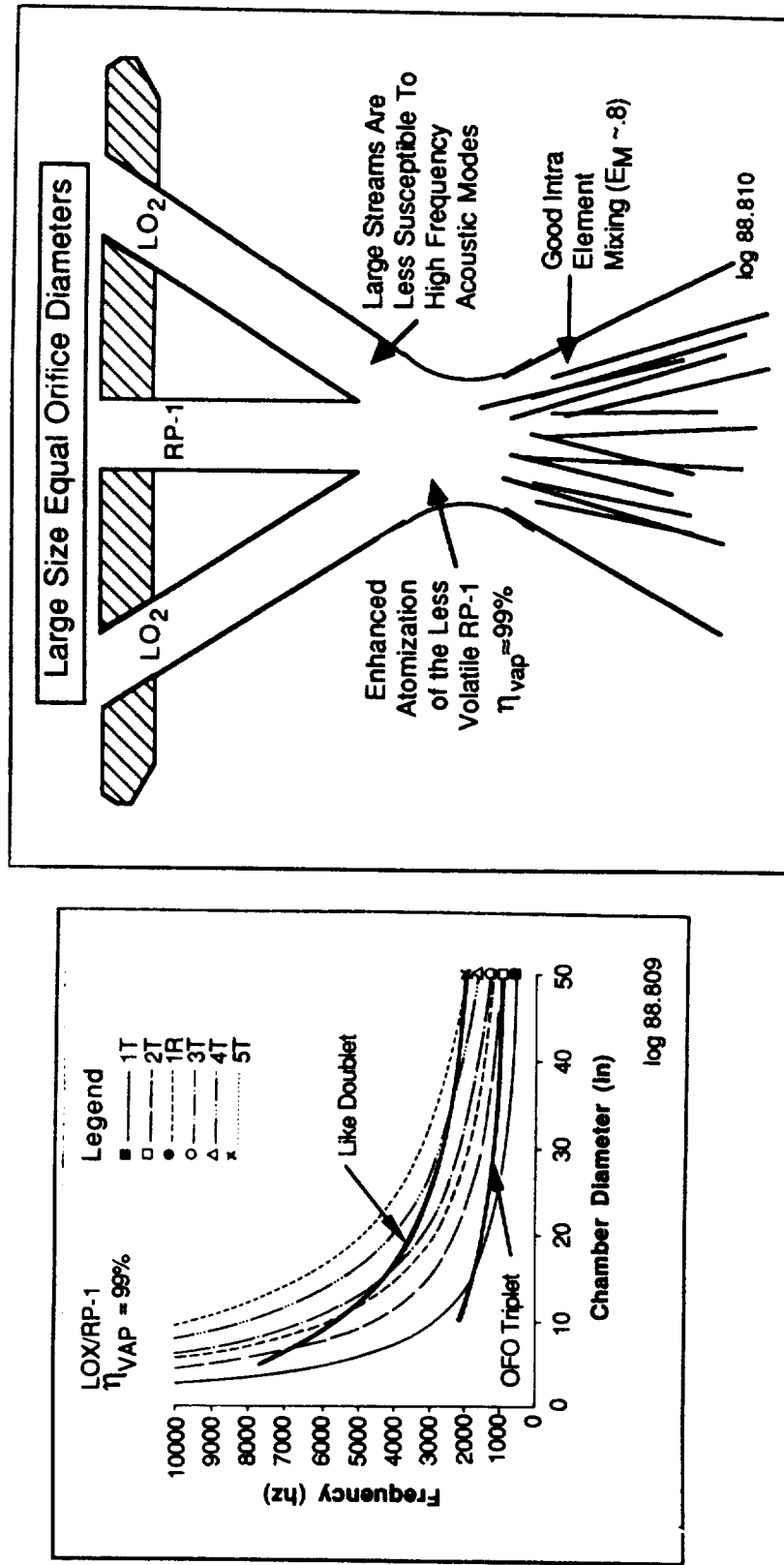
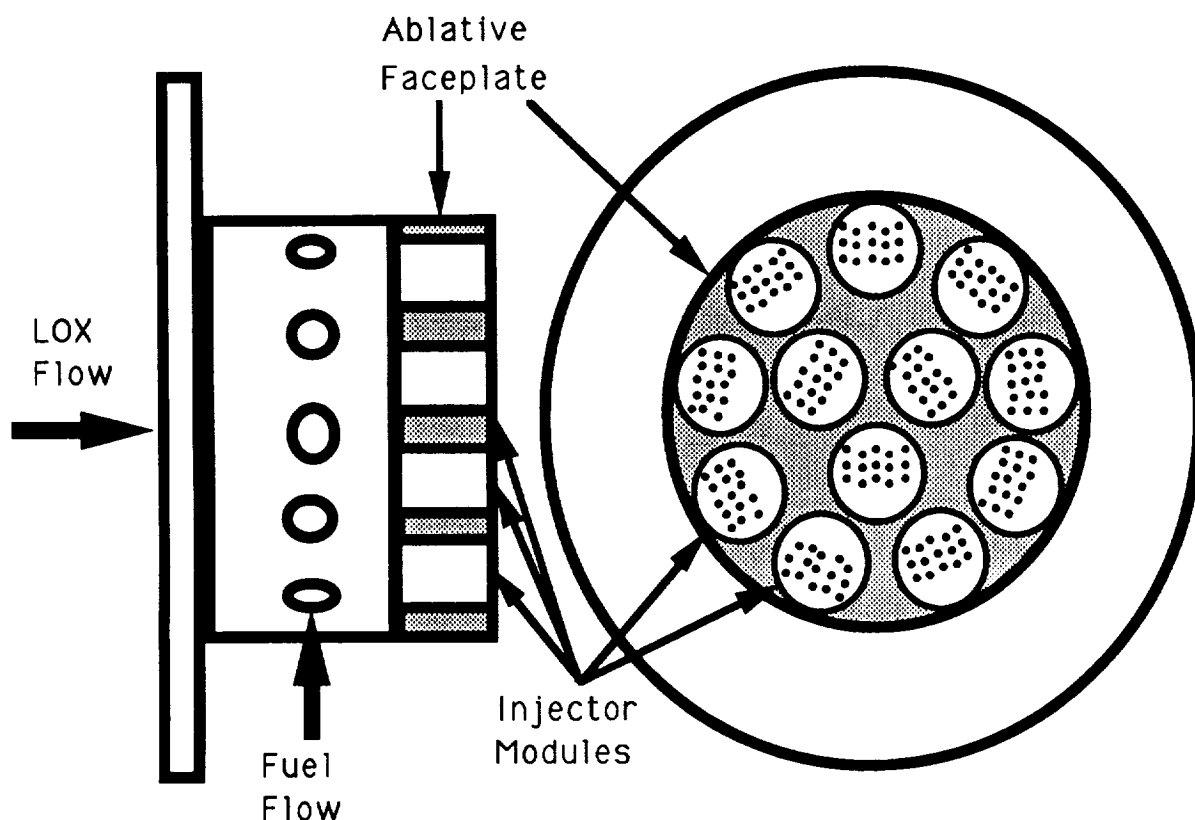


Figure 3.2.1 The O-F-O Triplet is the Best Element for LOX / RP

not a technical challenge as there are several ways to cool injector faces; active face bleed of propellants, circulation of propellants under the face surface, transpiration cooling, etc. However, active cooling of the injector face increases the cost of the injector significantly. Additional circulation of propellants for cooling purposes also increases the pressure drop through the injector. Both of these situations are in conflict with the design requirements.

The solution is to group the injection elements together and place them in copper modules for excellent heat conduction and face cooling. The areas between the modules are filled with an ablative material which has very high resistance to heat. In this way, critical injection areas are cooled and other areas are protected. This arrangement is shown below.



The modular approach introduces fabrication and cost advantages for the injector. A major risk in the fabrication of standard injectors is the hundreds of orifices that must be drilled to precise angles and depths. A single mis-drilled orifice can result

in a very expensive repair procedure or even rejection of the entire injector. The modular approach permits quantity production of the modules as discrete units which are individually inspected and accepted before assembly into the injector body.

The module size used in the subscale injector is identical to the fullscale configuration. This properly duplicates injection atomization and vaporization characteristics and avoids interpolation of data for the fullscale design. It also provides manufacturing data on actual module cost for the fullscale engine. The 4 inch module length was used to allow for a very long acoustic cavity to provide a wide damping range for testing. The actual cavity length will likely be much shorter, and the modules will protrude from the core assembly only a short distance in the actual full-scale design.

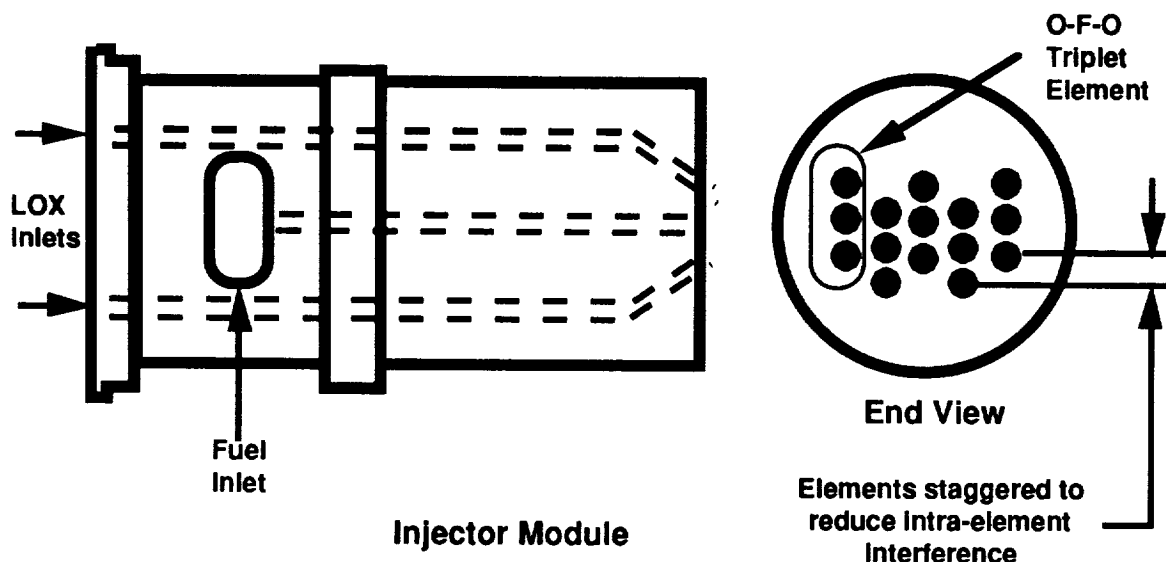
The **LOX Inlet** forms the back of the injector and is straightforward in design. A flat closure plate of CRES 304L was chosen for simplicity and low cost. The plate is penetrated by the inlet tube, which is 6 inch schedule 160 CRES pipe. A plenum is formed on the back side, as shown in figure 3.2.2, provides increased volume to slow the flow and distribute it evenly around the circular area. This plenum is formed with a 1.0 inch 304L plate which has 147 0.75 inch holes for flow distribution. A filter plate, made of perforated CRES 304L plate precedes the 1.0 inch plate and is brazed to it.

The LOX inlet also contains provisions for instrumentation to monitor propellant condition. One each temperature, pressure and high frequency pressure port is provided on the inlet tube. Lifting provisions, rated to 2500 lbs each, are provided at two places and are capable of lifting the entire injector after assembly or the injector end of the entire TCA when assembled. The calculated weight of the LOX inlet is 950 lbs.

The **core assembly**, as the name implies, is the heart of the injector and contains the injector modules as well as the face instrumentation. The core is assembled between the LOX inlet and the manifold.

The **injector modules** provide the flow passages for both the propellants and also contain the final injection orifices. They are constructed from copper alloy which has approximately 17% Zirconium added to increase tensile strength to approximately 24,000 psi at 70° F. Copper was selected for the modules so that the heat on the module face could be conducted rapidly away to the flowing propellants.

Each module contains five O-F-O triplet injection elements, as shown below. The design of each element is identical. The LOX flows through two 0.375 inch down-comers, which travel the length of the module, to an 30° angled injection orifice of 0.241 inch diameter. The impingement angle and position is tightly controlled to the fuel orifice within 0.005 inch in position. This is necessary to ensure good impingement and vaporization. Fuel is fed from a rectangular port in the side of the module and down through a single 0.241 inch injection orifice. To improve intra-element mixing, the modules are staggered by 0.250 inch as shown below.



External features of each module include two brazing surfaces which form the bond to the core weldment. The top joint, an interpropellant joint, is designed with a step which provides a positive contact between the module and the weldment, and reduces the wetted volume that the braze alloy must occupy. This design practically eliminates porosity in the brazed joint.

The core assembly also contains provisions for face thermocouples to measure module temperature as well as the face surface temperature between the modules. The thermocouple leads pass through the flange, along the weldment body, and up to the face. The module thermocouples are attached directly to the module by placing the thermocouple tip in a copper block and staking the block into a groove cut in the side of the module so that the block is flush with the injector face, as shown in Figure 3.2.3. Face temperature thermocouples are mounted in a holder, also shown in Figure 3.2.3.

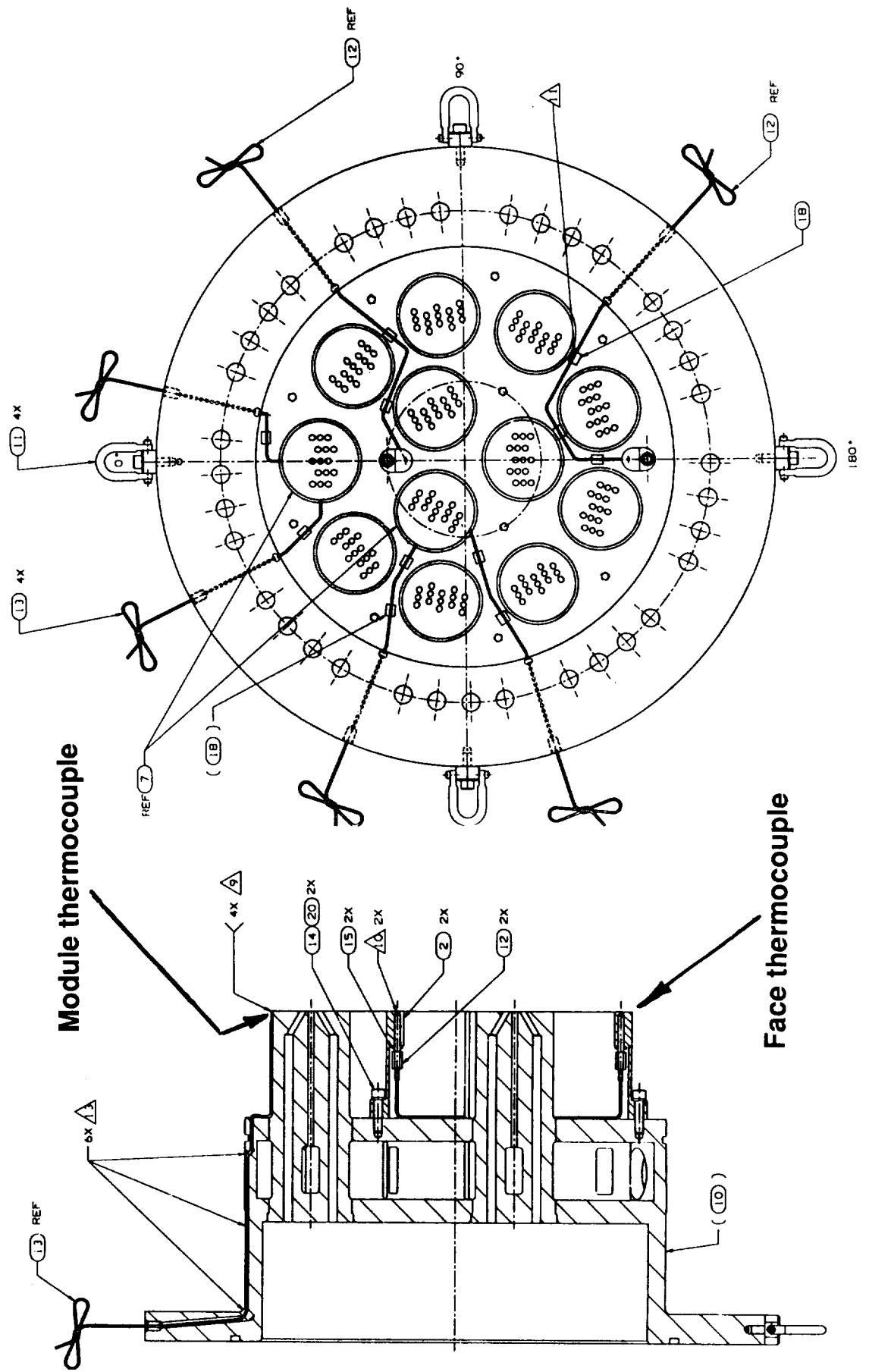


Figure 3.2.3 Face-mounted Thermocouples Measure Face Heat Flux

The **fuel manifold** supplies fuel from the injector periphery to the modules through a circular plenum. This manifold also contains an integral film-cooling injection ring which is fed from a separate circular manifold. This allows different film-cooling rates for specific engine operating points.

The design of the manifold is straightforward, directing fuel through the inlet connection, around the circular plenum, through a diffuser and filter plate combination and finally through radial passages to the core assembly. The filter / diffuser acts to distribute the flow evenly around the periphery and to trap any large particles that may be present.

The testing requirement for the independent control of the fuel film cooling requires a separate circuit and injection point from the fuel orifices. Injection on the face itself is not practical due to the modular configuration of the injector. The design challenge here was to pass the film coolant about 5 inches to the face surface without interfering with the modular injection. A circular ring was designed with small feed channels and 254 injection orifices at the end, as shown in Figure 3.2.4. The channels are formed by slotting the OD of an inner ring and brazing an outer solid ring over the inner ring to close out the channels. The injection orifices are then EDM'ed into the end.

The manifold contains only basic instrumentation ports for fuel temperature and pressure measurements. Two drains are provided at the low point to drain the manifolds between tests if necessary.

3.2.1 Ablative Faceplate

The modular design of this injector results in an open area between the modules which must be filled to prevent hot gas recirculation and protect leading edges of the modules. The open area is filled with an ablative material due to its low cost and high heat resistance. The material chosen for the faceplate is silica phenolic, which has demonstrated very low ablation rates in LOX / RP engines. For the faceplate, a compression molded design was chosen over a tape-wrapped construction to provide equal strength in all directions and avoid any lamination orientation problems. This fabrication method is also the lowest cost of the candidate composite techniques. Openings for the modules and attachment screws are machined. In production, these holes would likely be molded into the part. For the small quantity (3) being produced, the extra tooling costs required to do this were not justified.

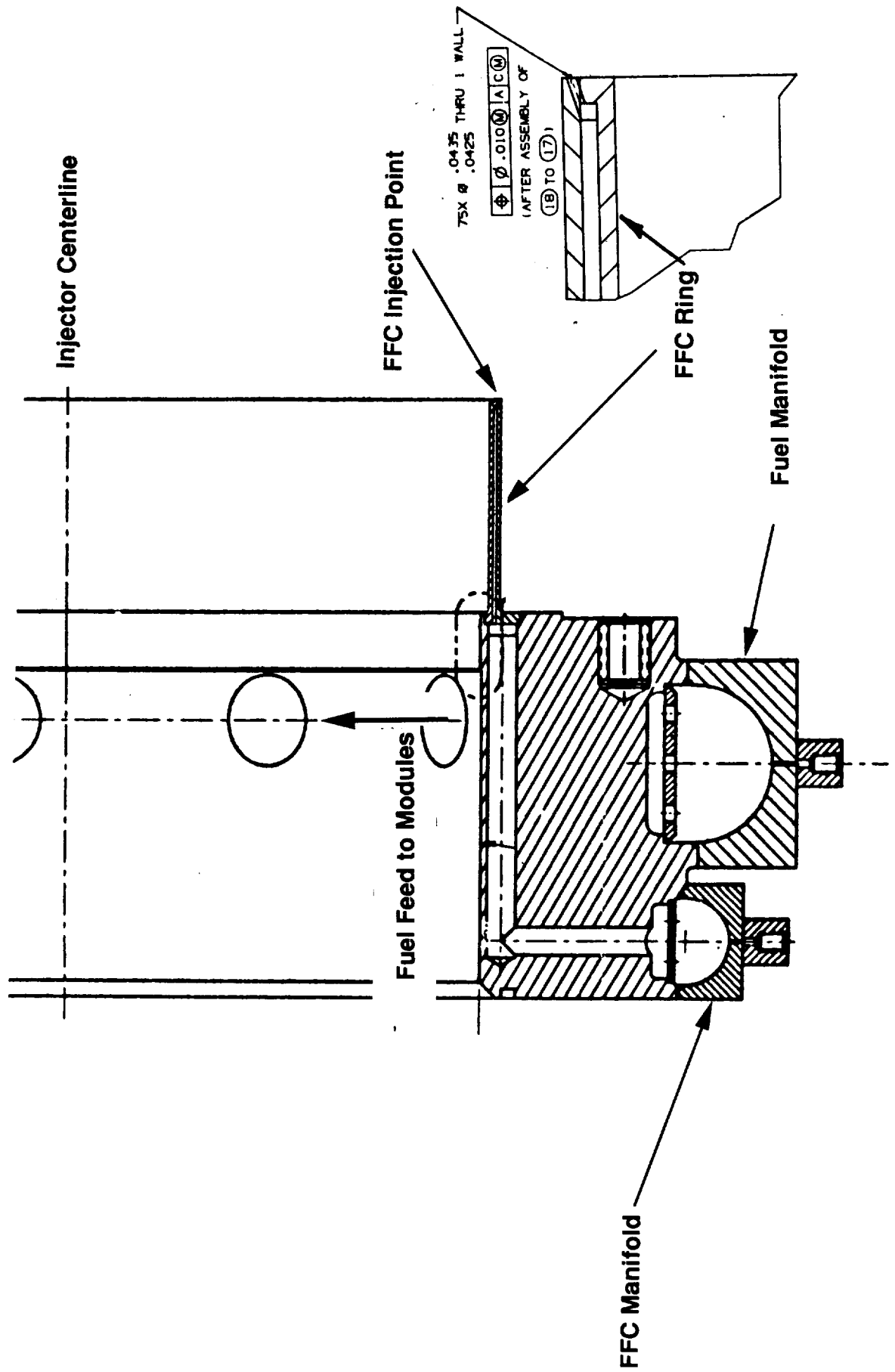


Figure 3.2.4 FFC Ring Injects Coolant to Injector Face

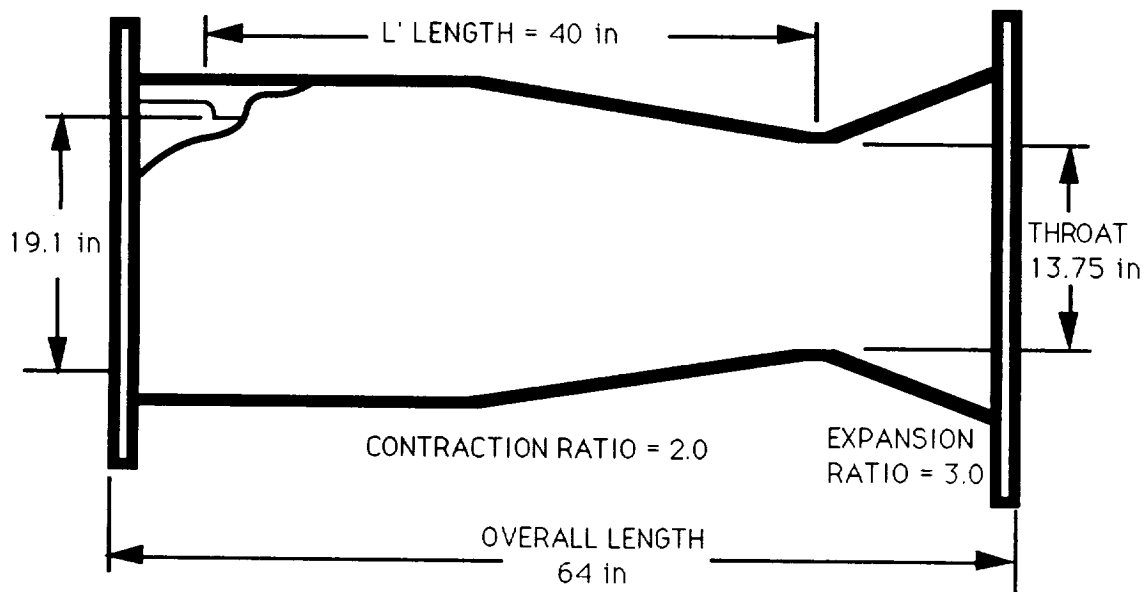
The primary data base for silica phenolic performance was developed in the late 1970's during Aerojet's M-1 program. This 1.5 million lb thrust engine utilized a silica phenolic chamber liner during development testing to reduce costs. Although the engine used LOX/Hydrogen as its propellants, the significant oxidizing combustion products (which contribute significantly to ablative recession rates) are slightly more oxidizing than LOX/RP products. Also, the chamber pressure (another significant recession factor) for this engine was 1040 psia, higher than the 720 psia pressure-fed value. The M-1 engine was tested for 144 sec on several liners and exhibited low ablative recession rates of about 2 mils/sec. This data, combined with several other development program results, gives high confidence that silica phenolic liners and faceplates will provide the required performance for this application.

Ablative chambers, nozzle extensions and other components have been manufactured on a production basis for over 15 years at Aerojet. The ablative and strength characteristics are well documented, as well as the manufacturing processes that produce high quality composite parts with few rejects.

3.3 CHAMBER DESIGN

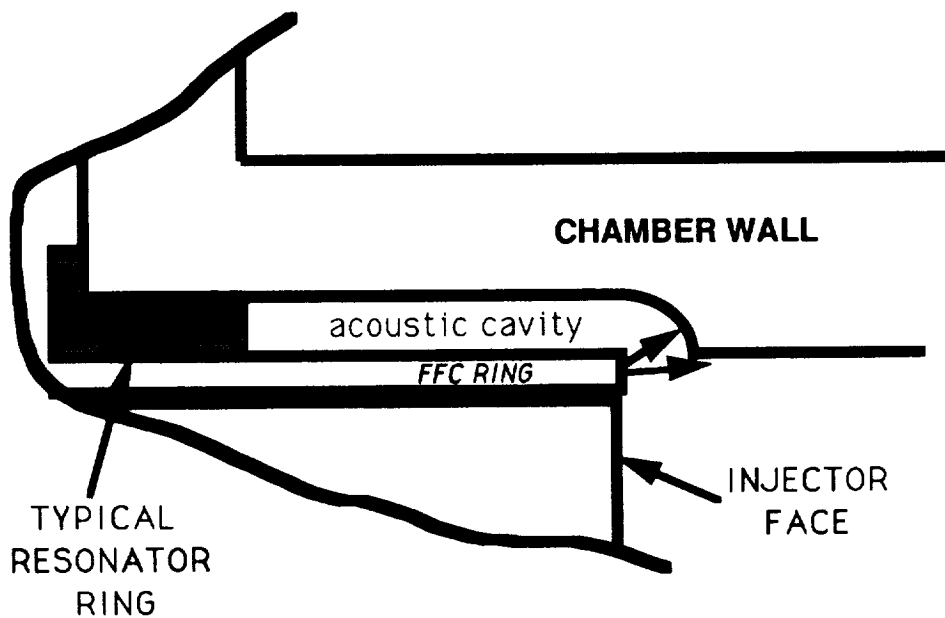
The chamber is a steel shell design to facilitate installation of high-frequency pressure transducers and thermocouples. An ablative liner configuration would make this data more difficult to obtain and would increase cost significantly.

The chamber was designed to be constructed by rolling and welding CRES 304L plate. This method is much cheaper than machining from a solid billet. The chambers long length (64 inches) and weight (1650 lbs) made the solid billet approach cost prohibitive. The chamber walls are approximately 1.65 inches thick. This thickness is determined so that, during a specified firing duration, there will be sufficient ambient temperature steel to contain the chamber pressures. This guideline is very conservative, but allows for testing variations and increased chamber life. The chamber configuration is shown below.



The chamber is designed at a subscale diameter to properly simulate the 1T / 3T relationship described in the requirements section. The combustion section diameter is 19 inches. The combustion length, L' , is selected due to the fact that the injector modules are full size, and the vaporization distance dictates the combustion length. Consequently, the combustion section is stretched slightly and has a resulting convergence angle of 6 degrees.

The chamber has an acoustic cavity built into the front section as a stability aid. The cavity is approximately 5 inches long and 0.75 inch wide as shown below. Provisions for mounting tuning devices, or resonators, are included to allow adjustment of the cavity depth during testing.



The chamber also has extensive provisions for instrumentation. There are 15 pressure ports and 23 thermocouple ports which extend along the length of the chamber at varying radial locations. These locations were selected to provide accurate information on film cooling effects and the axial combustion profile of the chamber. In addition, 5 high frequency pressure ports measure the combustion response and detect any instabilities. Instrumentation locations are shown in Figure 3.2.5.

The chamber also contains two ports for combustion stability bombs. These ports are approximately 5 inches from the injector face and oriented radially at 20 and 200 degrees. The upper port is a radial port, firing to the centerline of the chamber (across the injector face). The second port is a tangential port, firing across the bottom of the chamber. These two port configurations allow different ways of perturbing the combustion to better quantify combustion response.

3.4 INSTRUMENTATION

3.4.1 Temperature Measurement

Two types of thermocouples were used in subscale testing. Standard Type T junction thermocouples were used to measure the copper module face temperatures and co-axial Type K thermocouples measured the ablative injector face thermal

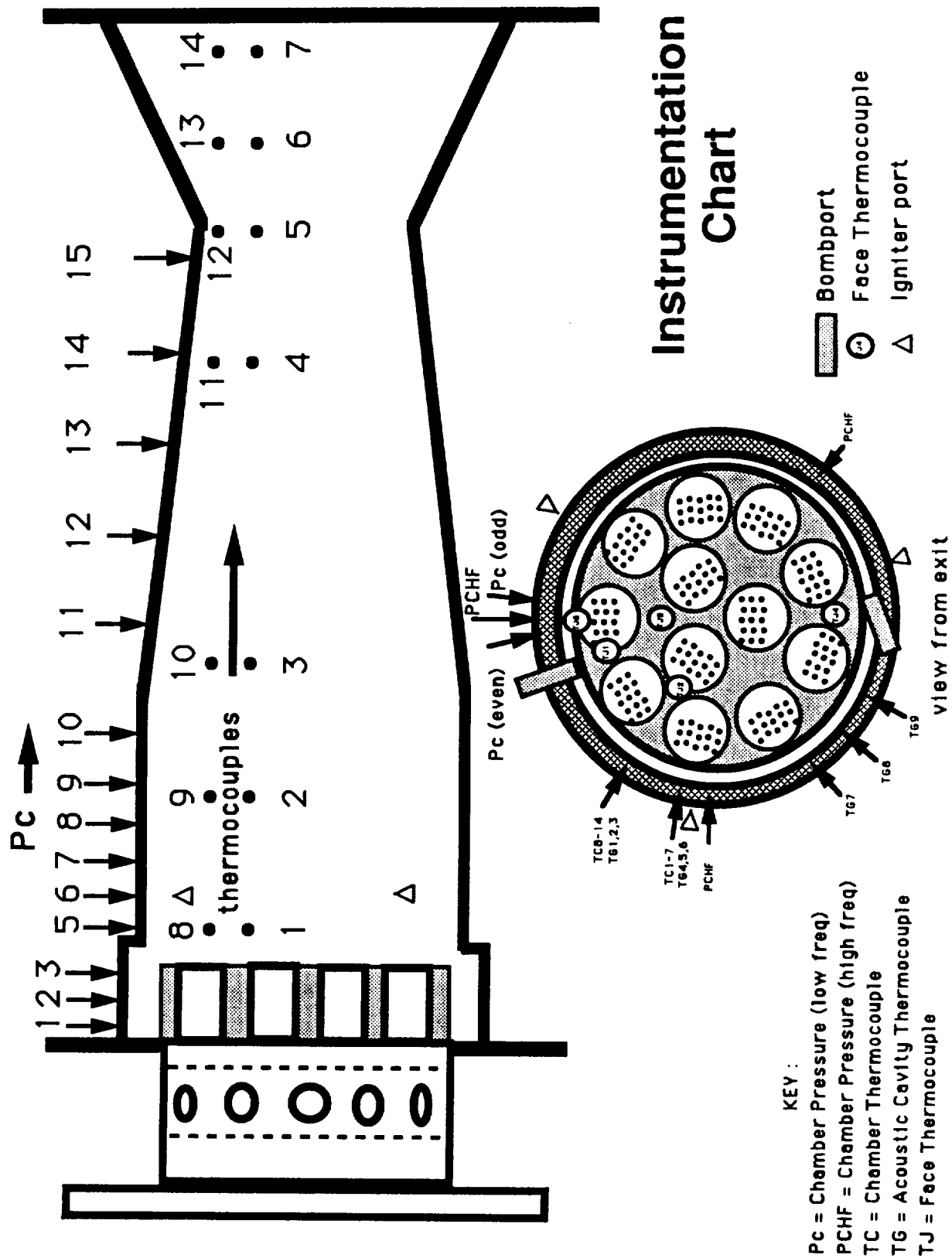


Figure 3.2.5 Extensive Instrumentation Monitors Engine Performance

environment and steel chamber wall temperature. Figure 3.2.5 shows the thermocouple locations in both the injector face and along the chamber wall.

Type T thermocouples were used on the copper modules in four locations, on both inner and outer row modules. These thermocouples provided the temperature histories on the outer edge of the front surface of a representative outer row module and an inner row module.

Type K thermocouples (TJ4 and TJ5) were mounted on steel supports which placed the tip of the thermocouple flush with the gas side surface and allowed surface heat flux to be inferred from the surface temperature history.

Chamber instrumentation consisted of two rows of 7 co-axial Type K thermocouples mounted at several axial locations, as shown in Figure 3.2.5, in the chamber and divergent section. Each row was either in line with an outer row module (TC1-7) or in between two outer modules (TC8-14) directly outboard of an inner row module. Each thermocouple was mounted flush with the gas side chamber wall surface. This approach directly measured gas side wall surface temperature enabling the surface heat flux to be inferred.

3.4.2 Pressure Measurement

Pressure measurements were divided into two distinct categories; low and high frequency. Low frequency transducers are used to measure most supply, differential, and chamber pressures for balance and performance calculations. The high frequency transducers are helium-cooled Kistler units designed to measure very rapid changes in pressure, and are used to determine combustion stability modes and amplitudes. Locations of the pressure instrumentation is shown in Figure 3.2.5.

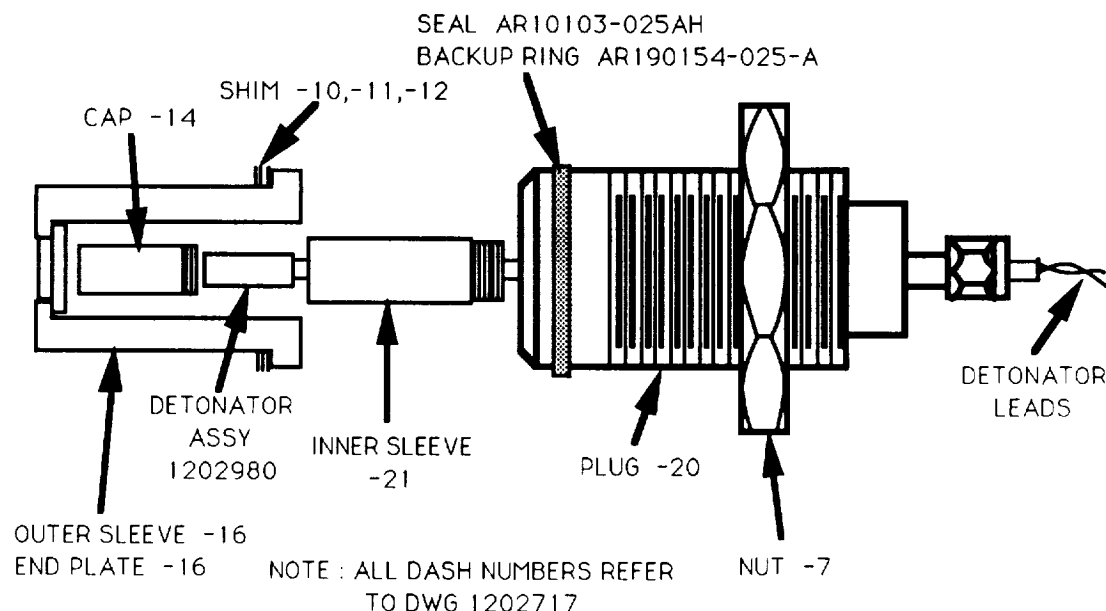
3.5 ANCILLARY HARDWARE

3.5.1 Bomb Components

The combustion stability bomb components were designed on another program and have performed well in other tests of similar engines. The components, shown below, include a plug assembly which mounts the remaining components. The detonator (explosive charge) assembly is placed inside a teflon cap which is screwed into the inner sleeve. The inner sleeve is made from high-strength A-286 stainless steel

and directs the charge inward into the chamber instead of allowing it to expand outward and potentially damaging the surrounding area. This is especially important with ablative chambers which can be easily damaged by the blast.

Bomb Port Assembly



The inner sleeve is then screwed into the plug and the detonator leads brought out through the end fittings. The outer sleeve is made from carbon phenolic material and is designed to protect the detonator from the combustion chamber heat load and prevent pre-ignition of the bomb. The outer sleeve is placed over the inner sleeve and the entire assembly is screwed into the chamber bombport. Shims are provided to allow adjustment of the outer sleeve to install it flush with the chamber wall. For each bombed test, all components except the plug and nut will be consumed and require replacement.

3.5.2 Resonators

Resonators were designed to fit into the chamber acoustic cavity to vary cavity depth. They are required to fine tune the cavity, and the resulting chamber acoustic response, to reduce or eliminate instabilities. Three different resonator configurations were designed; one for a full cavity, one to eliminate the cavity and several

blanks to be machined after test data determined the optimum cavity depth. The resonators are bolted into the front end of the chamber and are made of CRES 304L for low cost.

3.5.3 Proof Plate and Adapter

A proof plate and adapter were designed to assist in proof and leak testing. The proof plate is bolted to the end of the chamber and is rated to approximately 2000 psi proof pressure. The adapter , also rated at 2000 psi, can replace the chamber if it is desired to proof the injector without the chamber installed.

4.0 FABRICATION

Fabrication of the hardware was accomplished from June through December 1990. Of the six major components, the LOX inlet, core, manifold and chamber were made by a single vendor, Martinez and Turek, in Southern California. The resonator rings were made by a local vendor, Harris Machine and the ablative faceplate was made by Aerojet. Cleaning, final assembly and proof testing were performed by Aerojet.

4.1 INJECTOR

4.1.1 LOX Inlet

Fabrication of the LOX Inlet was a fairly straightforward process. The main body and plenum ring and distribution plate were all made from CRES 304L plate. The Inlet pipe is Schedule 160 CRES pipe with a forged Greylock standard hub welded on the end. All weld joints were TIG welded except for the plenum to body weld which utilized electron-beam welding to reduce warping.

The distribution plate incorporates a filter to screen large particles from the LOX stream and to further diffuse the LOX flow. This filter is made from CRES 304L perforated plate with 0.062 inch dia staggered holes. The filter is attached to the front side of the distribution plate by brazing. In any brazing operation, the most important considerations are cleanliness and proper fit between components. These parts were extensively cleaned and a fixture built to compress the items during brazing. The braze alloy was copper, chosen for its excellent fill properties, and brazing temperature was approximately 1700°F. The faceplate and screen are shown after brazing in Figure 4.1.1. After brazing, the distribution plate was ready for welding into the main body. This was an EB weld and resulted in the completed assembly, shown in Figure 4.1.2.

4.1.2 Core Assembly

The core was the most complex of the components. It consisted of a CRES 304L body, composed of two 1" thick plates which were welded into a circular housing, and twelve copper injector modules which were brazed into the housing.

The core body started as a weldment 1206093 as shown in Figure 4.1.3. The weldment was made from plate stock, which in some cases was rolled and welded. The weldment was stress relieved before final machining. Machining of the

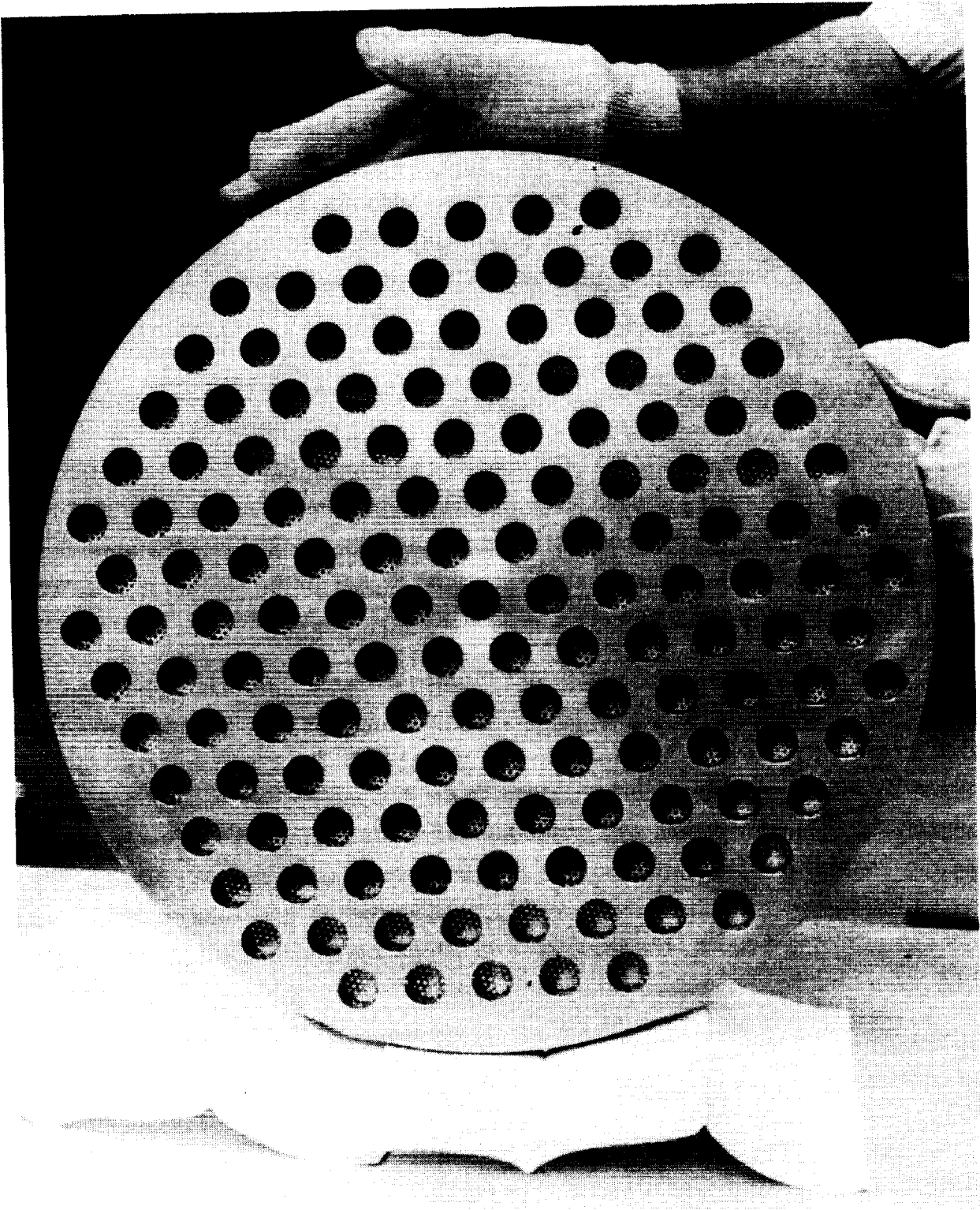


Figure 4.1.1 Inlet Plate and Screen After Brazing

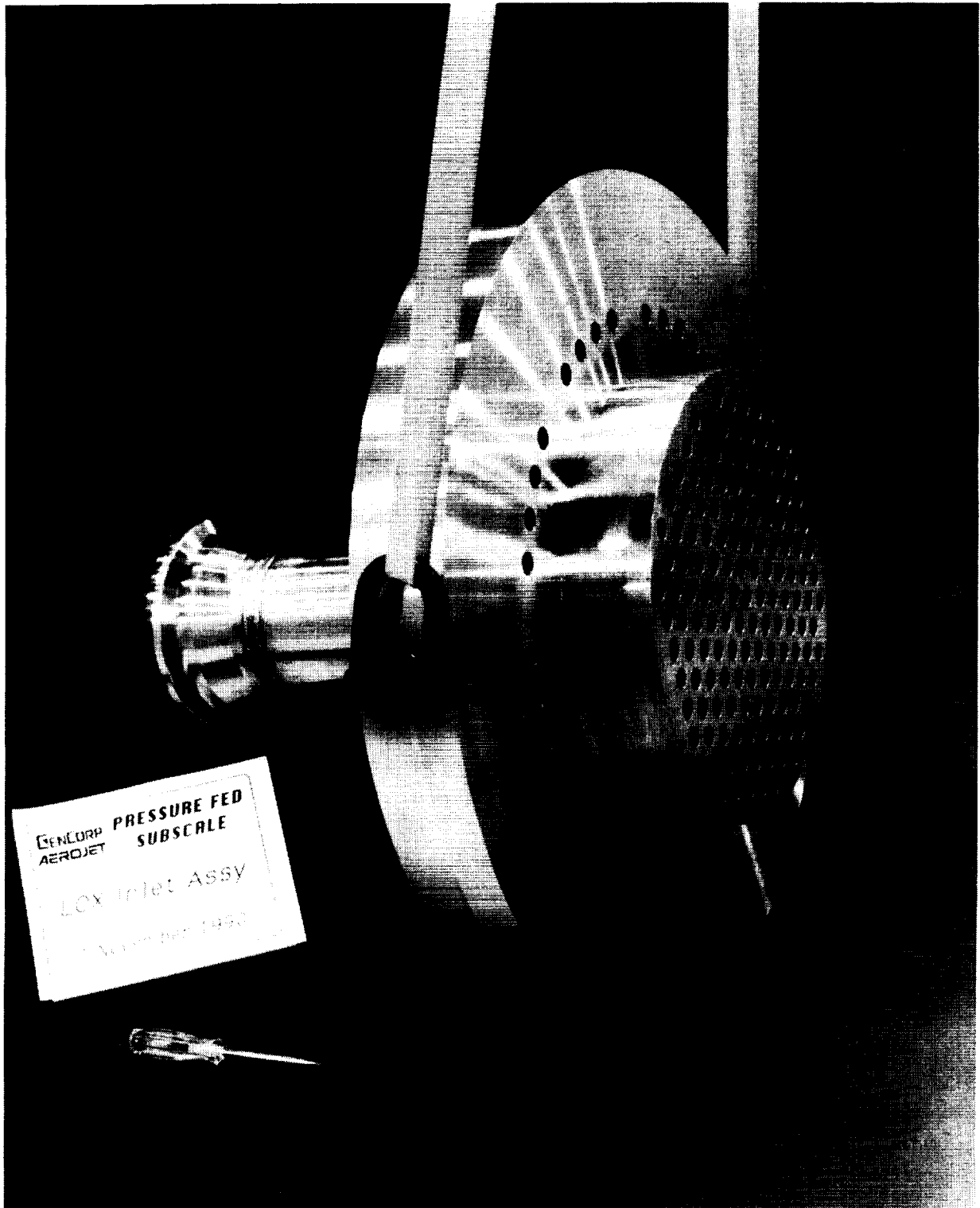


Figure 4.1.2 Completed LOX Inlet Assembly

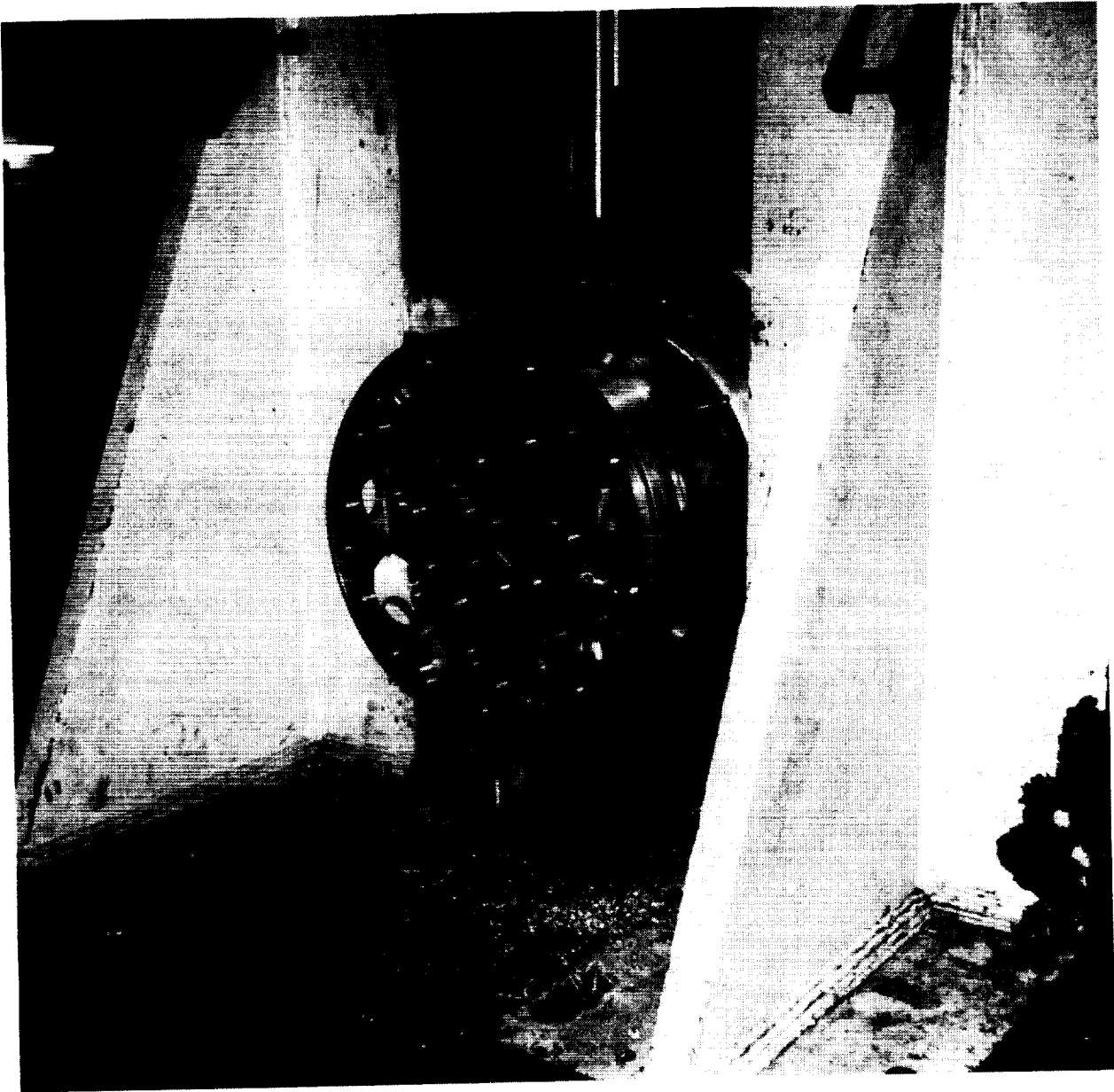


Figure 4.1.3 Core Assembly Weldment

ORIGINAL PAGE
BLACK AND WHITE PHOTOGRAPH

module bores was an important process, because the fit between the modules and their bores is critical for a good braze. The module bores were machined in two parallel plates with a concentricity of 0.005 in on the diameter.

The injector modules are constructed from Zirconium-Copper (.20% Zirconium) which has higher strength than OHFC copper. The modules were machined from 4.0 inches round barstock. Machining of the injection orifices, 0.241 and 0.380 inch holes, required a positional accuracy of 0.005 inch in their 7.5 inch length to ensure that they would intersect properly at the injection end. After some development of the machining operation, all of the modules were completed without error. The completed modules are shown in Figure 4.1.4.

Brazing of the modules to the core weldment required extensive setup and coordination, due to the size of the core and modules and to the braze preparation involved. The modules were prepared for brazing and inserted into the core, as shown in Figure 4.1.5. Cleanliness was of extreme importance, and components were constantly cleaned with alcohol.

Once the modules were inserted, a circle of braze alloy in wire form was placed above each braze joint and secured with special braze-compatible adhesive. The assembly was then instrumented and placed in the evacuated braze chamber. Brazing was performed at approximately 1750 ° F. Following cooling of the assembly, a leak check was made of each braze joint by pressurizing the fuel cavity with nitrogen to 50 psi. This required special fixturing and plugs to seal both the injection orifices and the side inlets. Three small leaks were noted during this test. A leak sealing procedure, devised prior to fabrication, utilized a braze alloy that melts at a slightly lower temperature than the original alloy. The alloy was placed on the leaking joints and the assembly was returned to the furnace. After the repair braze, the leak check was repeated confirming that the leaks had been successfully repaired.

The completed body was then placed in an assembly stand for the installation of thermocouples. The thermocouples were designed to measure both copper module temperature and the gas temperature at the face between modules. Four thermocouples were installed on the copper modules and two were mounted in support brackets. The thermocouple leads were potted in the passages with an



Figure 4.1.4 Injector Modules Can Be Mass Produced for Economy

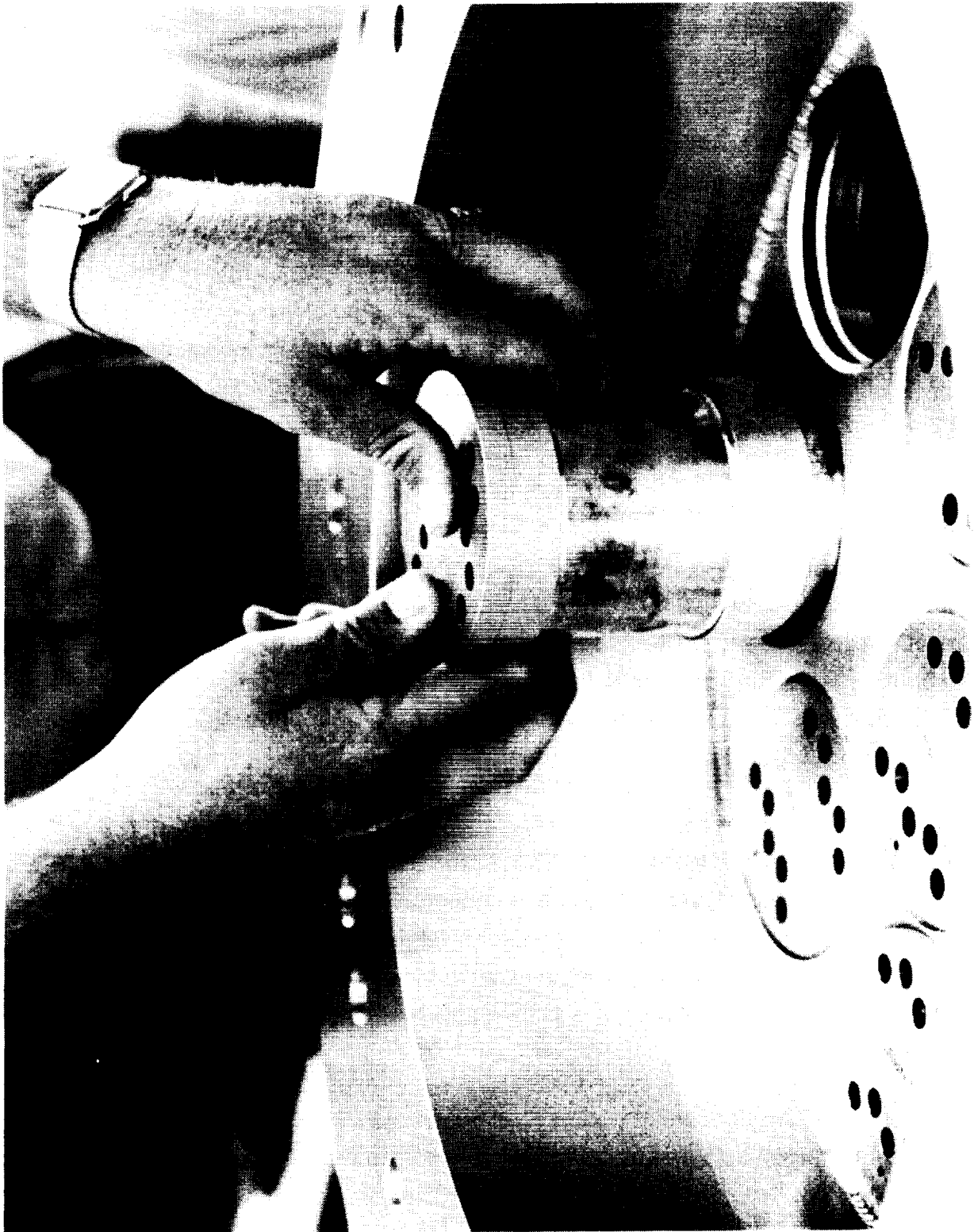


Figure 4.1.5 Modules are Inserted into Core for Brazing

epoxy filler to form a seal against the fuel manifold pressure. The sensing ends of the module thermocouples were staked to the module body using a copper plug as shown in Figure 4.1.6. Face thermocouples were mounted in support brackets, Figure 4.1.7, and the leads fed through the manifold passages and potted. A leak check was performed using the outside fitting to verify the seal between fuel pressure and atmosphere. No leaks were found.

4.1.3 Manifold Assembly

The manifold assembly was constructed entirely of CRES 304L. It consisted of several different components. The manifold actually contained two separate circuits, the fuel supply circuit and the fuel film cooling (FFC) circuit. A drawing of the manifold circuits is shown in Figure 3.2.4.

The manifold body was machined from a CRES billet and was straightforward in construction. Each manifold circuit had two circular strips welded to the perimeter as shown in Figure 4.1.8. The first strip, the distribution plate, controlled flow from the single inlet so that it would be distributed evenly around the perimeter and feed all modules. It was perforated with 0.38 inch holes and skip welded around the perimeter. The second strip served as a filter and consisted of perforated plate with 0.062 inch holes. This strip was welded on top of the distribution plate.

The FFC injection ring moved the FFC injection point to the face of the injector as shown in Figure 3.2.4. This required a ring with fine fuel passages almost 5 inches deep. Drilling of the 225 injection holes (with diameters as small as 0.042 inch) at that depth would have been cost prohibitive. The ring was constructed by machining an inner slotted ring and an outer solid ring and brazing them together as shown in Figure 4.1.9. The injection holes were then EDM'ed the short distance to the fuel passages. The completed ring was then attached to the manifold body by EB welding.

Each manifold circuit required an outer closure torus. The fuel circuit torus was constructed as one piece and electron-beam welded to the body. The FFC torus was installed as two pieces due to weld access and inspectability requirements. The inner half was electron-beam welded first and the weld was inspected. The second half was then welded on two perimeters. Inlet fittings were attached by standard TIG welding.

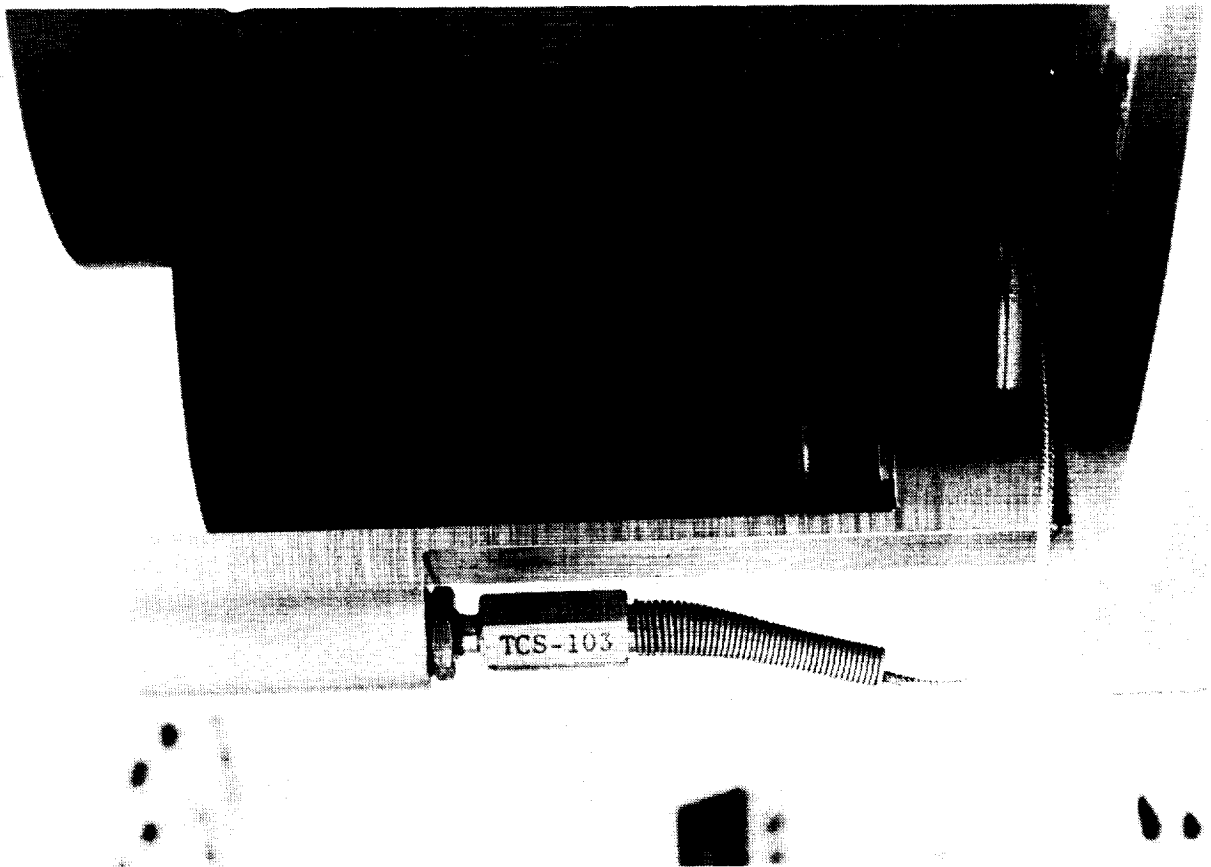


Figure 4.1.7 Face Thermocouples are Mounted in Stands

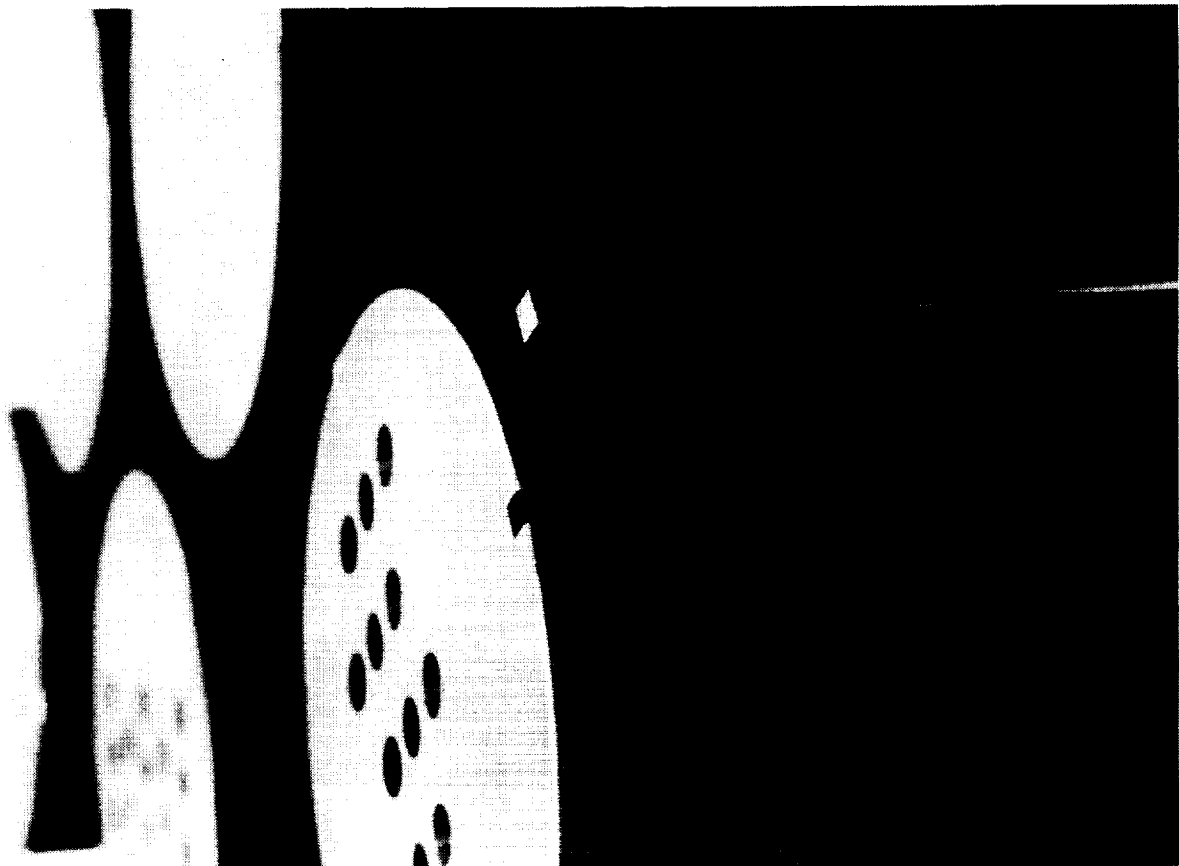


Figure 4.1.6 Module Thermocouples are Staked Directly to Modules

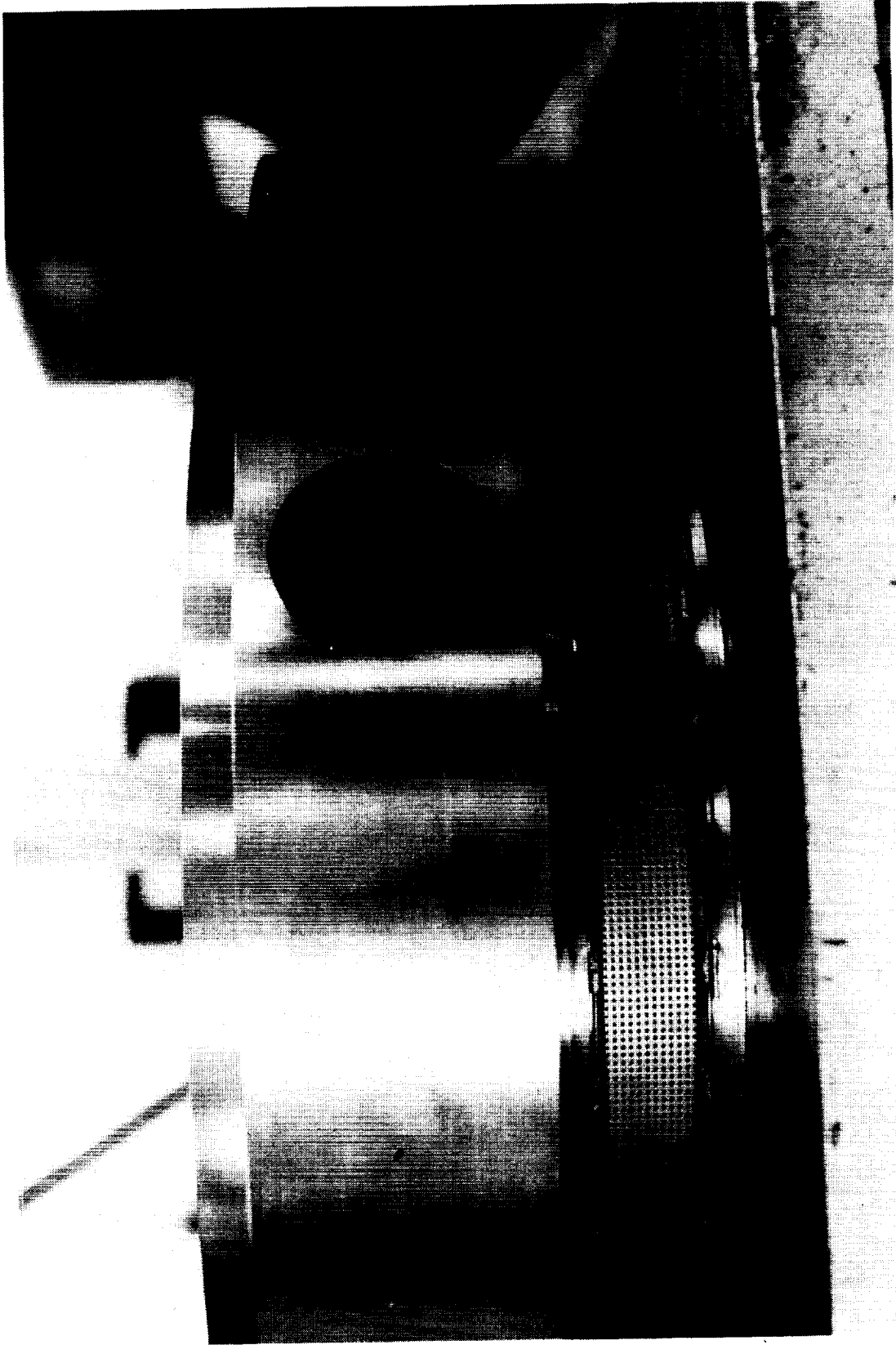


Figure 4.1.8 Distribution Plate (top circuit) and Filter (lower circuit) Condition Fuel Flow

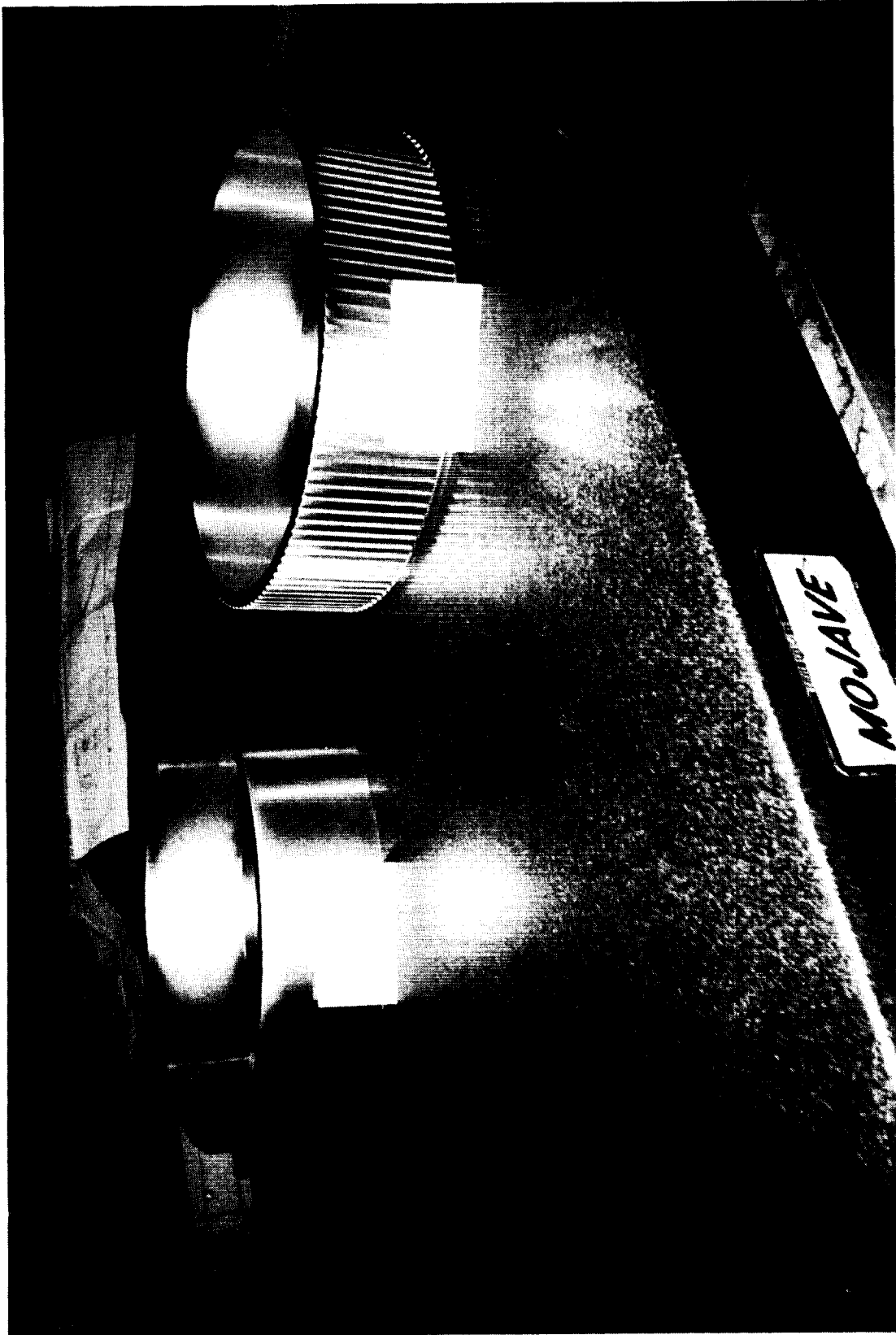


Figure 4.1.9 Concentric Rings Form FFC Injection Ring

Attachment and machining of instrumentation ports and fittings completed the manifold assembly. The completed assembly weighed approximately 900 lbs.

4.1.4 Ablative Faceplate

The ablative faceplate was molded and machined at Aerojet in the solid rocket motor manufacturing area which has extensive experience with ablative materials for nozzles and motor cases. Faceplates were molded and machined rather than molded to net shape, as would be done in production. The small quantity (3 faceplates) did not justify the construction of relatively expensive tooling.

Material for the faceplate was Fiberites MX-2600 Silica-Phenolic in the form of chopped 1/2-inch squares. This material was easy to use and mold. The 19 inch blank was molded using a vertical press which incorporated heated platens to maintain the proper molding temperature. The material was molded at an approximate pressure of 2200 psi and temperature of 250°F. The molding and curing process required approximately eight hours to complete. Figure 4.1.10 shows the loading of raw material into the mold.

Machining of the molded blank was accomplished using special diamond-tipped cutting tools as shown in Figure 4.1.11. The faceplate bores would likely be net-molded into the part in production quantities. The completed faceplate is shown in Figure 4.1.12.

4.2 CHAMBER

The chamber was constructed of CRES 304L plate which was rolled and welded for cost savings. The chambers large size (25 inches diameter and 64 inches long) made machining from billet stock cost/schedule prohibitive. Local imperfections inherent in welding were evaluated and judged to not be significant. Rolling of the 1.75 inches plate to tight diameters was not easily accomplished, but was successful after some trial bends. Inspection of the welds revealed porosity as large as 0.19 inch in some areas. Depending on the location and distance from the gas side wall, these

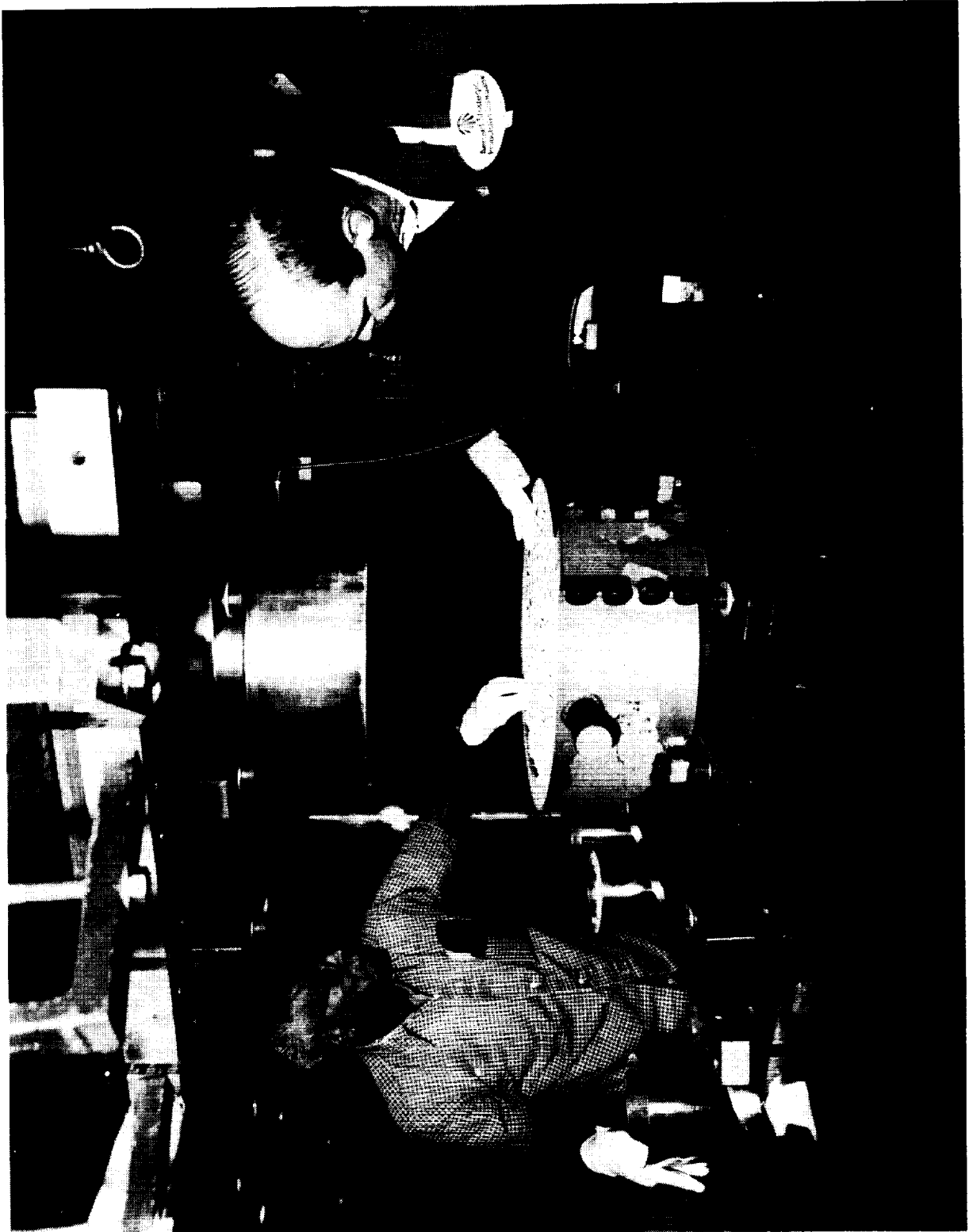


Figure 4.1.10 Faceplate is Compression Molded from Silica Phenolic Chips

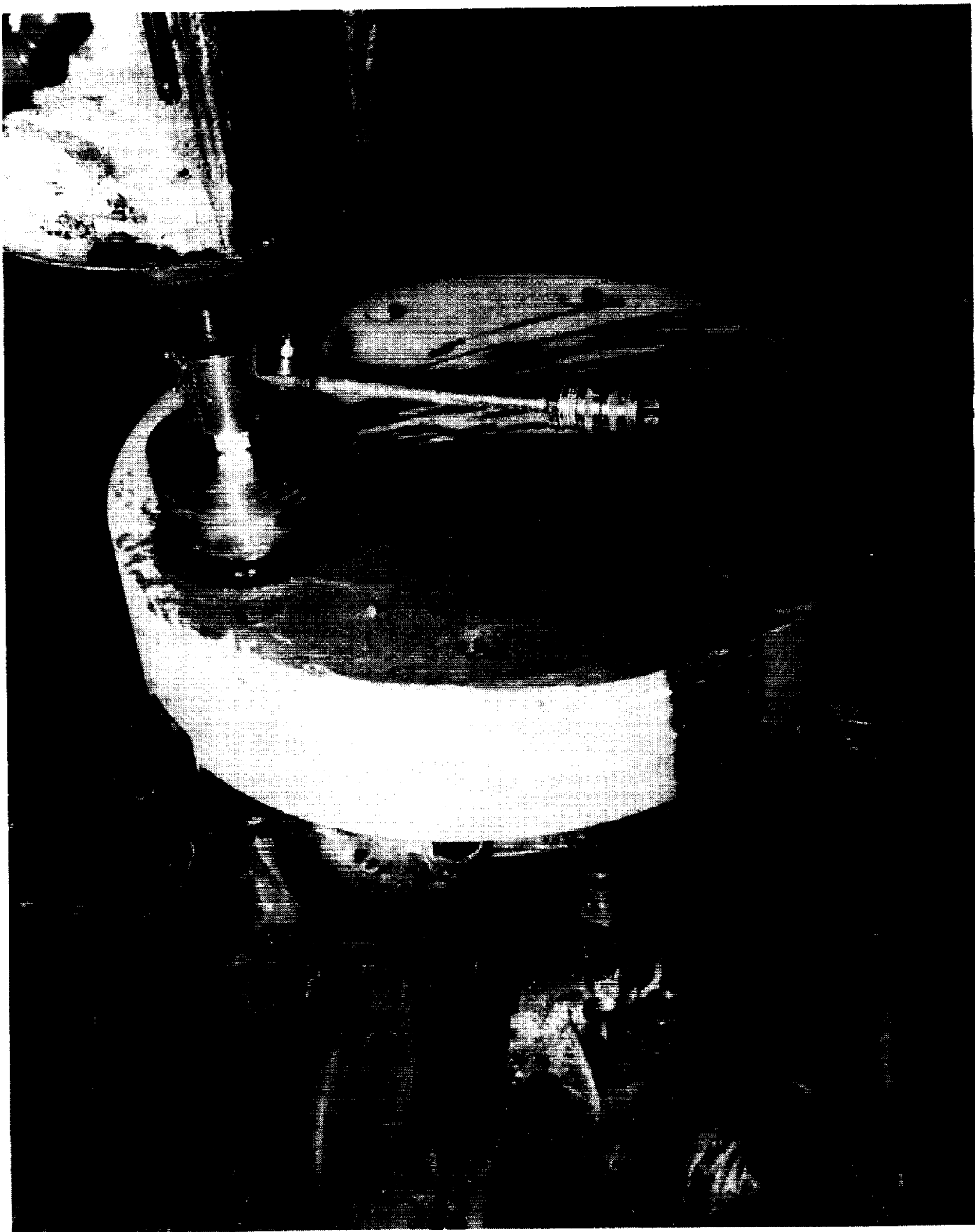


Figure 4.1.11 Faceplate Bores are Machined Using Special Tooling

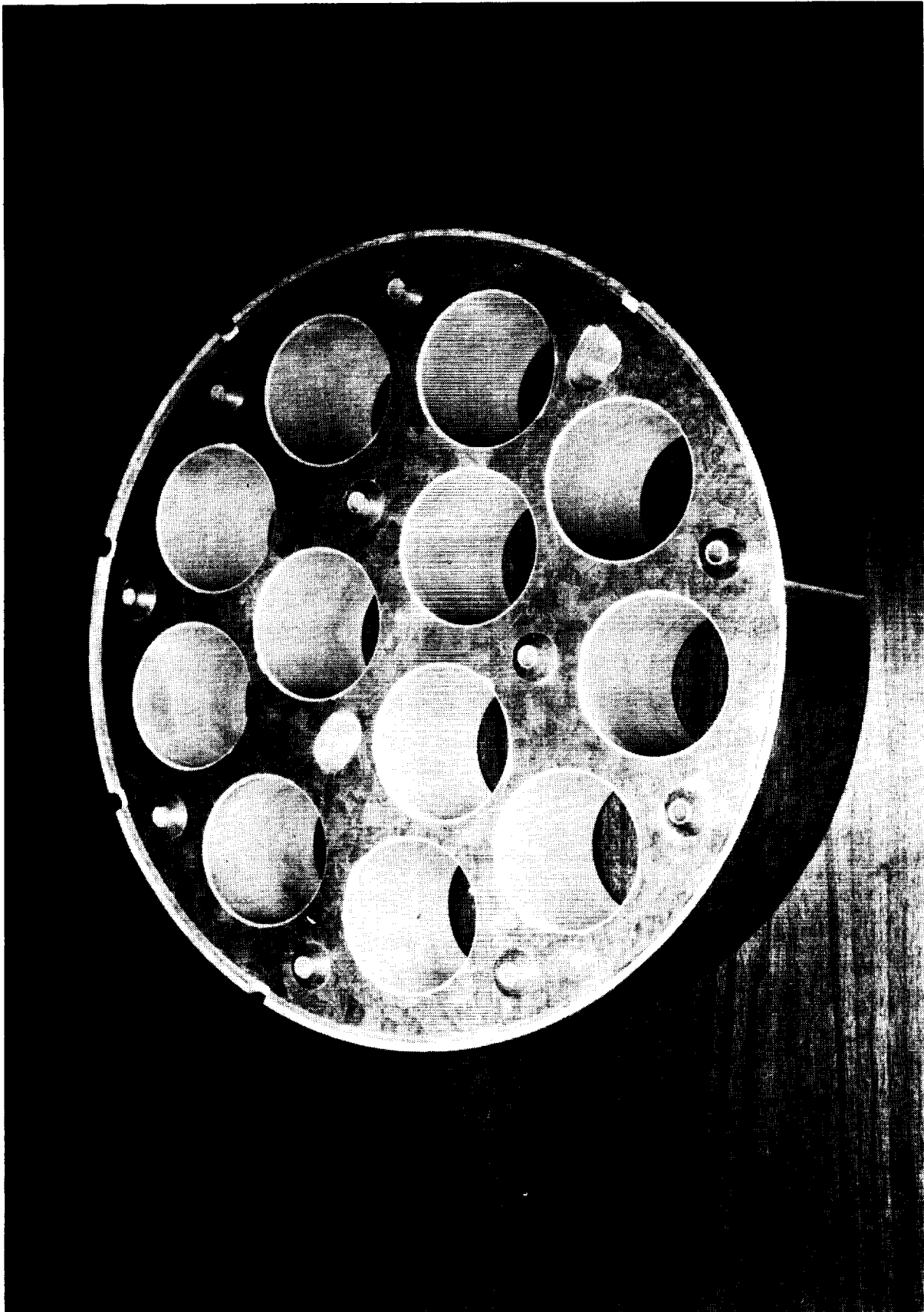


Figure 4.1.12 Completed Ablative Faceplate

imperfections were either repaired or accepted based on structural analysis. End flanges were cut from plate and welded to the tubular structure. Machining of the welded rough form was accomplished without incident.

The chamber assembly included several resonator rings of different lengths to tune the acoustic cavity. These rings were constructed from CRES 304L and incorporated a flange to bolt them to the front section of the chamber. Several spare rings were built so that they could be machined to the proper length after initial test results defined the proper cavity "tune". The acoustic cavity and the resonator are shown schematically in Section 3.2 .

Proof plates, adapter rings, and various miscellaneous hardware were also constructed to support assembly and testing. These components were procured well in advance of testing.

4.3 ENGINE ASSEMBLY

The engine was assembled at Aerojet in a clean area designed for hardware assembly per drawing 1206083. Assembly procedures were created and followed during the assembly process. The size of the hardware made handling difficult, sometimes requiring special lifting fixtures. A rolling assembly stand, shown in Figure 4.3.1 with the completed core assembly, was built which greatly assisted in the assembly process.

4.3.1 Cleaning

All components were cleaned to remove machining debris and oils per ATC-STD-4940, Level 1000 (1000 micron particle size). Particle size requirements are less severe than usual due to the large orifice diameters in the injector. In addition, all surfaces contacting LOX were cleaned and verified to ATC-STD-4940, Level 200K (for Hydrocarbon cleanliness).

4.3.2 Assembly

The injector assembly was assembled by placing the manifold on the assembly stand, dropping the core into it, and securing with temporary fasteners. The bolted units were then turned over, face instrumentation installed, and the leads secured to the core body. The ablative faceplate was then installed and torqued to specifications.

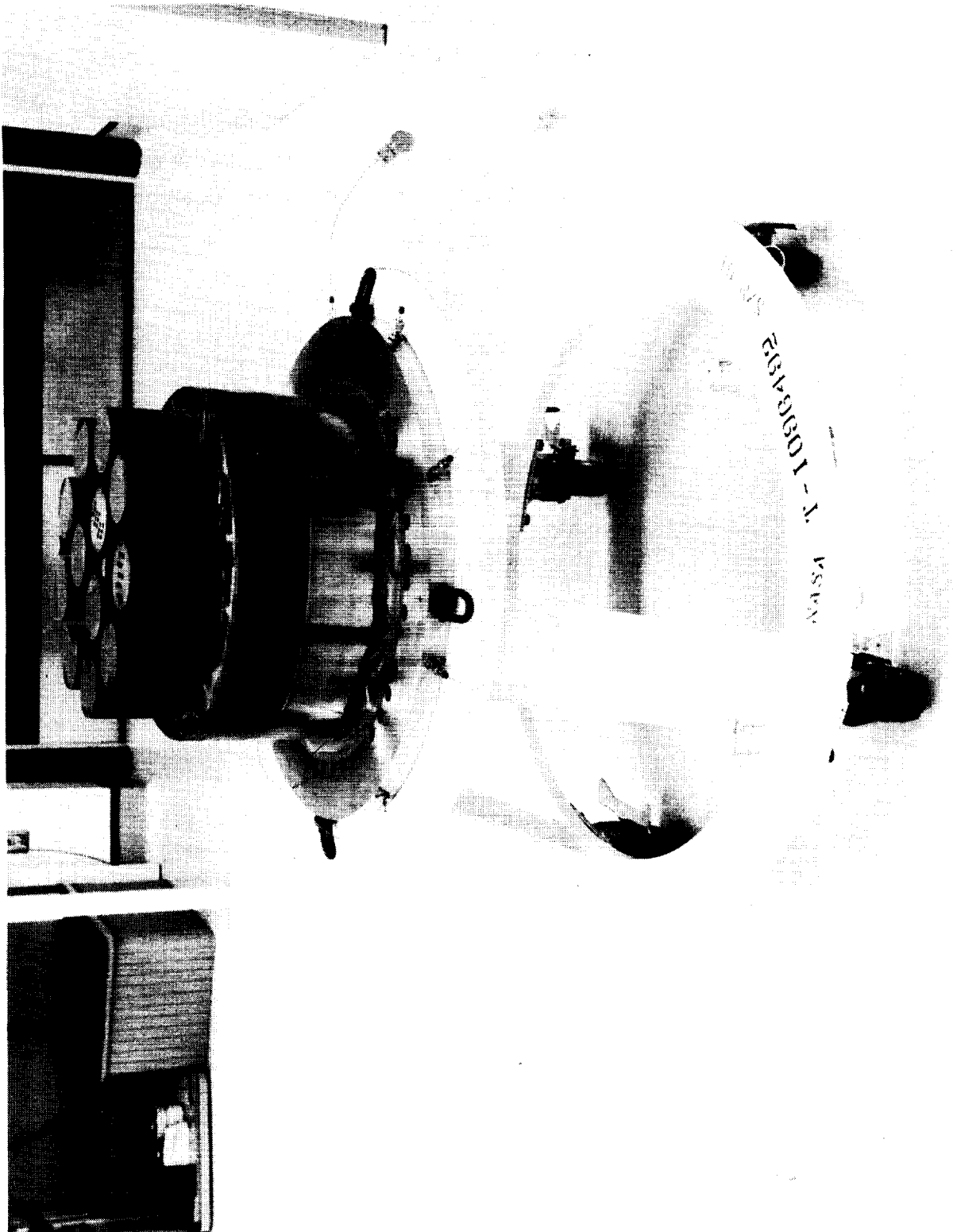


Figure 4.3.1 Rolling Stand Facilitates Assembly

ORIGINAL PAGE
BLACK AND WHITE PHOTOGRAPH

Perimeter gaps and boltholes were filled with high-temperature RTV sealant. The injector was turned over, and the LOX inlet was bolted and torqued to the manifold/core assembly to complete the injector.

The chamber was not attached to the injector until the injector had been mounted on the test stand. This was done to make handling easier and to avoid difficult propellant connections that would have to be made with the cumbersome unit. The engine components are shown in Figure 4.3.2.

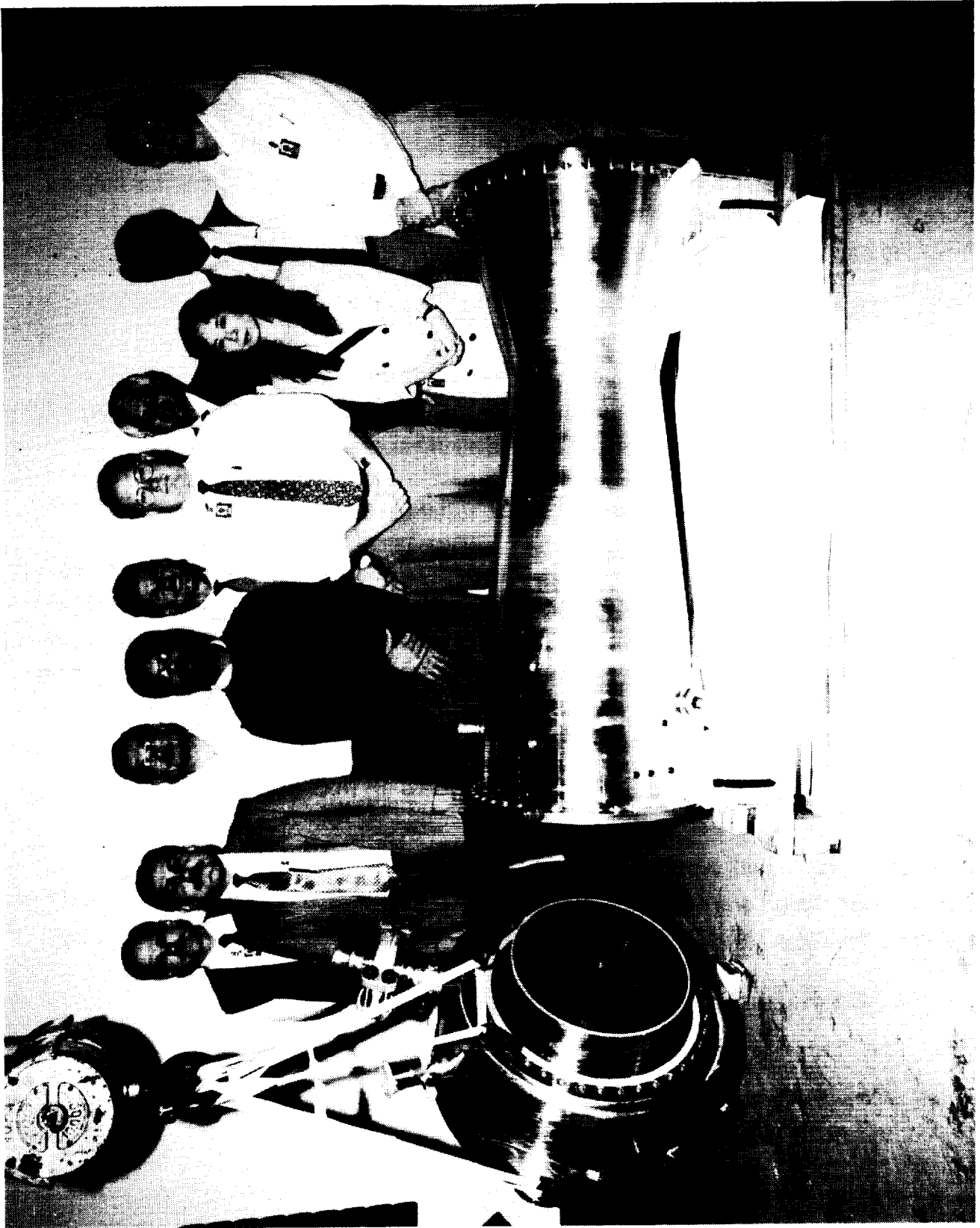


Figure 4.3.2 Completed Subscale Hardware

5.0 TEST PREDICTIONS AND RESULTS

5.1 TESTING PLAN

The test program objective was to obtain essential data for Low Cost LOX / RP-1 engine technology. Data requirements included combustion stability data, performance measurements at both on-design and off-design conditions, and thermal data for material compatibility studies. The test plan (Ref 2) organized testing into discrete blocks to ensure that specific, organized objectives were met.

5.1.1 Block I - Initial Operation (3 tests)

The first block contained three tests, one for LOX/TEA-TEB ignition and two tests for initial full Pc operation. These tests were performed to characterize start /shutdown transients and ignition performance.

5.1.2 Block II - Thermal / Performance (7 tests)

This block of testing had three purposes; verify engine operation and performance at different operating points of Pc and MR, establish the correct rate of film cooling by monitoring chamber wall temperature, and verify the ability of the combustion stability bombs to provide adequate chamber overpressure.

5.1.3 Block III - Stability (8 tests)

Block III tests were crucial tests designed to determine the baseline dynamic stability of the engine without damping devices. The acoustic cavity was blocked off with the full resonator, and the combustion perturbed with bombs shortly before programmed engine shutdown. By measuring stability of the engine without a damping device, predictions of damping requirements for subsequent tests were made.

5.1.4 Block IV - Pc and MR Mapping (6 tests)

Block IV tests were designed to measure engine performance and chamber wall temperatures with varying Pc and MR. Film coolant percentage was also varied to quantify its effectiveness.

5.1.5 Block V - Alternate Cavity (3 tests)

This block utilized an alternate cavity configuration designed from test data from Block III results. The effectiveness of the redesigned cavity was verified.

5.1.6 Block VI - Long Duration (1 test)

A long duration (≈9 seconds) test was scheduled to evaluate the durability of the injector faceplate. Wall temperatures on the steel chamber prevented this test.

5.2 TEST RESULTS

Testing was performed at Aerojets' Test Area "E" in Sacramento, CA during the period 16 October through 11 December 1991. A total of 32 tests were conducted, completing all of the planned test objectives with the exception of the long-duration test. During the 39 day testing period, approximately 17 days were consumed with hardware adjustments and configuration changes. The 22 testing days were required for the 32 tests, giving an average frequency of 1.5 tests/day. On several days, three tests were performed. This high test frequency can be credited to the following:

- Careful planning of the test matrix required the minimum hardware and test stand (propellant pressures) changes between tests.
- Redundant transducers for nearly every parameter minimized down time for instrumentation. Throughout the test program, no significant data was lost due to instrumentation malfunction.
- The diligence of the test crew in preparing the stand and readying the instrumentation minimized turn-around times.

Testing was conducted using established Aerojet policies and procedures for testing and safety. Each engine firing followed practices developed over many years of LOX/RP testing;

- A two level engine start was employed to establish proper functioning of components, valves and sensors before full thrust operation. At Level 1, approximately 30% of full chamber pressure, critical flow and pressure

"gates" must be met before the propellant valves were opened to their full open position. Additional gates were employed at Level 2 to ensure that the proper flow and pressures had been achieved.

- A combustion stability monitor (CSM) was used to detect instabilities and automatically terminate operation and minimize hardware damage. This system consisted of firing computer software which monitors a selected high-frequency pressure transducer.
- Test durations for this testing were relatively short (≈ 1 -2 seconds) due to temperature limitations of the steel chamber. However, thermal and engine performance data did reach steady-state values in this test duration.
- Axial thrust measurements were made for all tests. These provided more accurate calculations of engine performance than traditional pressure/area thrust calculations.

The first full chamber pressure (P_c) test, Test 2, ran stable and smooth for the full planned duration. This early success is very unusual. It was due to the careful pre-test calculations and transient analysis as well as the measurement of injector admittance, filling times and ignition timing by the test crew. Figure 5.2.1 is a log of tests performed and summarized results of each test.

Thermal tests in Block II were conducted with the baseline acoustic cavity configuration near the nominal operating point of 720 P_c and $MR = 2.8$. Several tests were automatically terminated by excessive chamber wall temperature in the combustion section. Fuel film cooling flow rate was increased to reduce wall temperature, but little effect was realized. Testing continued but was interrupted to replace a faceplate which sustained damage due to an assembly problem (discussed in section 5.6). Although durations in this Block were very short (0.2-0.5 seconds), thermal and bomb effectiveness data was successfully obtained.

Stability testing in Block III showed no spontaneous instabilities. Every bombed test was driven unstable, although some damped after 50-60 msec. Chamber pressures to 1030 psia and MRs to 3.7 were tested. All instabilities in this Block were in the 1T (first tangential) mode. This result confirmed the prediction that only simple

TEST OBJECTIVES (1)															RESULTS	
TEST		V	B	T	S	P	C	R	D	Pc	MR	FFC	DUR	CAV	Bomb	
										psia	core	% fuel	SS, sec	(type)	(type)	
													(2)		(3)	
APPROXIMATE DATA																
BLOCK I TESTS (Initial Operation)																
1	X									N/A	N/A	N/A	N/A	4.5"	none	smooth start transient
2	X									705	2.7	22%	0.2	4.5"	none	STABLE, good start, good performance
BLOCK II TESTS (Thermal)																
3		X	X	X	X	X	X	X	X	712	2.8	22%	0.2	4.5"	none	shutdown .2 sec--kill signal error
4	X	X	X	X	X	X	X	X	X	711	2.8	22%	0.4		none	shutdown .4 sec - high wall temp
5	X		X	X	X	X	X	X	X	696	2.4	27%	0.5		none	shutdown .5 sec - high wall temp
6	X		X	X	X	X	X	X	X	n/a	n/a	27%	0.2		6.5R	shutdown .2 sec - low Pc- faceplate damage
7	X		X	X	X	X	X	X	X	700	3.00	27%	0.5		6.5R	full duration- bombed unstable 1T-no damage
8		X	X	X	X	X	X	X	X	705	4.1	27%	0.2	V	6.5T	shutdown .2 sec- high wall temp
BLOCK III TESTS (Stability)																
9		X	X	X	X	X	X	X	X	N/A	N/A	22%	N/A	none	N/A	shutdown-fail to make POJ gate
10		X	X	X	X	X	X	X	X	480	2.4	22%	0.5	none	13R	bombed unstable-no chamber damage
11		X	X	X	X	X	X	X	X	N/A	N/A	22%	0.5	none	N/A	shutdown-failure to make ignition gate
12		X	X	X	X	X	X	X	X	504	2.7	22%	1	none	13R	stable for 1 sec-bombed unstable 1T
13		X	X	X	X	X	X	X	X	360	3.7		1	none	13R	stable for 1 sec-bombed u/s 1T
14		X	X	X	X	X	X	X	X	1030	2.2	V	1	none	none	stable for 1 sec-no bomb-some face damage
BLOCK IV TESTS (Pc , MR mapping/stability)																
15		X	X	X	X	X	X	X	X	715	2.8	22%	0.5	2"	13R	Stable. Bombed 40% Pc , damped quickly
16		X	X	X	X	X	X	X	X	716	2.3	22%	0.5		-	Stable. Bomb failed to ignite
17		X	X	X	X	X	X	X	X	735	2.3	22%	0.5		13R	Bombed unstable. 1T
18		X	X	X	X	X	X	X	X	762	4.1	22%	0.4		13R	Shutdown, wall temp. Bombed 10%, damped
19		X	X	X	X	X	X	X	X	521	2.8	22%	0.8		13R	Bombed 50%, damped quickly
20		X	X	X	X	X	X	X	X	680	2.5	16%	0.3		13R	Shutdown, wall temp. Bombed unstable 1T
21		X	X	X	X	X	X	X	X	737	2.1	16%	0.5		13T	Good thermal data. Bombed,some recovery
22		X	X	X	X	X	X	X	X	740	2.1	16%	0.7		13R	Shutdown,wall temp ..Bombed unstable 1T
23		X	X	X	X	X	X	X	X	725	3.3	16%	0.3		13R	Shutdown,wall temp...concludes 16% tests
24		X	X	X	X	X	X	X	X	728	2.9	27%	0.8		13R	Full duration..bombed, STABLE
25		X	X	X	X	X	X	X	X	730	4.1	27%	0.4		13R	Shutdown, Wall temp..
26		X	X	X	X	X	X	X	X	725	3.7	27%	0.8	V	13R	Full duration..bombed, STABLE..
27		X	X	X	X	X	X	X	X	735	2.9	22%	0.8	bitune	13R	Full duration, bombed 40%, DAMPED
28		X	X	X	X	X	X	X	X	735	2.2	22%	0.8		13R	Full duration, bombed 40%, DAMPED
29		X	X	X	X	X	X	X	X	729	3.9	22%	0.3		13R	Shutdown, wall temp...bombed,DAMPED
30		X	X	X	X	X	X	X	X	1026	2.9	22%	0.2		13R	Shutdown, wall temp...bombed, marginal damping
31		X	X	X	X	X	X	X	X	990	2.2	22%	0.8		13R	Full duration, bombed,DAMPED, 207K lbs thrust
32		X	X	X	X	X	X	X	X	955	2.8	22%	1	V	13R	Full duration, Bomb malfunction,,204,000 lbs thrust
Testing concluded -- ALL OBJECTIVES MET !!																
Notes: (1)	See table XV (Test Plan) for test objectives code-- X is major objective, √ is minor objective															
(2)	Duration is the minimum for SS measurements (3) Grain size/port type (R=radial, T= tangential)															

Figure 5.2.1 Test Program Met All Test Objectives

acoustic damping devices would be required for the full scale design. Some face damage was observed during the high P_c test in the form of copper loss on some of the modules. It was decided to terminate stability testing after this test and proceed with the next Block.

Performance testing in Block IV operated the engine over a wide range of conditions. A modified acoustic cavity, one with a 2 inch depth, was designed after analyzing results from Block I tests. This cavity improved the stability margin of the chamber. Many tests around the nominal operating point were now dynamically (bombed) stable. This Block of tests provided a wealth of performance and thermal data. After Test 26, all performance and thermal objectives had been met, but some instabilities were still occurring. A bituned acoustic cavity, discussed in detail in section 5.4.2, was installed and dramatically improved damping around the nominal operating point. Several tests were conducted and, with bomb overpressure of 40% P_c , the combustion instability was quickly damped. During this testing, thrust levels over 200,000 lbs were achieved.

The hardware was exceptionally durable, and was still performing well at the conclusion of testing. This result is commendable for a new design employing a unique injector configuration. The detailed results of the test program will be reported in the following sections:

- Performance Predictions and Results
- Stability Predictions and Results
- Thermal Predictions and Results
- Hardware Durability

5.3 PERFORMANCE PREDICTIONS AND RESULTS

5.3.1 Hydraulic Predictions and Results

Hydraulic predictions were made during the design phase to determine test stand hydraulic/control parameters and instrumentation requirements. Hydraulic analyses for the core and FFC circuits were performed by the calculation of individual losses for each flow branch. Accurate determination of injector hydraulics is essential for start transient predictions. Predicted values for the injector admittance (similar to the inverse of the hydraulic resistance) are shown below.

<u>Circuit</u>	<u>Kw</u>
Fuel	9.8 lbm-in./sec- $\sqrt{\text{lbf}}$
Fuel Film Cooling (FFC)	1.9 lbm-in./sec- $\sqrt{\text{lbf}}$
Oxidizer	20.6 lbm-in./sec- $\sqrt{\text{lbf}}$

5.3.1.1 Hydraulic Cold Flow

The subscale injector was cold flowed prior to hot fire to confirm the designed injector pressure drops and to establish balance requirements for the fuel film coolant circuit. The oxidizer circuit and the fuel core circuit of the injector were flowed using room temperature water flowing to 1 atmosphere back pressure. Supply pressures were varied over a range from 20 to 65 psid to characterize hydraulic admittance (Kw). Resulting Kw's are shown plotted versus the circuit pressure drop for both the oxidizer and fuel in Figure 5.3.1. Predicted Kw values were within 4% of cold flow measured values. The injector cold flow spray pattern was also checked visually and was found to have no visual flow anomalies.

5.3.2 Combustion Predictions and Results

The ROCCID computer program, Ref 3, was used to predict the combustion characteristics for the injector. The analysis assumed that 25% of the core flow mixed with the 16% fuel film coolant periphery flow, which was the nominal predicted film coolant required. A mixing efficiency parameter value of 0.85 Em was used for both the core and barrier streams, resulting in a four-streamtube model. The atomization length calculated by the model was reduced based on hot-fire test results from a previous LOX/RP program (Ref 1).

The predicted static combustion pressure profile is shown in Figure 5.3.2 along with a measured static pressure profile from hot fire Test 24. Close agreement between predictions and test data, including the point at which the static pressure initially drops (indicating the start of combustion) confirms the assumption of short atomization distance.

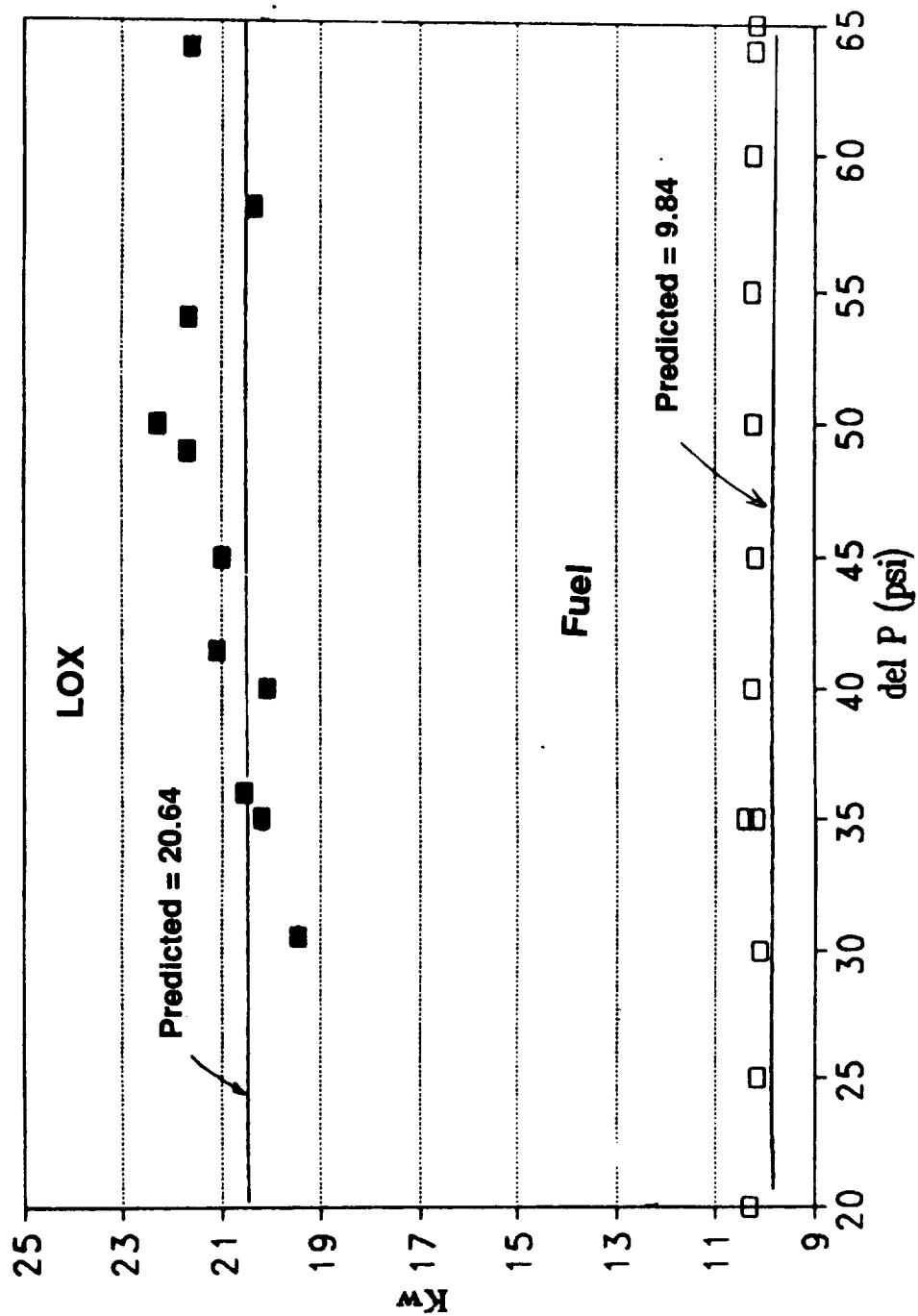


Figure 5.3.1 Measured Injector Admittance Closely Matches Predicted Values

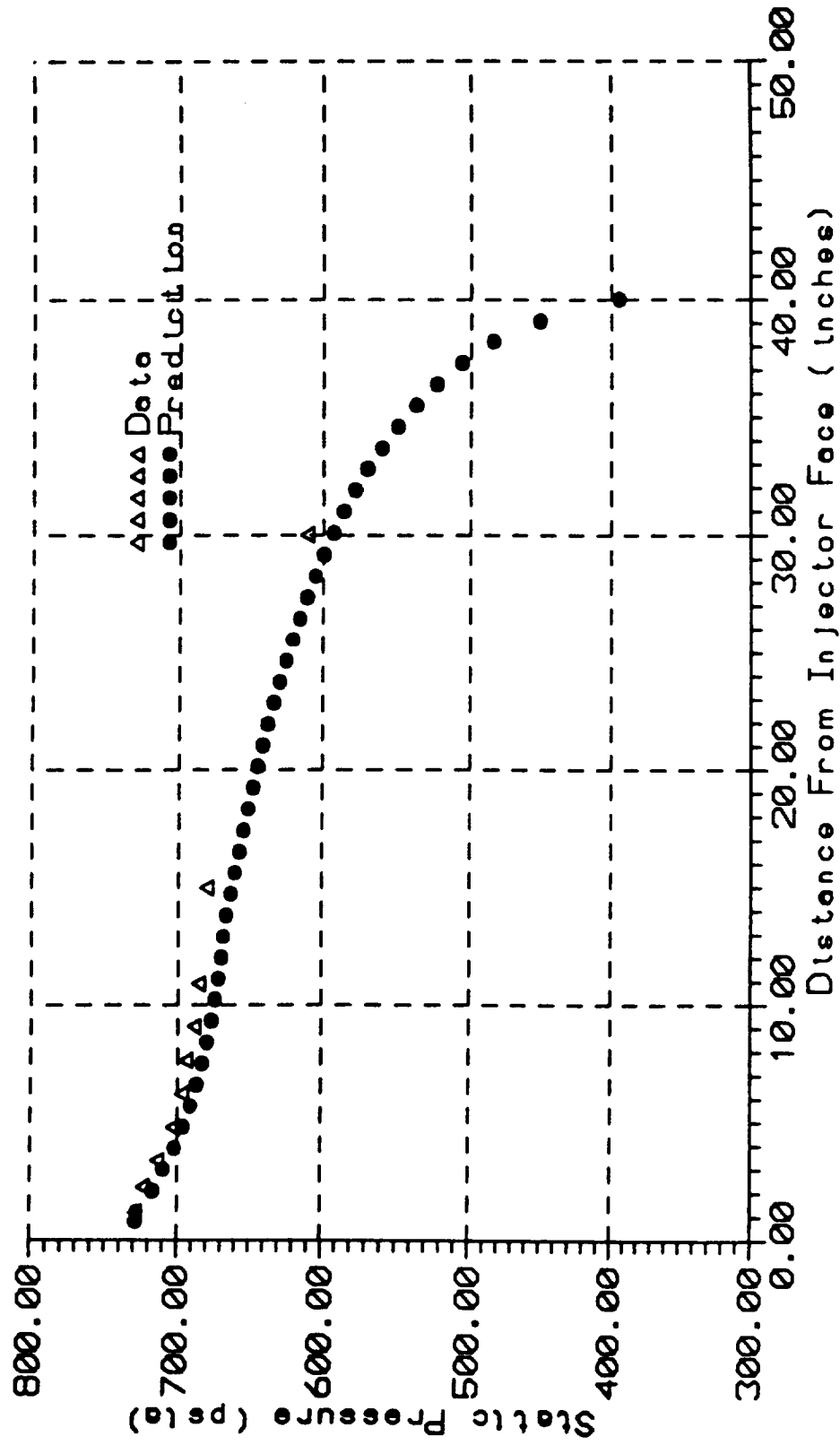


Figure 5.3.2 Combustion Pressure Profile Matches Predictions

Predicted characteristic velocity, which is a measure of combustion efficiency, versus both fuel film coolant percentage and core mixture ratio is shown in Figure 5.3.3. Note that the highest combustion performance occurs at a MR of about 2.4 to 2.5. This prediction was confirmed by test data which also indicated highest performance at an MR of 2.5, which will be discussed in the performance section.

Close correlation between the predicted combustion response and measured response validates the analytical tools used for design of the injector.

5.3.3 Performance Predictions and Results

Injector efficiencies were predicted using the ROCCID program and are shown plotted versus the overall injector mixture ratio in Figure 5.3.4. The C^* and energy release efficiency of an injector is a combination of vaporization and mixing efficiencies as shown. The corresponding predicted delivered specific impulse is also shown versus overall injector mixture ratio.

5.3.3.1 Performance Results Summary

Performance data was obtained for most of the 32 engine firings. Three fuel film cooling rates were tested during hot fire; 15%, 22% and 27% of core fuel flow. Chamber pressures fired fell into three distinct ranges of low, nominal and high. The low range covered 350 to 500 psia, the nominal from 696 to 743 psia, and the high range from 954 to 1033. These chamber pressure values are based on the Pc-3 measurement which was located immediately downstream of the resonator cavity lip. Figure 5.3.5 summarizes the performance data for the twenty-two hot fire tests in which test data is reported. Remaining tests contained either transient or redundant data and were not used for data analysis.

Overall injector efficiency, including the loss associated with 22% FFC, was approximately 91% for the nominal chamber pressure of 720 psia, and 94% for the high (~1000 psia) chamber pressure tests at an overall mixture ratio of 2.2. Injector core efficiencies, backed out from these overall efficiencies with a calculated FFC loss, are 97% for the nominal Pc and 99+% for the high Pc. Overall injector efficiency for the nominal chamber pressure, low FFC (~15%) tests, for which there was valid data only at an overall mixture ratio of ~1.75, performed at the same level as the high Pc tests at this MR, was about 95-97%. This test at low FFC is representative of

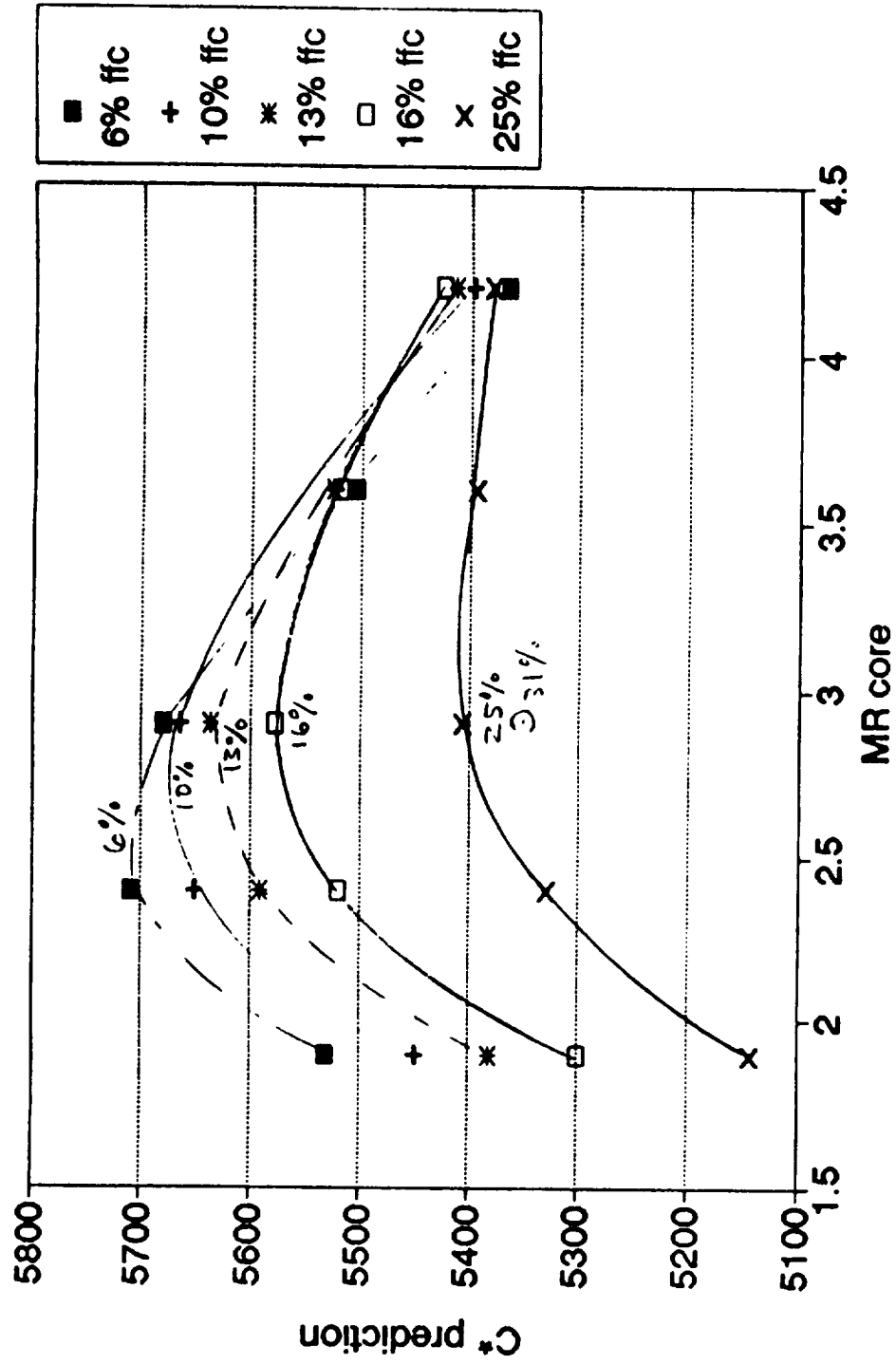


Figure 5.3.3 Combustion Efficiency is Greatest Around Core MR = 2.5

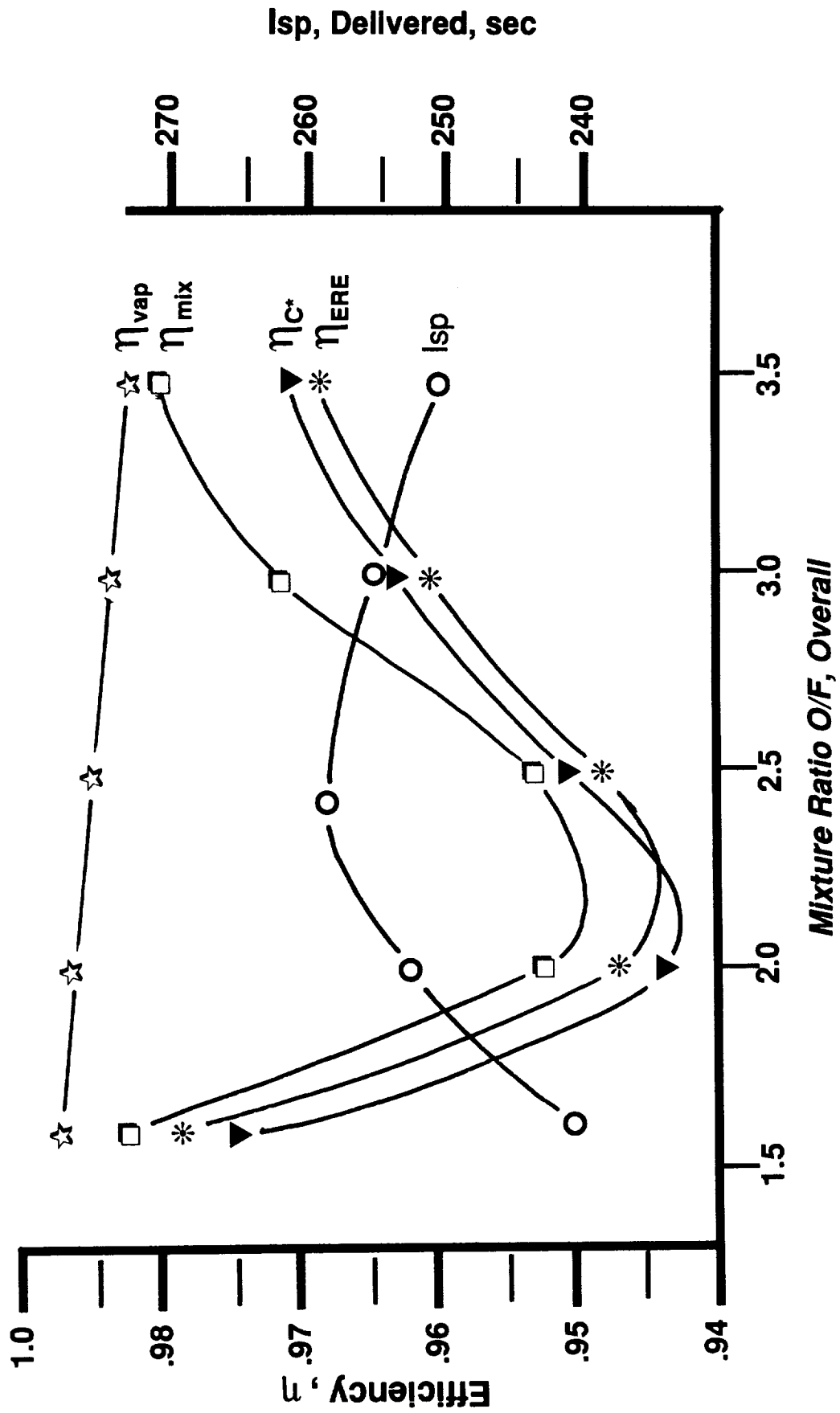


Figure 5.3.4 Injector Efficiencies Combine to Give Greatest I_{sp} at about $MR = 2.4$

Pressure Fed Technology Program

Test No.	Chamber Pressure (psia)	MR overall	FFC %	MR core	Isp vac measured (sec)	Cstar measured (ft/sec)	Isp PI (MRoa) (sec)	Isp PI (w/FFC) (sec)	Efficiency Injector	Efficiency FFC	Efficiency core	Fuel Inj delta P (psid)	LOX Inj delta P (psid)
2	702	2.015	21.2	2.56	261.1	5702	278.2	264.3	0.938	0.950	0.988	211	292
3	714	2.144	21.7	2.74	256.0	5637	280.7	263.5	0.912	0.939	0.972	219	307
4	721	2.178	22.0	2.79	256.0	5700	281.1	263.1	0.911	0.936	0.973	214	328
5	696	1.805	26.0	2.44	254.4	5609	271.0	261.8	0.939	0.966	0.972	186	279
12	503	2.119	21.5	2.70	254.8	5601	280.3	263.8	0.909	0.941	0.966	115	155
13	354	2.809	21.2	3.57	249.4	5500	279.0	261.8	0.894	0.940	0.951	45	97
14	1033	1.741	22.0	2.23	257.6	5588	267.9	262.6	0.962	0.980	0.981	553	574
15	717	2.150	21.8	2.75	256.0	5609	280.8	263.4	0.912	0.938	0.972	213	307
16	733	1.606	21.4	2.04	253.3	5589	260.5	260.0	0.972	0.998	0.974	304	272
17	738	1.688	21.8	2.16	253.3	5580	265.4	261.8	0.954	0.986	0.968	294	286
18	715	2.866	21.7	3.66	250.6	5508	278.2	261.2	0.901	0.940	0.958	152	380
19	498	2.109	21.7	2.69	254.1	5576	280.1	263.7	0.907	0.942	0.964	113	151
21	739	1.743	15.1	2.05	257.5	5727	268.0	263.3	0.961	0.983	0.978	418	282
22	743	1.763	15.2	2.08	258.5	5751	269.0	263.8	0.961	0.981	0.980	415	286
24	729	2.071	26.4	2.81	253.3	5600	279.4	260.6	0.906	0.933	0.965	189	326
25	730	2.896	25.9	3.91	247.3	5530	277.8	256.3	0.890	0.923	0.972	114	400
26	726	2.663	26.7	3.63	249.2	5530	280.7	255.3	0.888	0.910	0.976	127	384
27	743	2.288	21.8	2.93	257.2	5690	282.0	262.7	0.912	0.932	0.979	270	329
28	734	1.668	21.3	2.12	251.3	5591	264.4	261.4	0.951	0.989	0.961	351	283
30	1032	2.171	21.9	2.78	265.3	5835	281.0	263.2	0.944	0.937	1.008	505	649
31	1008	1.653	22.3	2.13	258.3	5698	263.5	261.1	0.980	0.991	0.989	652	523
32	954	2.115	22.5	2.73	261.7	5536	280.2	263.1	0.934	0.939	0.995	531	632

Figure 5.3.5 Performance Testing Summary

the fullscale engine, which should require only 10-13% FFC due to its higher temperature ablative liner and smaller chamber surface area-to-volume ratio.

NOTE: Throughout the test program, a discrepancy in the redundant flowmeters for both the fuel and oxidizer circuits required that corrections be made in performance data. In all cases where a discrepancy occurred, the flow measurement resulting in a lower performance value was used. Consequently, performance values presented in this report may be slightly lower than would be expected in operation.

5.3.3.2 Performance Results Discussion

Specific Impulse. The measured specific impulse, I_{sp} , corrected to vacuum conditions, is shown plotted versus mixture ratio for the nominal (~700 psia) chamber pressure tests with the three different percentages of fuel film coolant in Figure 5.3.6, and for a constant FFC of 22% at three different chamber pressures in Figure 5.3.7. Both figures include a curve of the theoretical "perfect injector" I_{sp} with zero percent FFC and a curve of the theoretical "perfect injector" I_{sp} with a calculated fuel film coolant loss. These curves have been included to show that the injector efficiency can be calculated from the measured data using these theoretical values. These theoretical curves include the nozzle losses for divergence, kinetics and boundary layer, but assume 100% propellant vaporization and a uniform mixture ratio profile across the injector face, i.e., perfect mixing. Overall injector efficiency can be determined by dividing the measured I_{sp} by the theoretical "perfect injector" I_{sp} . The curve which includes a fuel film coolant loss was determined by estimating how much of the core gas mixes with the periphery fuel film coolant to create a barrier stream tube and then mass weighting the core and barrier I_{sp} 's. An injector core efficiency can be determined by dividing measured I_{sp} by this theoretical "perfect injector" with FFC loss. It should be remembered, however that the accuracy of this core efficiency is dependent on the accuracy of the FFC loss that was calculated, and there is some uncertainty in that number.

Fuel Film Coolant Performance Loss. Calculation of the fuel film coolant loss is dependent on determining how much of the core flow mixes with the fuel film coolant. In order to estimate the percentage of the core that mixes with, or becomes entrained in the periphery fuel film coolant, adiabatic wall temperature was

Pressure Fed Technology Program

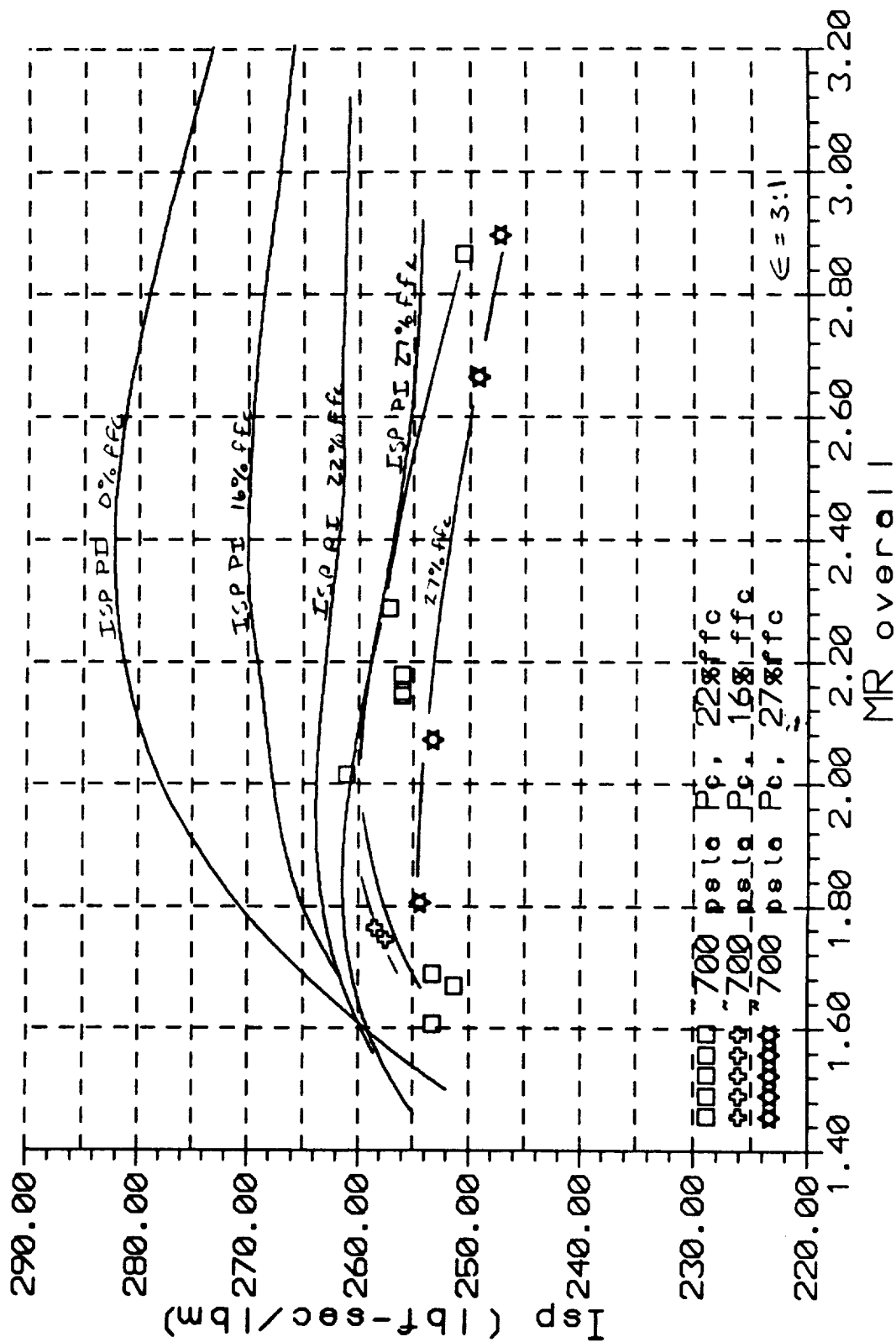


Figure 5.3.6 Specific Impulse Varies with Percent FFC

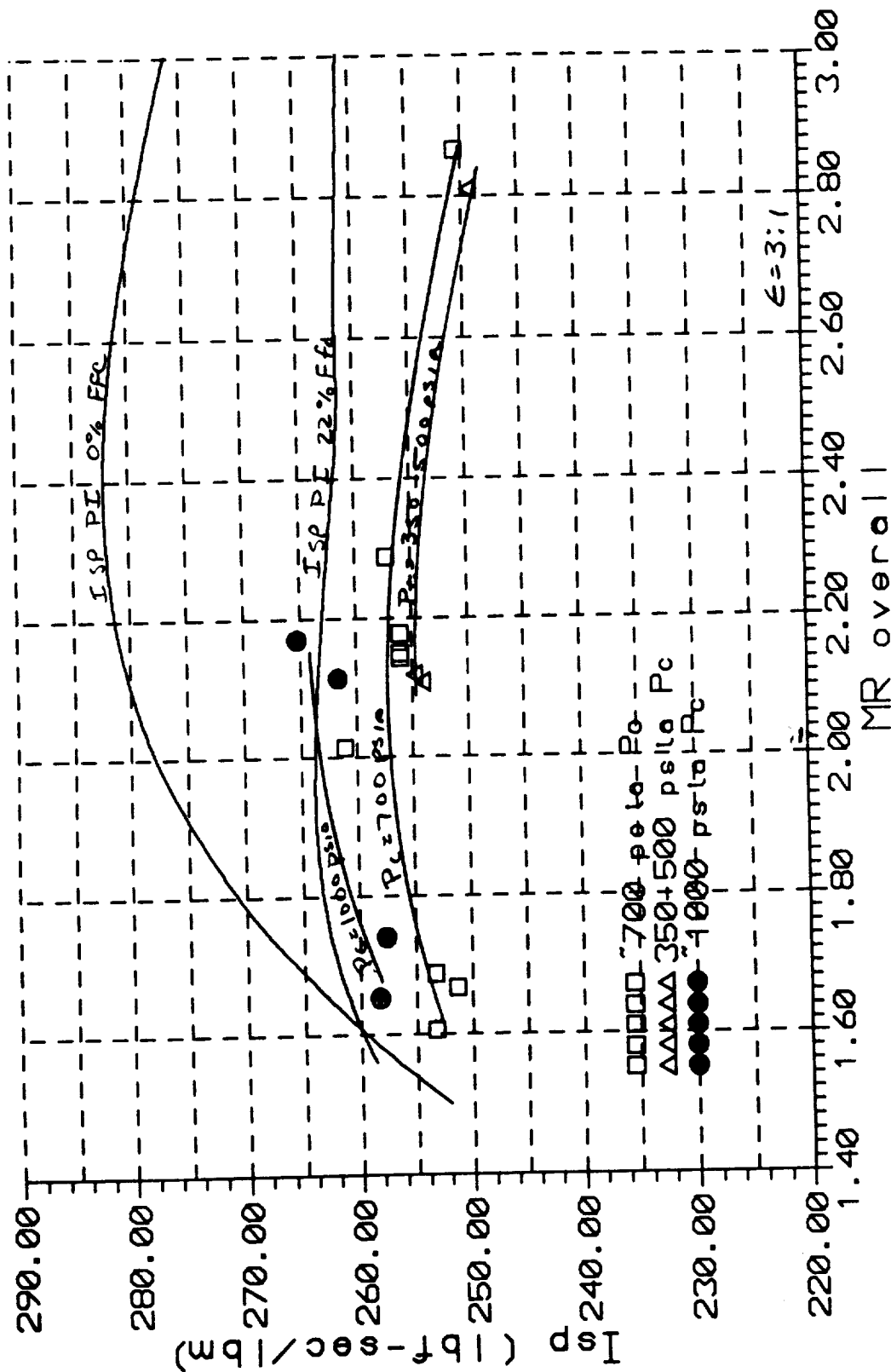


Figure 5.3.7 Specific Impulse Varies with P_c

obtained from the thermal data for two nominal mixture ratio Tests 24 and 27. Test 24 was run with 27% FFC and Test 27 was run with 22% FFC. A barrier mixture ratio was determined for each of these tests that would give a gas temperature equal to the adiabatic wall temperature. From this barrier mixture ratio and the amount of fuel film coolant injected, the percentage of the core that would need to mix with the FFC to obtain that mixture ratio was calculated. Core entrainment fractions calculated from these tests were 16.6% for Test 24 and 18.5% for Test 27. Consequently, an approximate value of 17.5% was decided upon for core entrainment percentage. This value was used for all of the different FFC amounts. A plot of the fuel film coolant efficiency versus the overall injector mixture ratio, for the three approximate FFC percentages at which the tests were run, is shown in Figure 5.3.8.

Injector Efficiency Based on Isp. Overall injector efficiency, including both core and periphery film coolant losses, was calculated for all of the performance tests and is also presented on Figure 5.3.5. This injector efficiency is shown plotted versus the overall injector mixture ratio on Figure 5.3.9. Overall injector efficiency decreases with increasing mixture ratio, similar to the calculated fuel film coolant efficiency.

The high chamber pressure tests (~1000 psia P_c) exhibited a higher overall injector efficiency than the nominal and low pressure tests. There was also an apparent difference in injector efficiency between the different fuel film coolant tests. The two low fuel film coolant (~15% FFC) tests had an overall injector efficiency of the same order as the high chamber pressure tests, which were run at ~22% FFC. Injector efficiencies for the 27% FFC tests were approximately 1% lower than that for the 22% FFC tests at overall mixture ratios greater than about 2.2. These trends do not exactly match the predicted trend in Figure 5.3.8, however they do validate the general trends for predicted FFC efficiency. At an overall MR of 2.2 and 22% FFC, overall injector efficiency was approximately 91% for the nominal chamber pressure tests and 94% for the 1000 psia chamber pressure tests.

Fuel film coolant efficiency was calculated for each test (based on the %FFC that was measured for that test) and is tabulated in Figure 5.3.5. These fuel film coolant efficiencies were used to calculate injector core efficiency, also tabulated in the performance summary table. Calculated core efficiencies are shown plotted versus core mixture ratio in Figure 5.3-10. Injector core efficiency is flattened

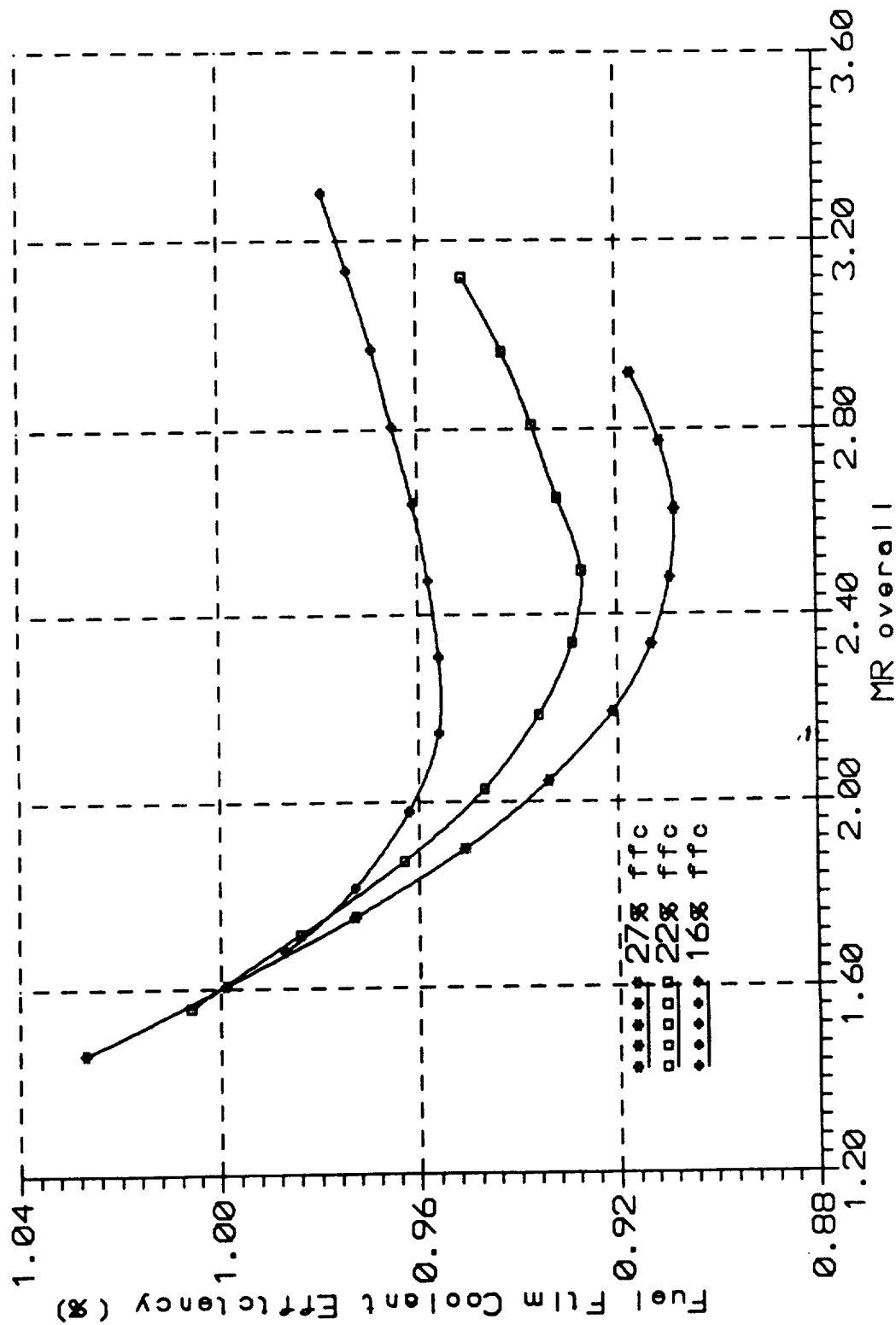


Figure 5.3.8 Fuel Film Cooling (FFC) Efficiency Changes with MR

Pressure Fed Technology Program

Propulsion Division

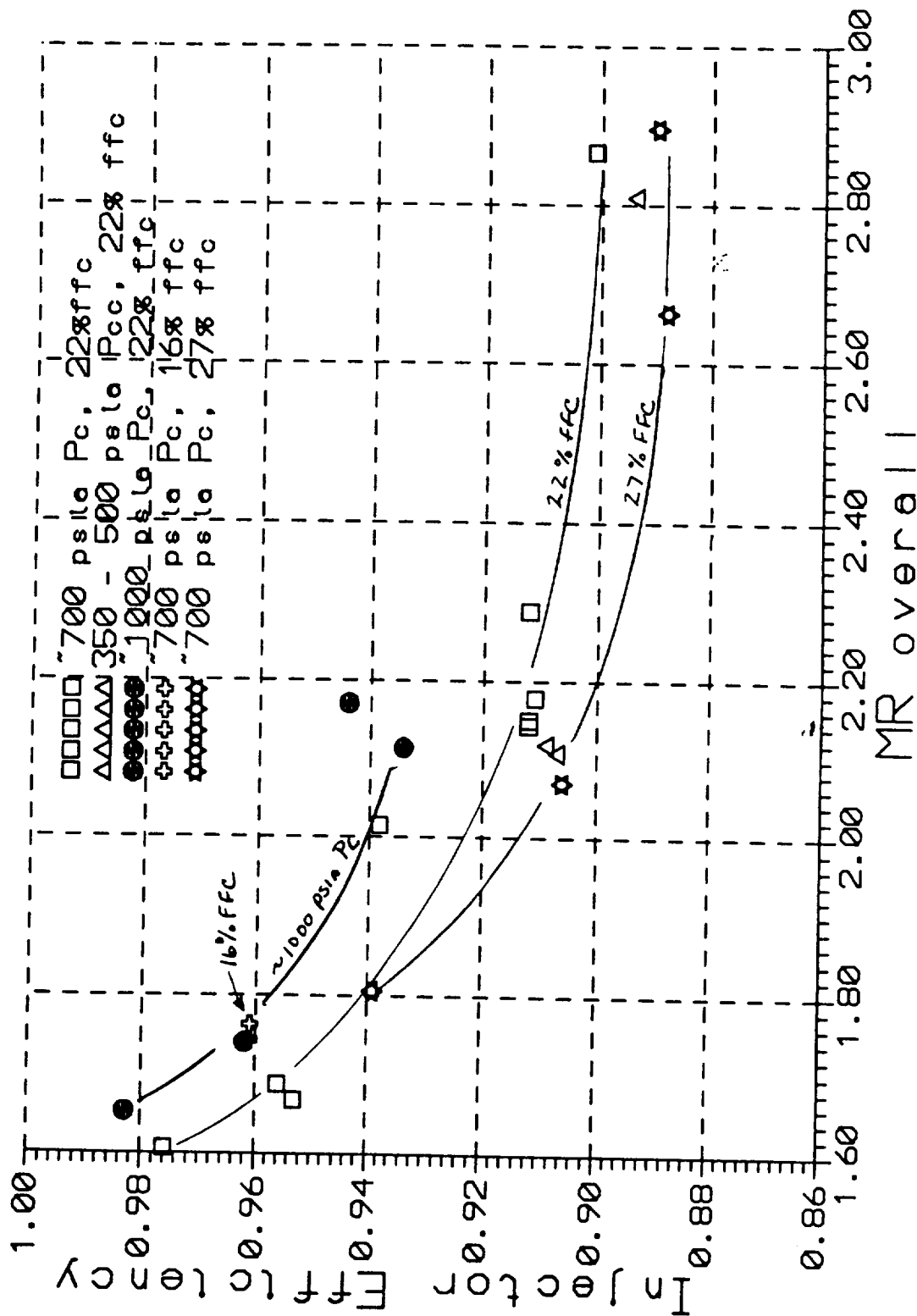


Figure 5.3.9 Injector Efficiency Decreases with MR Increases

Pressure Fed Technology Program

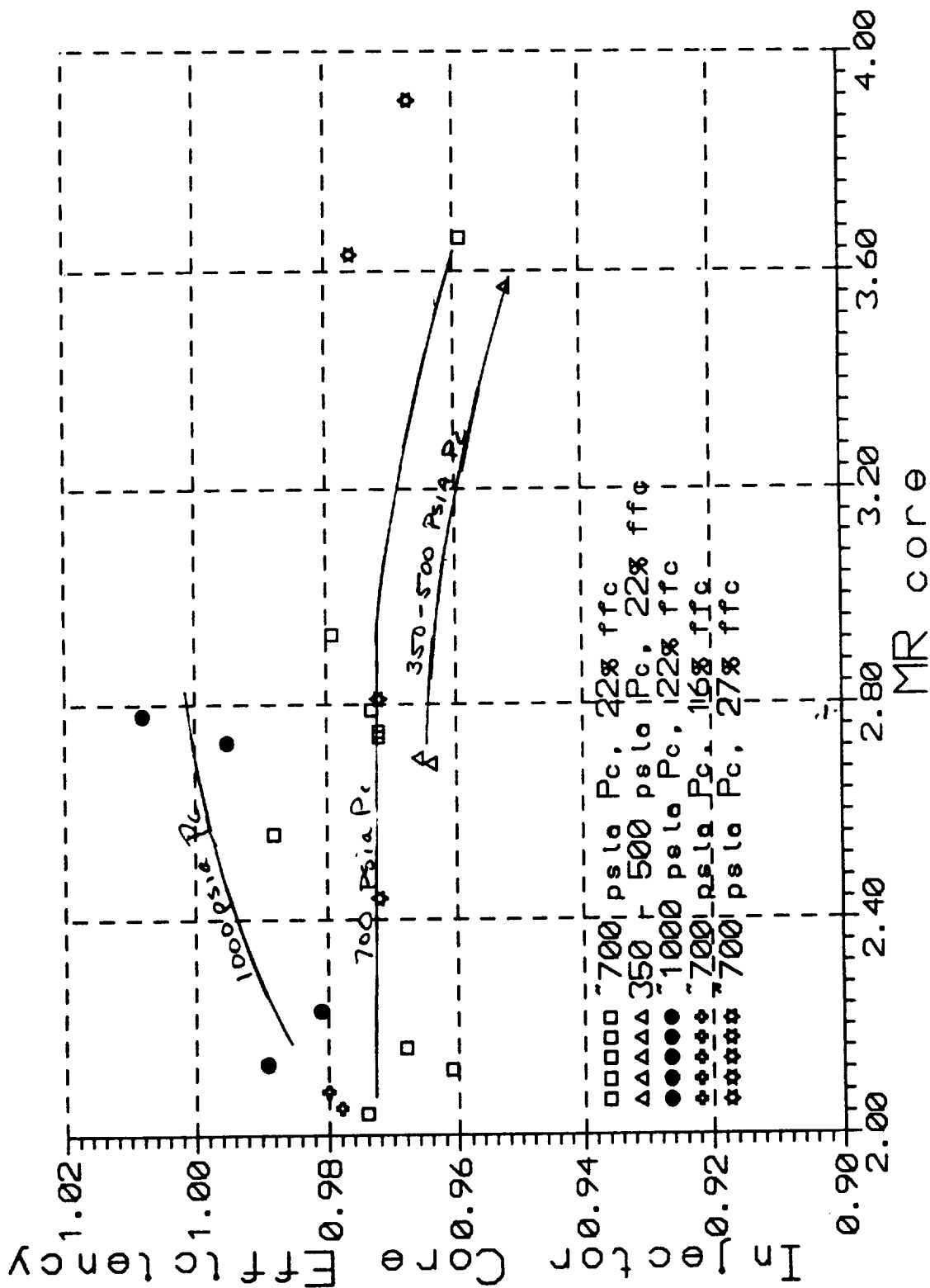


Figure 5.3.10 Core Efficiency Changes as MR Increases

out by removal of the fuel film coolant efficiency. From core mixture ratios from 2.0 to 2.9, core efficiency remains constant at approximately 97% within the data scatter of $\pm 1\%$. The few data points at around 3.6 core MR suggest that efficiency may be starting to tail off. At a core MR of 2.8, the injector core efficiency was approximately 97% for the nominal P_c tests and approximately 99+% for the 1000 psia P_c tests. The unrealistically high core efficiency ($\geq 100\%$) for one of the high P_c tests could be a result of inaccuracies in accounting for other losses. Nominal pressure nozzle losses were used for the analysis of the high pressure test data. There could be slight reductions in boundary layer and kinetics losses at the higher P_c . However, these losses are small at the nominal chamber pressure (almost negligible kinetics loss and a 1.4 lbf-sec/lbm boundary layer loss) so this error would be on the order of tenths of a percent. The most likely explanation for the error is the FFC loss, where an over accounting of this loss would artificially raise the core efficiency. This bias on core efficiency would be applicable to all the tests and so would not alter the apparent relationship between injector efficiency and chamber pressure.

Injector core efficiencies for all performance tests and also for just the tests with core MR's of between 2.7 and 2.8 are plotted versus chamber pressure, and fuel and oxidizer injector pressure drops in Figures 5.3-11. These plots indicate that there is a correlation of injector core efficiency with either chamber pressure or injector pressure drop. The slight drop in efficiency with increasing mixture ratio (higher oxidizer pressure drop and lower fuel pressure drop) points to fuel injector pressure drop as the source of the increased efficiency. Analytically, this is also more supportable since the fuel vaporization is the limiting factor on the vaporization efficiency and increased pressure drop will reduce drop size, enhancing vaporization. This suggests that injector efficiency could be improved at the nominal chamber pressure by increasing fuel injection pressure drop. The impact of this change on the stability characteristics of the injector would also need to be investigated.

5.4 STABILITY PREDICTIONS AND RESULTS

5.4.1 Stability Predictions

Combustion stability characteristics were predicted prior to testing using the ROCCID computer code (Ref. 3). Some of the input parameters were

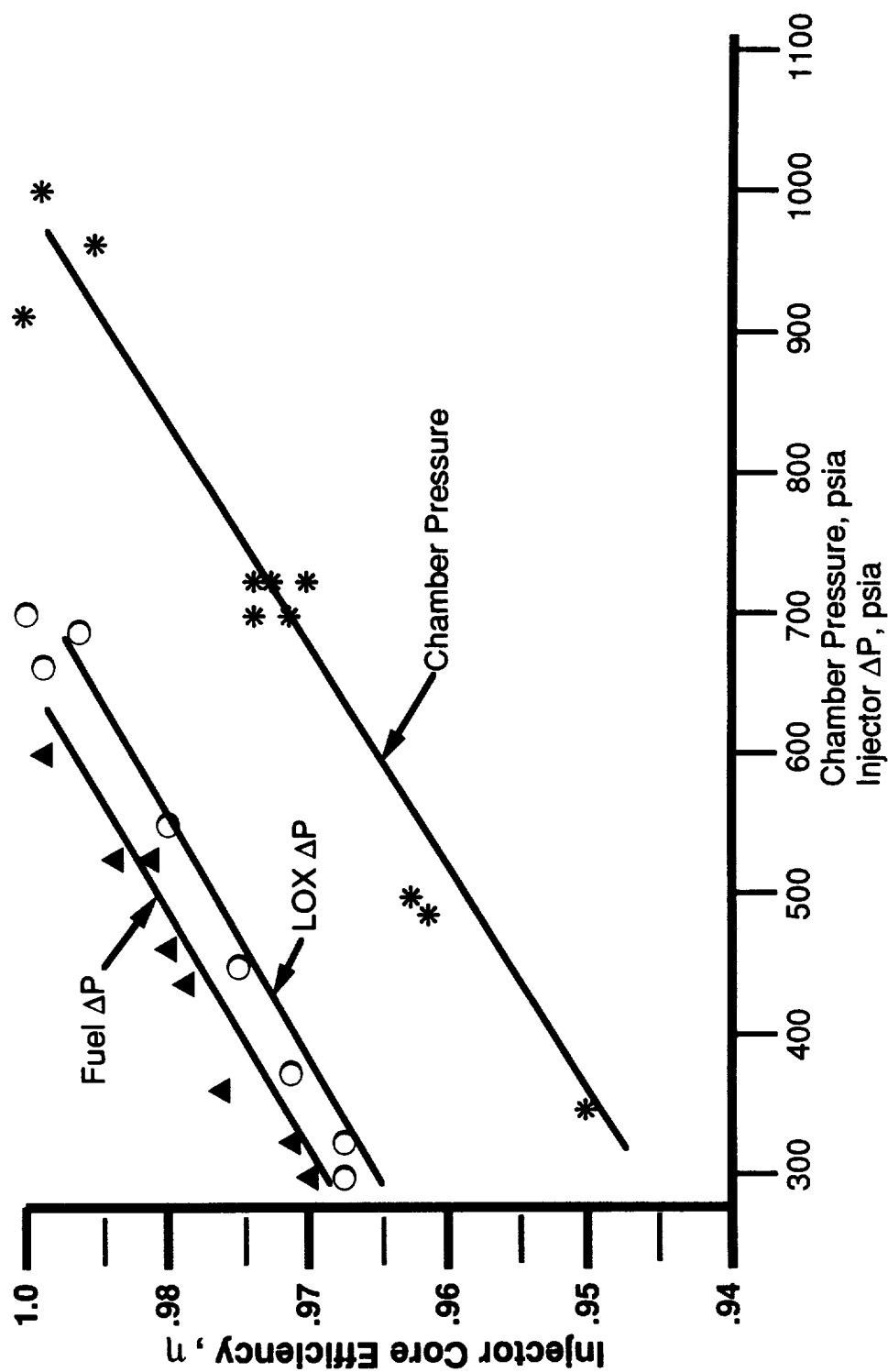


Figure 5.3.11 Injector Efficiency Increases with Chamber Pressure and Injector ΔP

anchored using existing F-1 and LOX/HC Injector Characterization Program (Ref. 1) data base.

5.4.1.1 Chug Prediction

Calculations indicated that marginal chug chamber pressure would be approximately 361 psia and the chug frequency is approximately 67 Hz. Test results showed that the engine was chug stable at all operating conditions tested. Chamber pressures in all tests except Test 13, where the chamber pressure was measured to be approximately 354 psia, were above the predicted marginal pressure. Some tests briefly encountered chug instabilities at a frequency of approximately 80 Hz during early parts of the start-up transient where the chamber pressures were extremely low and the injector cavities may not have been completely filled. The instabilities disappeared quickly as mean chamber pressures rose to steady-state values.

5.4.1.2 High Frequency Stability

High frequency (acoustic) stability characteristics were predicted only for the chamber configuration without acoustic cavities. No predictions were made for chamber with any of the cavity configurations prior to the testing because it is difficult to predict cavity gas temperature and related sound speed with reasonable accuracy.

The engine configuration without acoustic cavities was predicted to be stable at a chamber pressure of 500 psia and an overall mixture ratio of 2.45. Test results, however, showed that the engine configuration was dynamically unstable at chamber pressures as low as 354 psia. The configuration without acoustic cavities was predicted to be spontaneously unstable at approximately the nominal operating point. Although this configuration was not tested at the nominal operating point, operation at high P_c during Test 14 was stable without perturbation. Therefore, the nominal operating point is expected to be stable without perturbation. Test 7, with a 4-inch monotuned cavity, was demonstrated to be dynamically unstable near the nominal operating point. The configuration without acoustic cavities was predicted to be dynamically unstable (triggered by combustion perturbation bomb) in both 1T and 2T modes at high chamber pressure, approximately 1000 psia, and in the mixture ratio range between 1.5 and 2.5. Although chamber pressure and mixture ratio in test 14 corresponded to the operating conditions for which predictions were made, comparison

between prediction and test result could not be made because combustion perturbation bomb was not used in this test. Tests using chamber configuration with bituned cavities (Tests 30 and 31) showed that operation at high chamber pressures could indeed be driven unstable with bombs at not only the 1T but also higher modes. Since the chamber with acoustic cavities was tested to be dynamically unstable at higher chamber pressure, it can be argued that the chamber without acoustic cavities would be dynamically unstable at high chamber pressure.

The results shown in Figure 5.4.1 confirm that the a priori prediction of rocket engine stability remains very difficult. The ROCCID program is the latest stability model and utilizes correlations from several different sources to attempt a stability solution. Much work is still required in this area to develop reliable stability models capable of stability predictions.

5.4.2 Stability Results

Stability testing was performed to determine injector combustion characteristics for a range of chamber pressures and mixture ratios. Combustion stability was the most important goal for this injector. Engine system stability margin is essential to flight reliability. Stability tests were conducted by examining chamber acoustic response under a variety of damping conditions. The following chart summarizes the configurations that were used.

<u>Test Series</u>	<u>Test Numbers</u>	<u>Acoustic Cavity Configuration</u>
1	2 thru 8	monotune, 4 in. depth
2	9 thru 14	no cavity
3	15 thru 26	monotune, 2 in. depth
4	27 thru 32	bitune, 1.82/2.76 in. depth

A summary of the combustion stability test results is provided in Figure 5.4.2. Tests for checking out engine operation (Test 1) and aborted tests (Tests 9 and 11) were not included in the table. The table lists test number, oxygen and RP-1 manifold pressures, chamber pressure, core and overall mixture ratios, and oxygen and RP-1 injection pressure drops. In addition, cavity configuration, combustion perturbation bomb size, bomb over-pressure, amplitude and frequency of chamber pressure oscillation, bomb damp time, and the Kistler transducer number from which presented stability

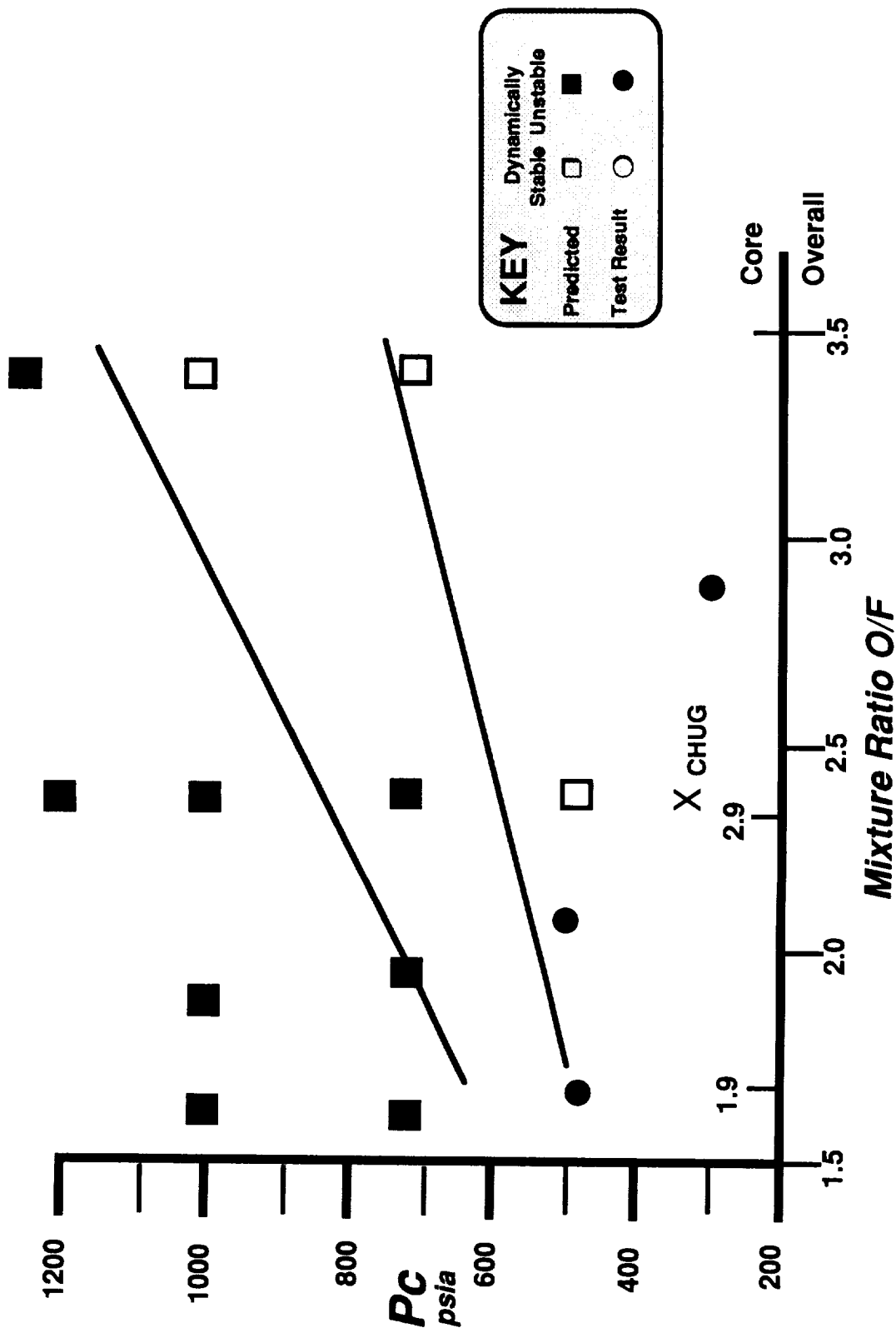


Figure 5.4.1 Stability Predictions for Chamber with No Cavities

**Test Number
Date**

2	3	4	5	6	7	8	10	12	13
10/16/91	10/17/91	10/17/91	10/21/91	10/21/91	10/30/91	10/31/91	11/07/91	11/08/91	11/14/91

OPERATING CONDITIONS

Oxygen Manifold Pressure (psia)	994	1021	1049	975	1017	1002	1087	633	659	451
SP-1 Manifold Pressure (psia)	912	933	935	882	917	864	809	605	619	398
Chamber Pressure, PC3 (psia)	702	714	721	696	619	702	705	481	503	354
Mixture Ratio - Overall	2.02	2.12	2.13	1.81	1.86	1.88	2.56	1.54	2.12	2.80
Mixture Ratio - Core	2.56	2.71	2.72	2.65	2.53	2.54	3.42	1.95	2.70	3.56
Oxygen Injection Pressure Drop (psid)	292	307	328	279	398	300	383	152	155	97
SP-1 Injection Pressure Drop (psid)	211	219	214	186	298	162	104	124	115	45

STABILITY DATA

Cavity Tune No. of Each Type	Monotone	Monotone	Monotone	Monotone	Monotone	Monotone	Monotone	No Cavities	No Cavities	No Cavities
Cavity Depth (in)	4.52	4.52	4.52	4.52	4.52	4.52	4.52	1	1	1
Cavity Width (in)	0.75	0.75	0.75	0.75	0.75	0.75	0.75	n/a	n/a	n/a
Bomb Size (grains 80X)	0.00	0.00	0.00	0.00	0.00	0.00	0.00	n/a	n/a	n/a
Bomb Direction (Radial or Tangential)	n/a	n/a	n/a	n/a	Radial	Radial	Tangential	Radial	Radial	Radial
Bomb Overpressure (psid)	n/a	n/a	n/a	n/a	102	280	0	280	230	160
Kistler No.	all	all	all	all	1	1	all	3	1	3
Stable or Unstable	Stable	Stable	Stable	Stable	Stable	Bomb U.S.	Stable	Bomb U.S.	Bomb U.S.	Bomb U.S.
Amplitude (psid p-p)	n/a	n/a	n/a	n/a	n/a	1085	n/a	260	282	120
Oscillation Frequency (hz)	n/a	n/a	n/a	n/a	n/a	1298	n/a	1327	1298	1760
Bomb Dump Time (msec)	n/a	n/a	n/a	n/a	<2	n/a	n/a	n/a	n/a	n/a

COMMENTS

Stability	No Bomb	No Bomb	No Bomb	No Bomb	Bomb overpressure seen only on PC1/F1	Bomb Overpressure Was Not Seen on any PC1/F's

Figure 5.4.2 Stability Testing Summary

Pressure Fed Technology Program

Propulsion Division

Test Number
Date

14 15 16 17 18 19 20 21 22 23
11/14/91 11/19/91 11/19/91 11/20/91 11/20/91 11/20/91 11/22/91 11/22/91 12/02/91 12/02/91

OPERATING CONDITIONS

Oxygen Manifold Pressure (psia) 1607
RP-1 Manifold Pressure (psia) 1586
Chamber Pressure, PC3 (psia) 1033
Mixture Ratio - Overall 1.75
Mixture Ratio - Core 2.24
Oxygen Injection Pressure Drop (psid) 574
RP-1 Injection Pressure Drop (psid) 553

STABILITY DATA

	14	15	16	17	18	19	20	21	22	23
Cavity Tune	No Cavities	Monotune	Monotune	Monotune	Monotune	Monotune	Monotune	Monotune	Monotune	Monotune
No. of Each Type	1	1	1	1	1	1	1	1	1	1
Cavity Depth (in)	n/a	1.82	1.82	1.82	1.82	1.82	1.82	1.82	1.82	1.82
Cavity Width (in)	n/a	0.75	0.75	0.75	0.75	0.75	0.75	0.75	0.75	0.75
Bomb Size (grains BOX)	0.00	13	13	13	13	13	13	13	13	13
Bomb Direction (Radial or Tangential)	n/a	Radial	Radial	Radial	Radial	Radial	Radial	Tangential	Radial	Radial
Bomb Overpressure (psid)	n/a	224	330	330	110	300	300	100	200	150
Kistler No.	n/a	1	all	1	1	3	3	1	1	3
Stable or Unstable	Stable	Stable	Stable	Stable	Stable	Bomb U.S.	Bomb U.S.	Bomb U.S.	Bomb U.S.	Stable
Amplitude (psid p-p)	n/a	n/a	n/a	399	n/a	n/a	222	66	236	n/a
Oscillation Frequency (hz)	n/a	n/a	n/a	1298	n/a	n/a	1298	1711	1327	n/a
Bomb Damp Time (msec)	n/a	10	n/a	n/a	<2	12	n/a	50	n/a	<2

COMMENTS

Stability	No Bomb	Bomb Overpressure Was Not Seen on any PCHF's	Marginally Stable in Amplitude and Recovery Time

Figure 5.4.2 Stability Testing Summary (cont'd)

Pressure Fed Technology Program

Test Number	24	25	26	27	28	29	30	31	32
Date	12/03/91	12/03/91	12/03/91	12/10/91	12/10/91	12/11/91	12/11/91	12/11/91	12/12/91
OPERATING CONDITIONS									
Oxygen Manifold Pressure (psia)	1054	1130	1109	1099	1006	1127	1681	1531	1587
RP-1 Manifold Pressure (psia)	917	844	852	1014	1086	931	1536	1661	1485
Chamber Pressure, PCS (psia)	729	730	726	743	732	727	1032	1008	954
Mixture Ratio - Overall	2.08	2.88	2.68	2.28	1.65	2.75	2.16	1.65	2.12
Mixture Ratio - Core	2.82	3.88	3.65	2.92	2.09	3.43	2.77	2.13	2.74
Oxygen Injection Pressure Drop (psid)	326	400	384	355	273	400	649	523	632
RP-1 Injection Pressure Drop (psid)	189	114	127	270	354	204	505	652	531
STABILITY DATA									
Cavity Tune	Monotone	Monotone	Monotone	Bitune	Bitune	Bitune	Bitune	Bitune	Bitune
No. of Each Type	1	1	1	4/8	4/8	4/8	4/8	4/8	4/8
Cavity Depth (in)	1.82	1.82	1.82	1.82/2.67	1.82/2.67	1.82/2.67	1.82/2.67	1.82/2.67	1.82/2.67
Cavity Width (in)	0.75	0.75	0.75	0.75/0.75	0.75/0.75	0.75/0.75	0.75/0.75	0.75/0.75	0.75/0.75
Bomb Size (grains RDX)	13	13	13	13	13	13	13	13	13
Bomb Direction (Radial or Tangential)	Radial	Radial	Radial	Radial	Radial	Radial	Radial	Radial	Radial
Bomb Overpressure (psid)	168	100	100	125	280	48	120	170	0
Kistler No.	3	3	3	3	3	1	1	2	all
Stable or Unstable	Stable	Stable	Stable	Stable	Stable	Stable	Bomb U.S.	Bomb U.S.	Stable
Amplitude (psid p-p)	n/a	n/a	n/a	n/a	n/a	n/a	105	455	n/a
Oscillation Frequency (hz)	n/a	n/a	n/a	n/a	n/a	n/a	2568	1268	n/a
Bomb Damp Time (msec)	<3	<2	<2	10	20	<2	60	40	n/a
COMMENTS									
Stability	PCIF4 and 5 PCIF1 and 4 Bomb shows Overpressure largest oscillation was Not seen on 69 psid at 25 psid at any PCIF's 3529 Hz 2196 Hz								

Figure 5.4.2 Stability Testing Summary (cont'd)

data was obtained are listed. In general, stability data such as bomb over-pressure, damp time, and amplitude are obtained from the transducer which recorded the largest value of chamber pressure amplitude or bomb over-pressure.

5.4.2.1 Stability Results

Combustion perturbation bombs were used to drive combustion instabilities and generated over-pressures in the range of approximately 7 to 58 percent of mean chamber pressure. There were no chug (feed system related) instabilities in any of the tests. All combustion instabilities were acoustic instabilities, and were induced by combustion perturbation bombs. There were no spontaneous combustion instabilities.

Chamber pressure response to a perturbation in a typical stable combustion test is shown in Figure 5.4.3. In this particular test, bomb over-pressure was approximately 224 psid and the perturbation damped out after approximately 10 msec. In a few stable combustion tests, the perturbation damped out almost instantaneously, as shown in Figure 5.4.4. , where the Test 25 chamber response to a perturbation is shown.

Chamber pressure response to a perturbation in a typical unstable combustion test is shown in Figure 5.4.5. In this particular test, bomb over-pressure was approximately 200 psid (27% of P_c) and the perturbation grew to a slightly larger amplitude. A waterfall plot showing the evolution of the power spectral density (PSD) of the chamber pressure is shown in Figure 5.4.6. A PSD plot of the chamber pressure is shown in Figure 5.4.7. The PSD plot was obtained by averaging for a 100 msec period that included approximately 50 msec before and 50 msec after the chamber pressure perturbation. Figure 5.4.8 shows that the high-frequency pressure transducers in the propellant manifolds and the accelerometers mounted on the outside of the combustion chamber detected instabilities and accurately provided the values of resonant frequencies. These instruments were demonstrated to be well-suited in supplementing the high-frequency pressure transducers in the combustion chamber for stability data. The figures show several resonant frequencies existing simultaneously. The first resonant frequency corresponds to the 1T acoustic frequency of the combustion chamber, which is approximately 1325 Hz. Other resonant frequencies, 2679, 4063, 5388, and 6772 Hz appeared to be harmonics of the 1T mode.

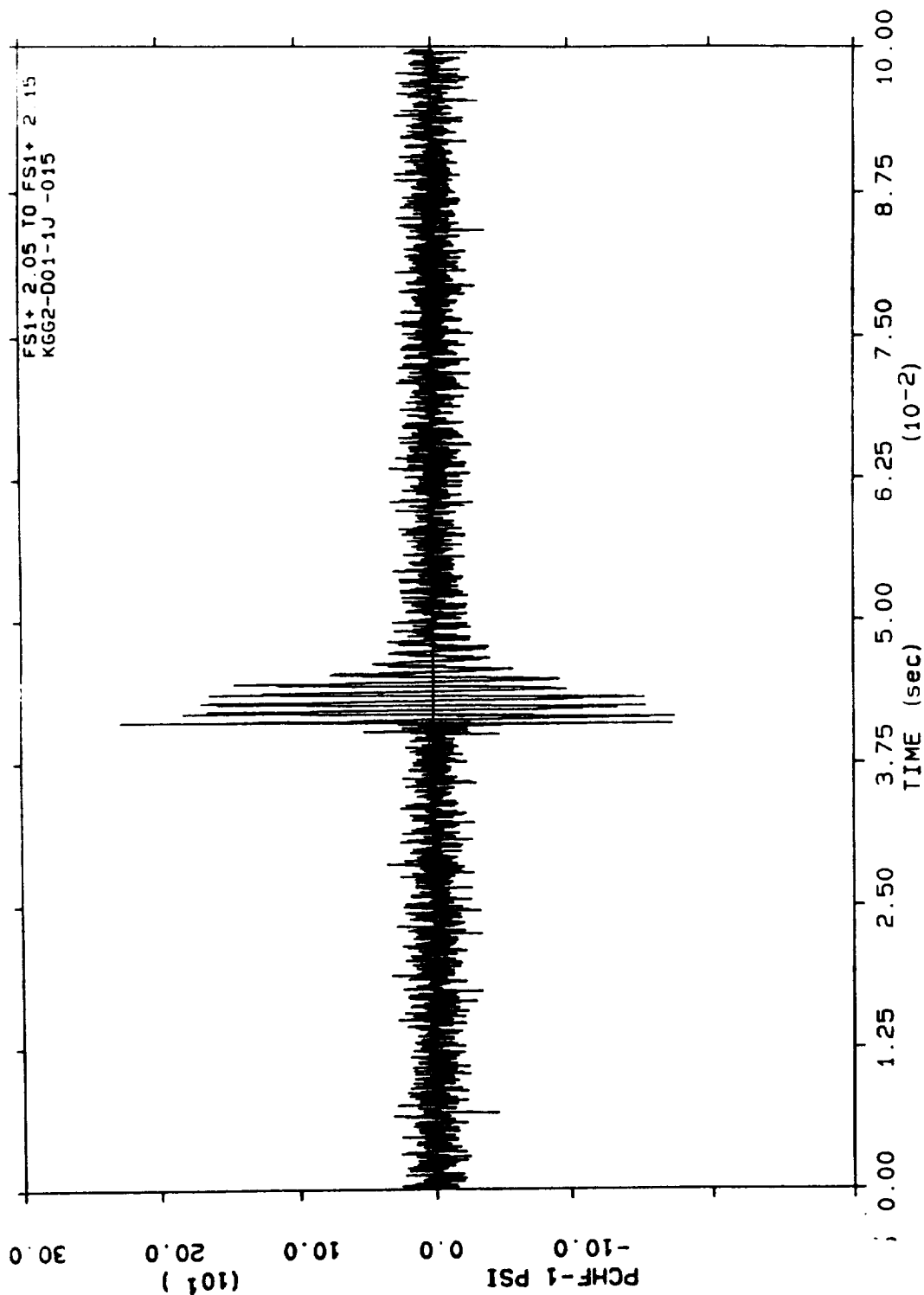


Figure 5.4.3 A Typical Induced Instability which was Damped Quickly (Test 15)

Pressure Fed Technology Program

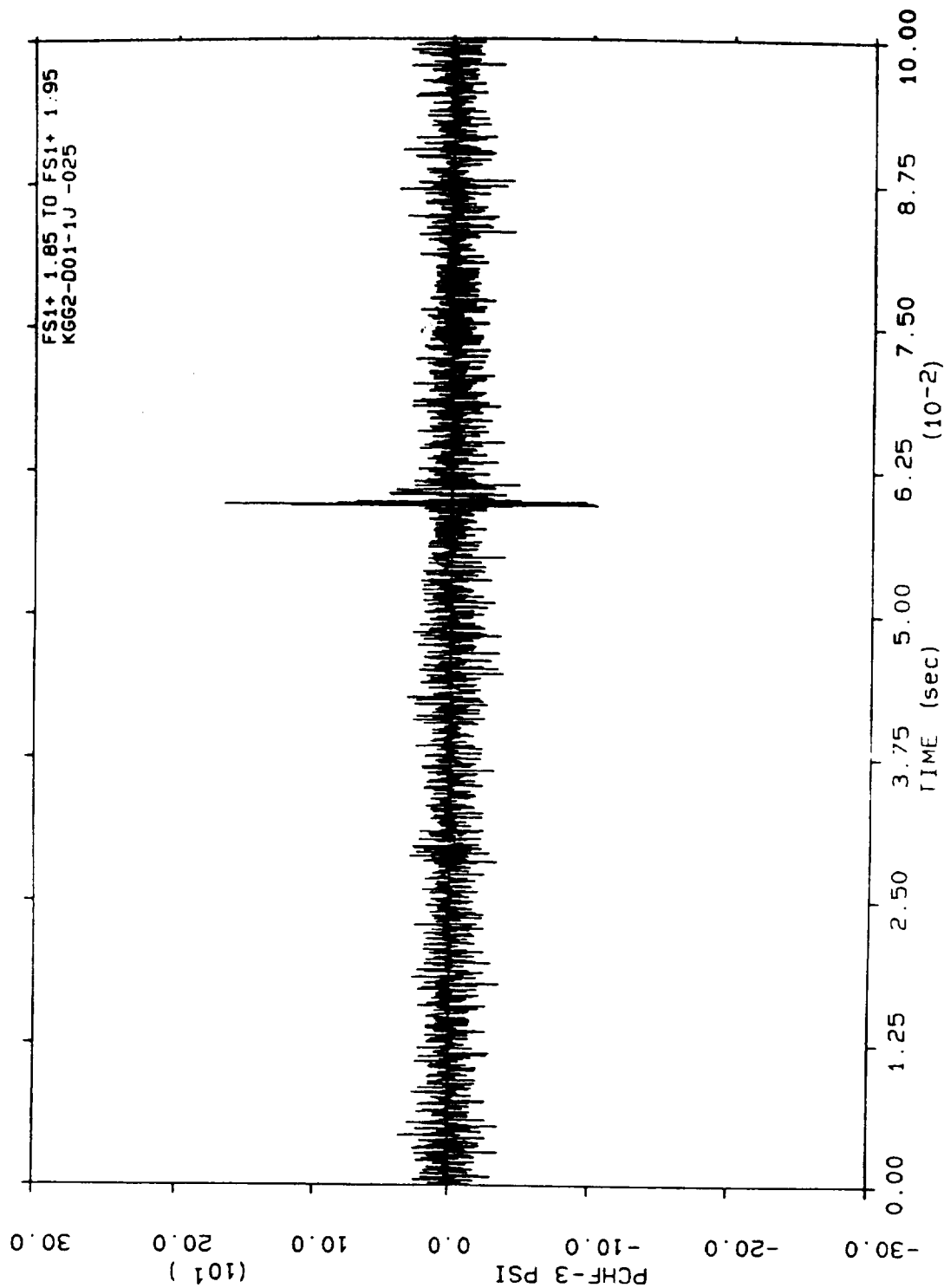


Figure 5.4.4 This Induced Instability Damped Almost Instantly (Test25)

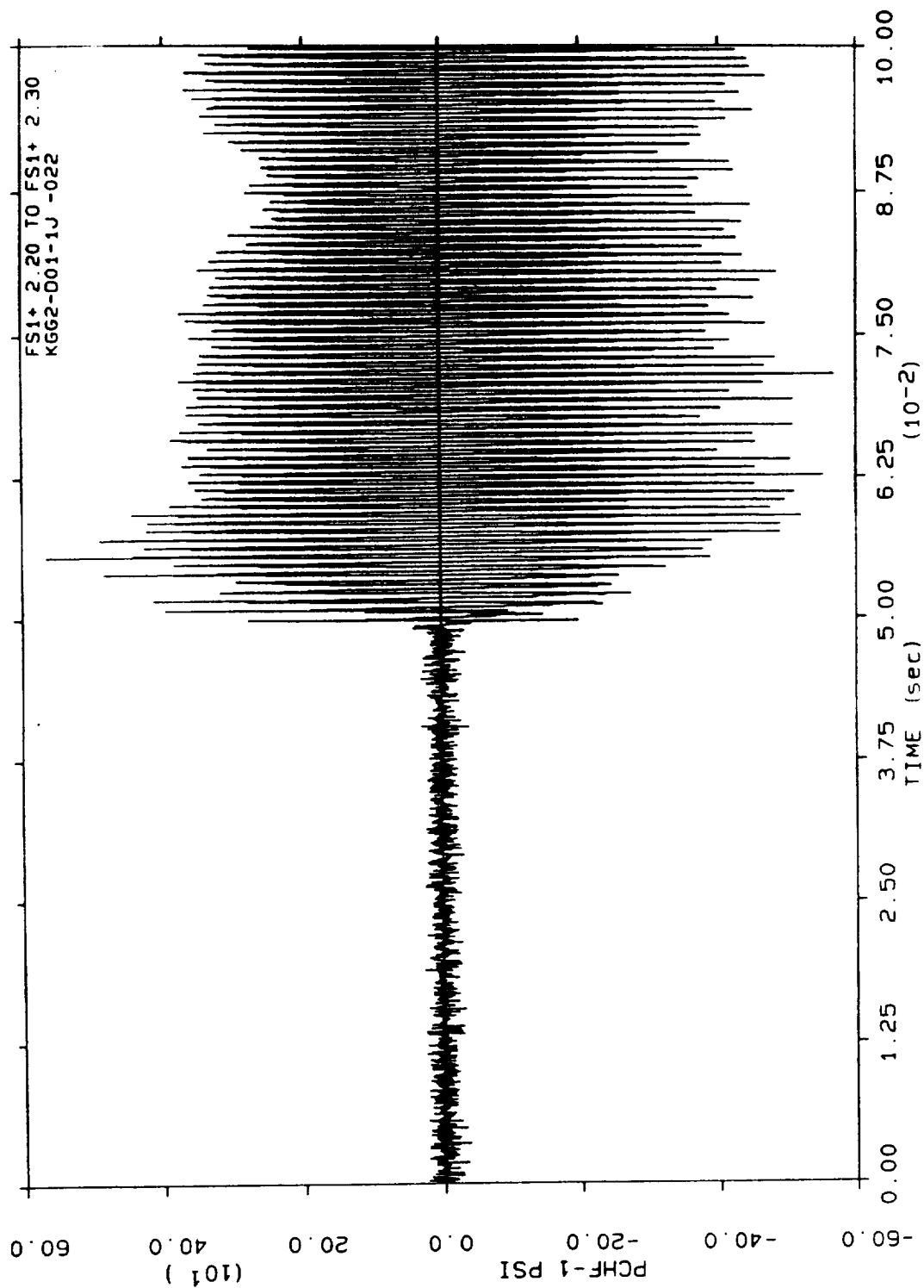


Figure 5.4.5 A Typical Induced Instability which Remained Unstable (Test 22)

Pressure Fed Technology Program

Propulsion Division

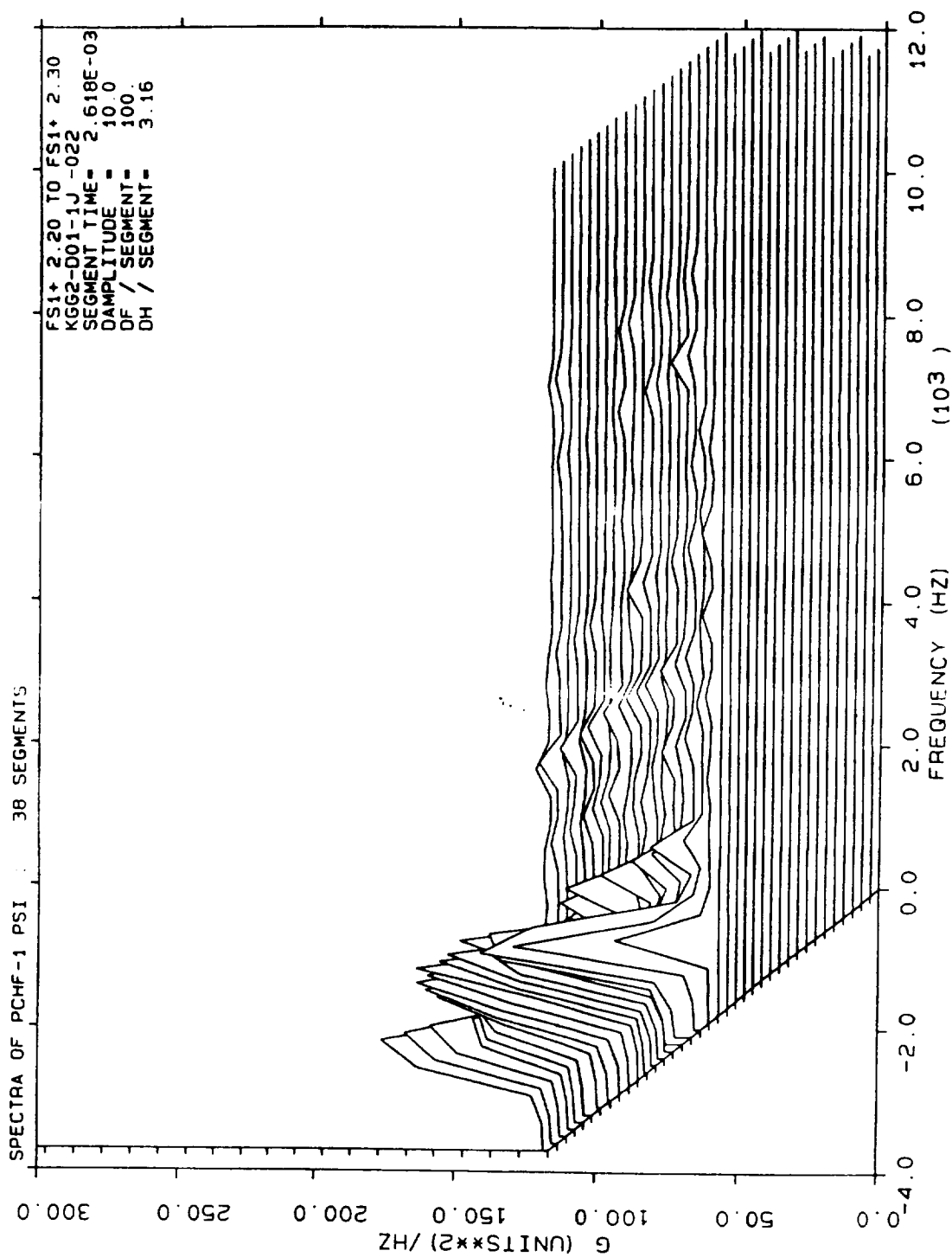


Figure 5.4.6 "Waterfall " Plot of Test 22 Shows the Evolution of the Instability

Pressure Fed Technology Program

Propulsion Division

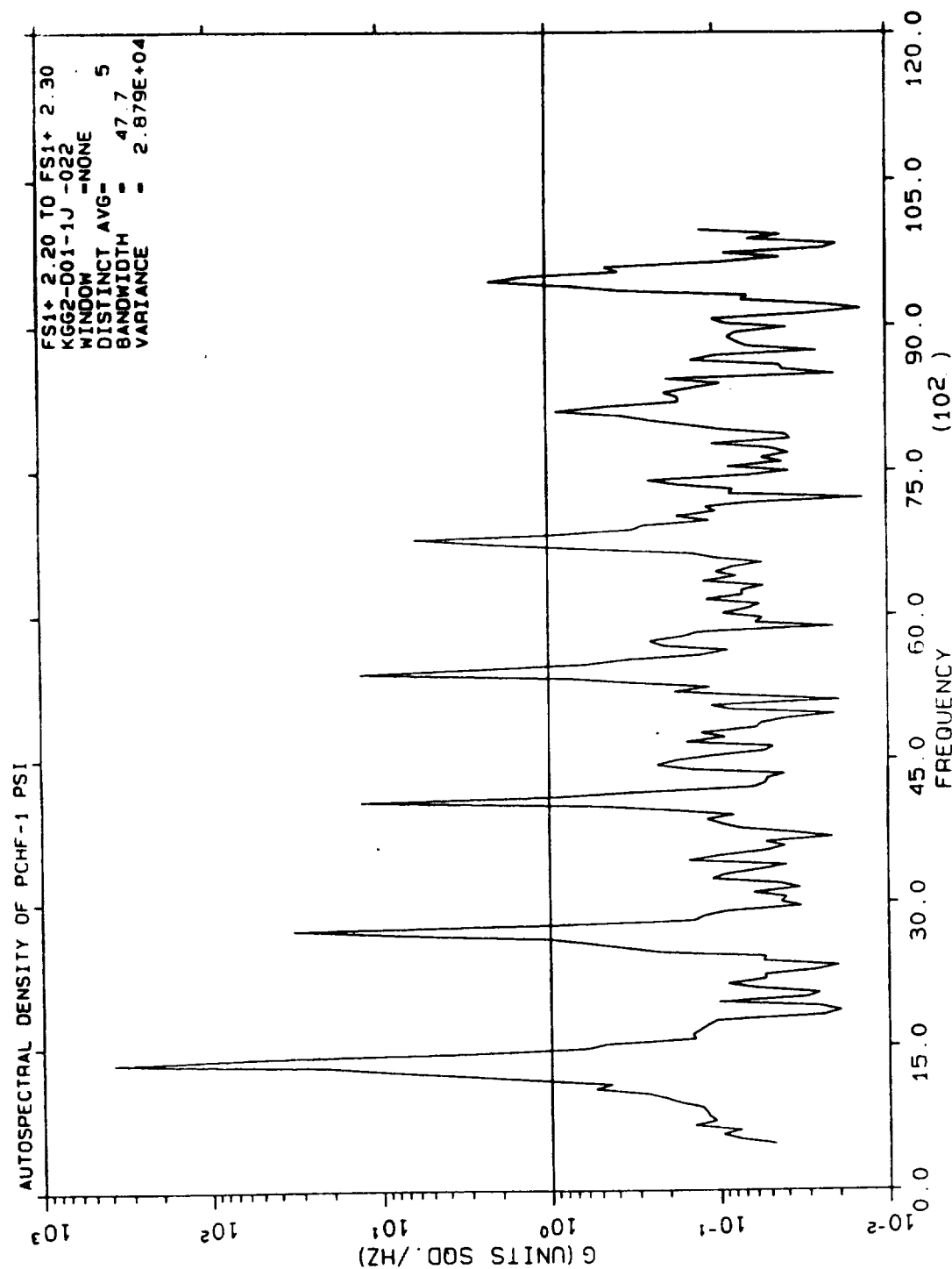


Figure 5.4.7 Power Spectral Density (PSD) Plot Shows Unstable Frequencies

Pressure Fed Technology Program

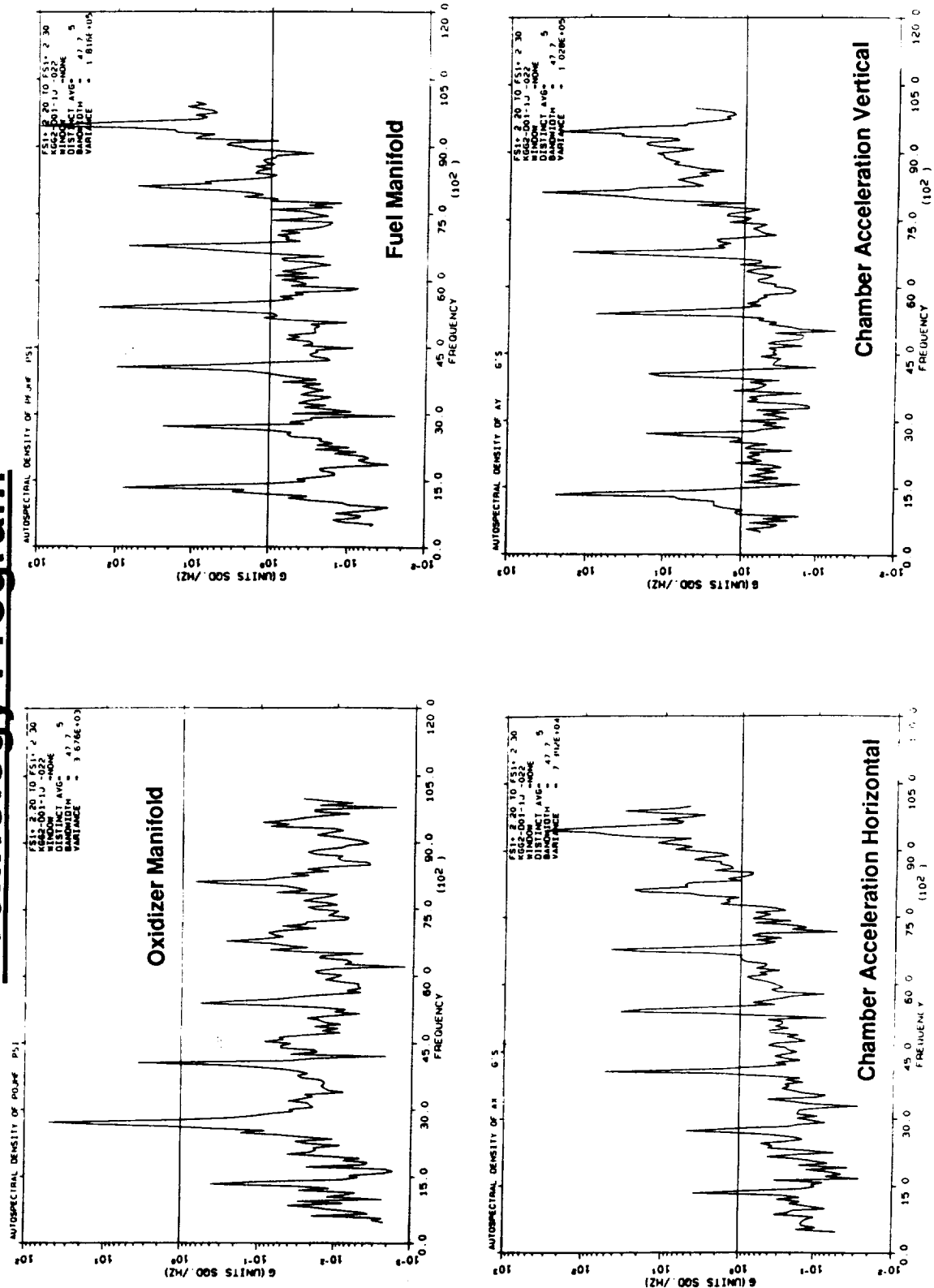


Figure 5.4.8 PSD Plots of Manifold Pressures and Chamber Accelerations
Confirm Instabilities

In the first test series, an engine configuration with a 4-inch deep cavity was tested. The primary objectives of this test series were to check out engine operation, and to obtain combustion performance and thermal data. Nevertheless, stability data was also obtained from this test series. Gas temperature inside the cavity was measured to estimate the speed of sound in the cavity and used to tune the cavity in subsequent tests. In this test series, tests 2, 3, 4, and 5 were stable. Dynamic stability characteristics are not known since no combustion perturbation bombs were used in these tests. Combustion perturbation bombs were used in the next three tests resulting in combustion instability in only test 7. Tests 6 and 8 were dynamically stable.

Measured temperature of the gas inside the cavity (between 250 and 500°F) indicated that the 4-inch deep cavity may have been too long to be effective for the 1T mode. Cavity gas temperature can infer a cavity sound speed, as shown in Figure 5.4.9, allowing optimization of acoustic damping. Low cavity gas temperature, and the low speed of sound inside the cavity, probably limited the effectiveness of the 4-inch deep cavity. The low cavity gas temperature resulted from improper impingement of RP-1 fuel film cooling (FFC) stream onto the cavity entrance. Following test series 2, the chamber diameter at the cavity entrance was slightly enlarged to reduce or eliminate FFC cavity impingement. This resulted in more FFC flow down the chamber wall, which provides cooling for the chamber and throat region, and higher cavity gas temperatures which were nearer predicted values. A stability map for series 1, showing stability results for each test, is shown in figure 5.4.10.

In the second test series, the chamber was tested without acoustic cavities (the cavities were blocked with a full resonator ring) to determine the baseline combustion stability characteristics. Almost all tests were dynamically unstable. Tests 9 and 11 were aborted. Tests 10, 12, and 13 were dynamically unstable. Test 14 was stable, but dynamic stability characteristics could not be deduced since no combustion perturbation bomb was used in this test. (See figure 5.4.11 for the stability map). This test series provided valuable data on the baseline acoustic response of the chamber and confirmed the need for acoustic damping devices.

In the third test series, the acoustic cavity was shortened to increase the stability margin. The HIFI chamber response model was used to size the new cavity using cavity gas temperatures measured in previous tests. Cavity depth in

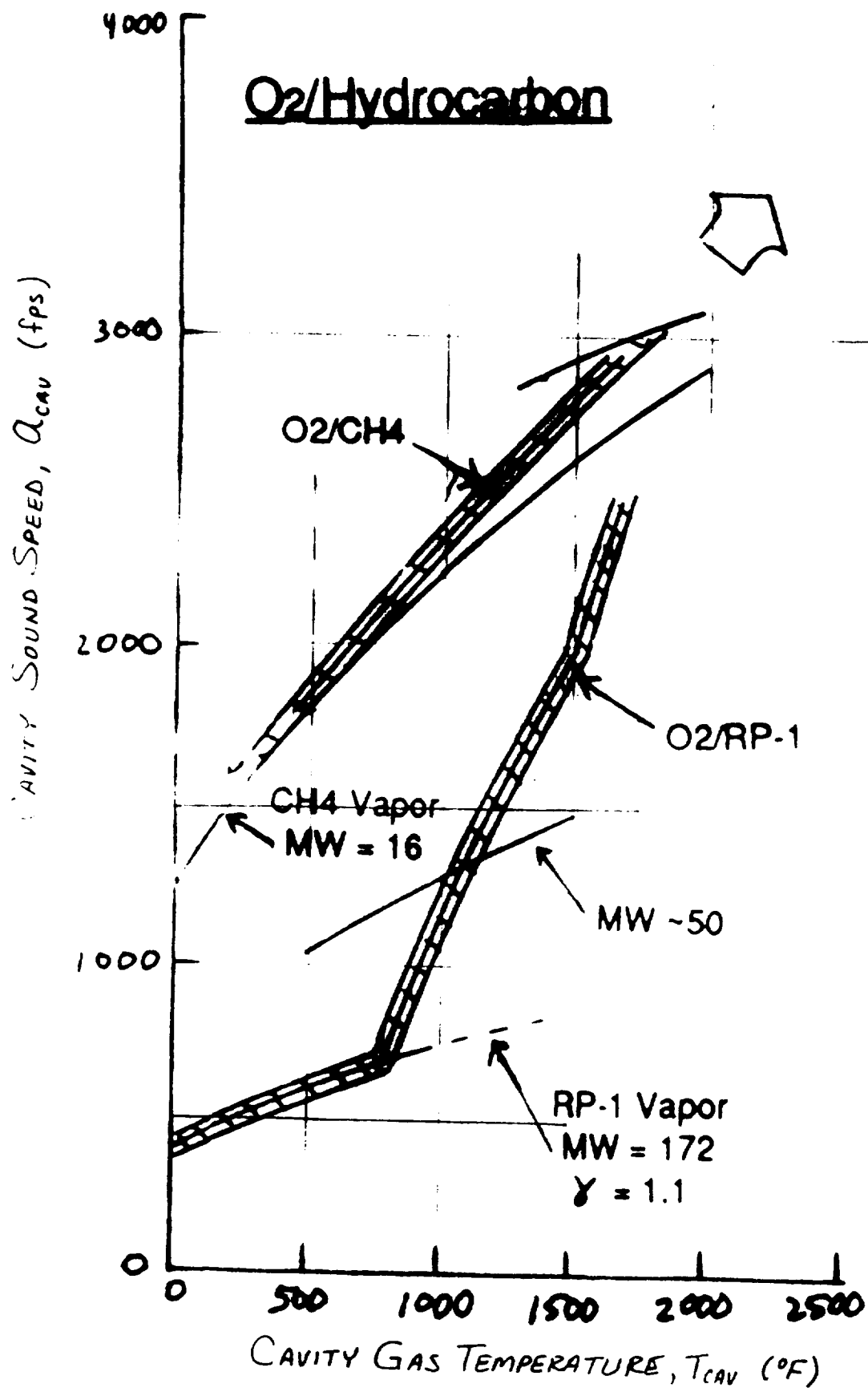


Figure 5.4.9 Acoustic Cavity Gas Temperature can Infer Gas Composition and Cavity Sound Speed for Cavity Damping Optimization

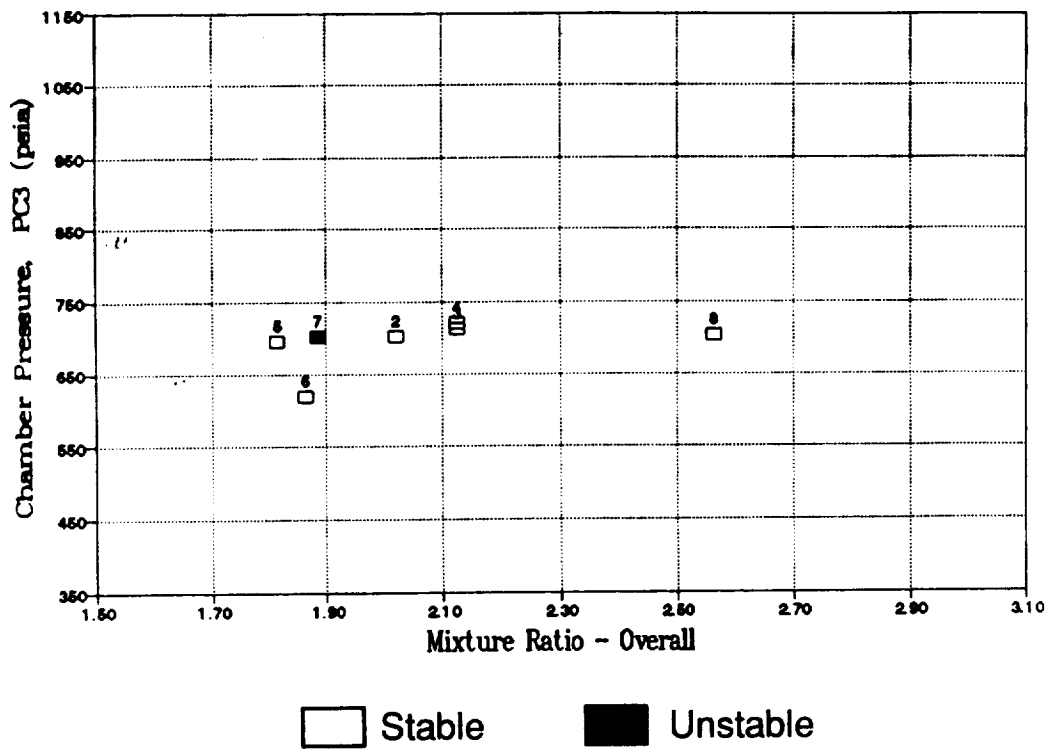


Figure 5.4.10 Stability Map for Series 1, 4 inch Cavity

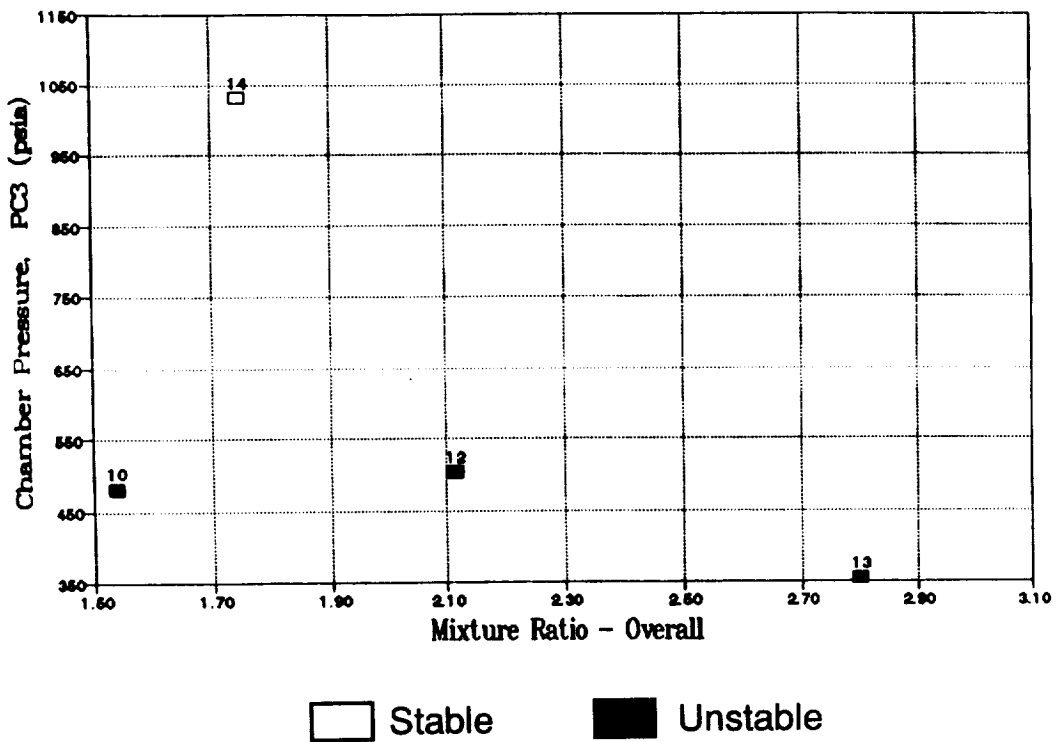


Figure 5.4.11 Stability Map for Series 2, No Cavity

this test series was 2 inches. The shallower cavity significantly improved the stability margin as shown on the stability map, figure 5.4.12. Combustion was dynamically stable over a larger range of mixture ratio and chamber pressures, including the nominal operating point. It should be noted that the nominal operating point had been previously tested to be dynamically unstable in a chamber with a 4-inch deep monotuned cavity (Test 7).

Following the third series tests, it became clear that an effective cavity design for widely varying operating points (P_c , MR and FFC rates) was unlikely. Unfortunately, acoustic cavities are effective only in a specific range of conditions. Cavity depths were based on the speeds of sound inside the cavity that were inferred from the cavity gas temperatures measured during previous tests. Parametric evaluation of different cavity distribution was made using the computer code HIFI . Results are shown in Figure 5.4.14. In this figure, a dimensionless parameter, Y_{\min} (the inverse of the chamber response) c was plotted for several cavity configurations as a function of the cavity gas temperature and speed of sound inside the cavities. Cavity configurations with higher value of Y_{\min} over the range of the cavity sound speed provide better damping.

To damp instabilities over a wider range of operating conditions, a "bituned" cavity configuration, consisting of cavities with 1.82 and 2.67 inch depths, appeared to be a good compromise. This cavity configuration, shown below, was predicted to be effective over a cavity speed range from 600 to 1500 ft/sec. The bituned cavity was fabricated by machining one of the several blank resonator rings available.

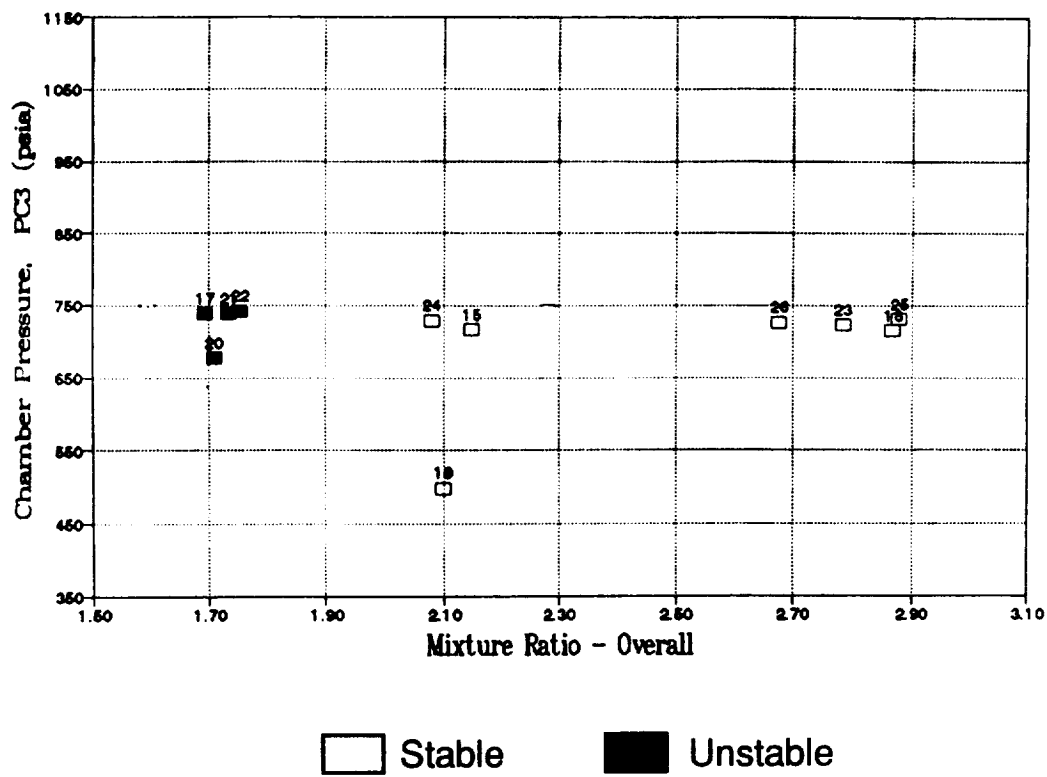


Figure 5.4.12 Stability Map for Series 3, 2 inch Cavity

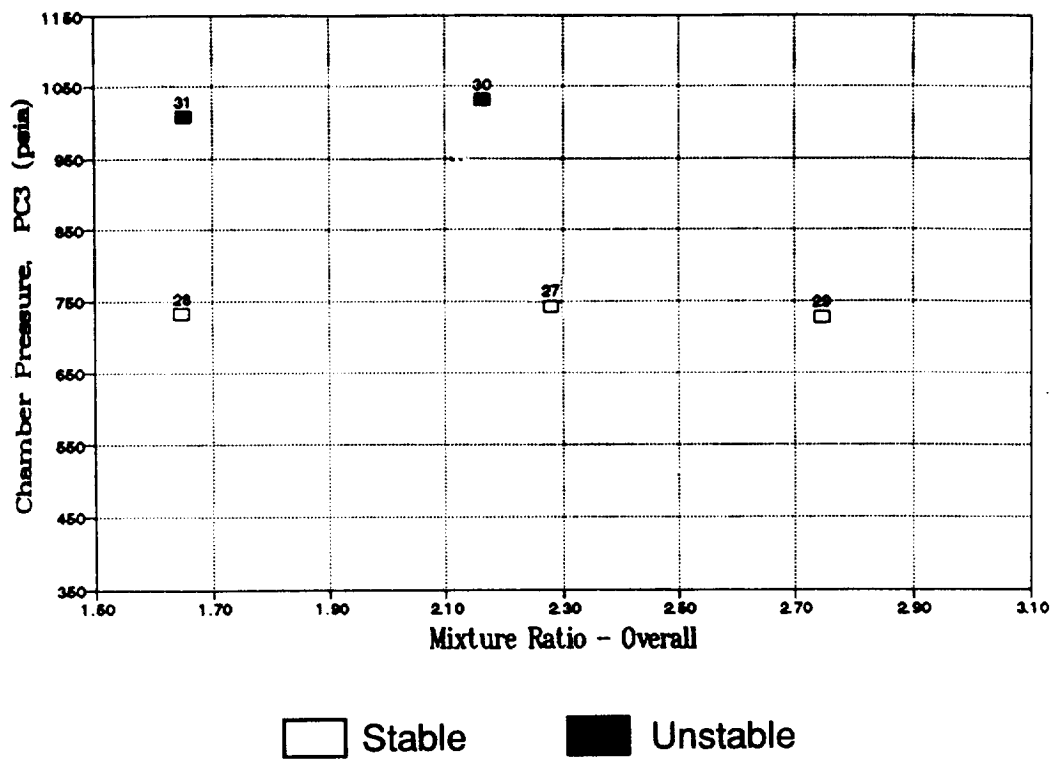


Figure 5.4.13 Stability Map for Series 4, Bituned Cavity

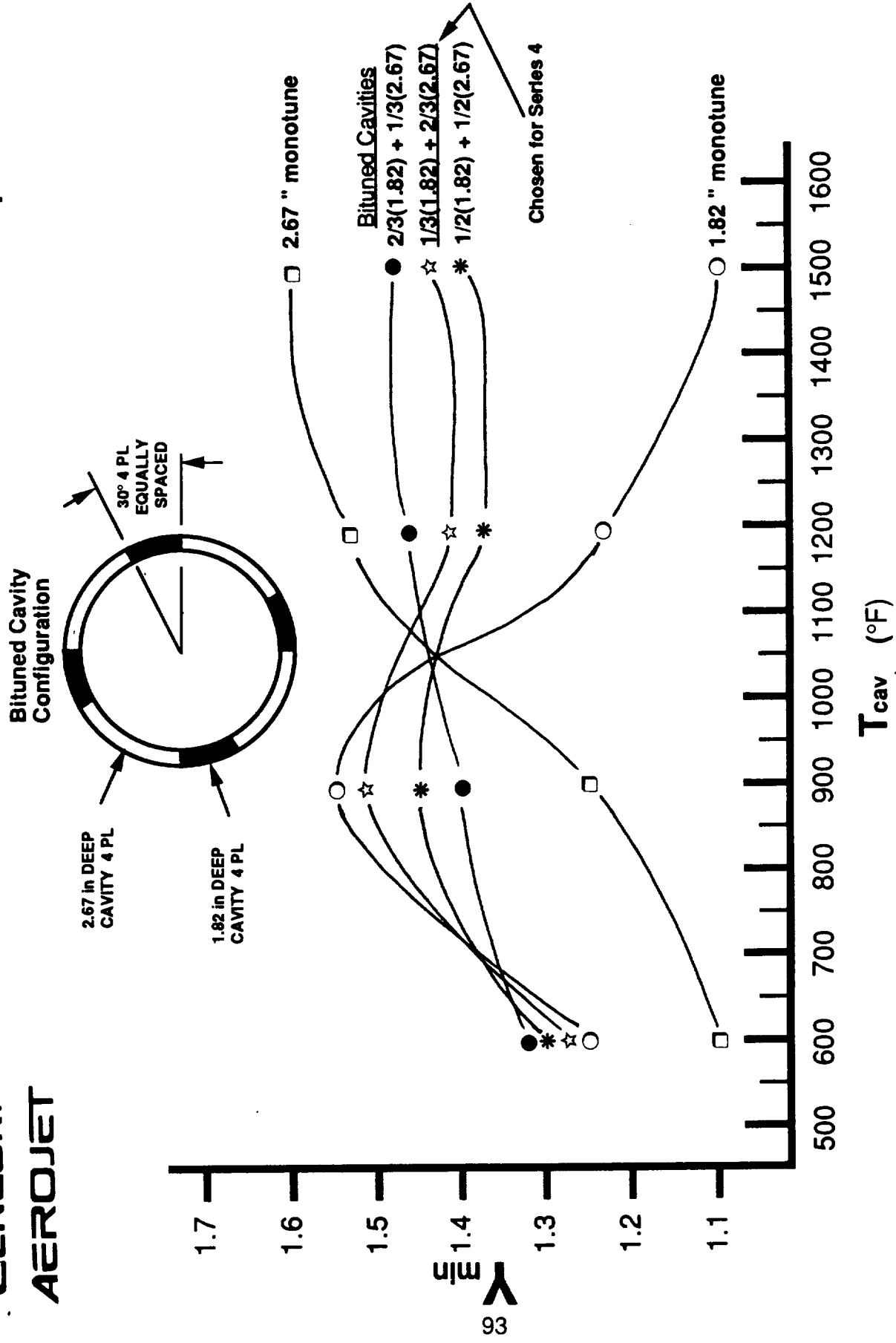
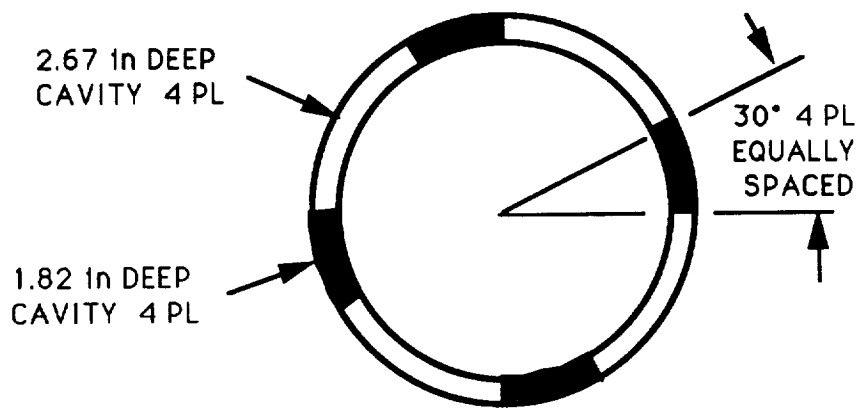


Figure 5.4.14 Cavity Damping Ability Varies with Gas Temperature



Bituned Cavity Configuration

Both cavities were intended to damp out the 1T mode. Cavity depths differed so that over the range of cavity gas temperatures, at least one of the cavities would provide some damping for the 1T mode.

Test results, Figure 5.4.13, shows that the bituned cavity configuration improved the stability margin. Combustion was stable over a larger range of mixture ratio, including not only the nominal operating point but also at the low mixture ratio of 1.65 (Test 28) where previous tests with a monotuned cavity (Tests 17, 21 and 22) were unstable. In addition to Test 28, Tests 27 and 29, were demonstrated to be dynamically stable. Note that Test 29 was at relatively high overall mixture ratio of 2.75. Although a perturbation bomb was used in Test 32 (954 psia), an over-pressure was not seen on any of the transducers, and this test point is not shown on the stability map. Higher chamber pressures were tested in Tests 30 and 31 to determine if higher instability modes could be excited as predicted. Test results indicated that 1T and 2T modes were excited in Test 31, and that 1T, 2T and 3T modes were excited in Test 30. Figure 5.4.15 shows the waterfall plot of the chamber pressure in Test 30. The figure shows PSD peaks at the 3T and 2T frequencies in addition to the peak at the more common 1T frequency. This result suggests that higher modes may exist at the higher chamber pressures.

Summarizing the stability test results and conclusions for the full-scale design:

- Acoustic Cavity Required
 - Combustion was dynamically unstable in tests without a cavity where combustion perturbation bombs were used. No test was spontaneously unstable. The absence of higher mode instabilities, 2T and 3T, at the nominal operating point indicates that simple damping devices will be sufficient for the fullscale design.
- Chug Stable.
 - No chug instabilities were encountered at steady-state operation even at chamber pressure as low as 354 psia. Since chug instabilities are a result of feed system coupling to the combustion process, this result confirms the injector as a highly throttleable design.
- Dynamically Stable with Bituned Cavity
 - Bituned cavities were effective in providing dynamically stable combustion at nominal P_c and over a wide range of mixture ratios (overall 1.59 to 2.88). The bituned cavity may be instrumental in providing fullscale damping at both nominal and throttled operating points.

5.5 THERMAL PREDICTIONS AND RESULTS

5.5.1 Methodology

Thermal data was required at varying operating conditions and chamber positions to characterize the combustion process and to determine material requirements for component compatibility. The injector and chamber were highly instrumented to acquire extensive temperature data.

Characterization of the combustion process was required to establish the degree of fuel film coolant (FFC) entrainment into the combustion stream. This was done by comparing the adiabatic wall temperature from two tests with different FFC rates, determining a barrier mixture ratio, and determining the amount of film coolant that must have been entrained to achieve this mixture ratio. This information is critical in determining the amount of FFC required for the full scale ablative design.

Determination of surface heat flux is required to design the copper injector modules for steady state operation. Face mixture ratio and combustion gas recirculation velocity is required to predict heating rates for the ablative face, which will lead to prediction of surface ablation rate. This was done by measuring the temperature of the module body and the temperature at the face surface and applying a time dependent surface temperature boundary condition to a semi-infinite slab, subsequently inferring the associated surface heat flux. Combustion gas temperatures can be derived from calculated surface heat flux vs. measured surface temperature. A correlation of combustion gas temperature vs. mixture ratio leads to estimates of the local wall mixture ratio. The resulting boundary conditions are then used to correlate various injector face thermal compatibility prediction models, to determine the injector face heat flux and the resulting mixture ratio of the recirculating combustion products at the injector face.

Chamber temperature measurements were used to determine the effectiveness of the fuel film cooling (FFC) and generate design data for the design of the fullscale ablative chamber liner. Utilization of co-axial Type K thermocouples allowed chamber gas side wall temperature to be measured directly. Two of these thermocouples (TC2 and TC5) were used to automatically terminate engine operation when a pre set temperature limit was exceeded to minimize steel chamber erosion during the tests. Additionally, since the chamber wall is thick (1.5 inches) relative to the short (<1.0 second) firing duration, outside wall temperature remains ambient during the firing and it can be analytically treated as a semi-infinite slab. Gas side wall heat flux can be inferred along with an estimate of the local adiabatic wall temperature and heat transfer coefficient if the local mixture ratio and chamber pressure are constant. The adiabatic wall temperature can be used to determine fuel film cooling design requirements to achieve a specific wall mixture ratio. Low cost fuel film cooled engine performance can be optimized for allowable surface recession rates with an ablative silica phenolic chamber which can withstand 4°R design temperatures compared to < 2500°F with instrumented steel heat sink chambers.

5.5.2 Thermal Predictions and Results

5.5.2.1 Injector Face

Thermal predictions were made for the steady state operating temperature of the copper modules at both nominal P_c and 10% above nominal P_c using a 3-D computer model. A uniform boundary condition was applied along the front face of the modules only. Gas side boundary conditions were calculated based on an injected core mixture ratio of 2.9 which corresponds to a gas temperature of 5621°R. In reality, actual mixture ratio near the modules should be higher due to the much lower vaporization rate of RP1 relative to LO₂ resulting in a lower recovery temperature than predicted.

The maximum steady state temperature of the modules for a 726 psia chamber pressure was predicted to be 1113°F. This was predicted to occur at the edge farthest from the orifices as shown by the red area in Figure 5.5.1. This is the location where the propellant conduction cooling path to the orifices is the longest.

These predictions were compared to actual test data from thermocouples TJ1, TJ2, and TJ6. Test 4 was the best test for obtaining module temperatures. This test was approximately 0.4 sec. duration at a chamber pressure of 711 psia and core mixture ratio of 2.8. TJ1 read much higher than TJ2 and TJ6 for Tests 3 and 4, which was unexpected. Photographs of the injector face taken after Test 6 indicated that the copper plug into which the TJ1 had been inserted had separated from the module into which it was peened, resulting in an incorrect temperature measurement of the module. Figure 5.5.2 shows the temperature vs time curves for the remaining thermocouples TJ2 and TJ6. This data shows that the modules did not reach steady state temperatures during any of the tests, although the slope of the temperature rise was very small at the termination of the test. It can be inferred from the temperature histories from Test 4 that the maximum steady state temperatures of the modules should be less than 750°F for nominal operating conditions; which is 263°F less than the prediction.

The ablative face experienced very little recession throughout the test matrix. This is partly due to the short firing durations but mainly due to relatively benign boundary conditions at the injector face. Limited temperature data was available from TJ4 and TJ5 due to the injector face damage incurred during the shut-down transient of Test 6. Figures 5.5.3 and 5.5.4 shows the temperature response of

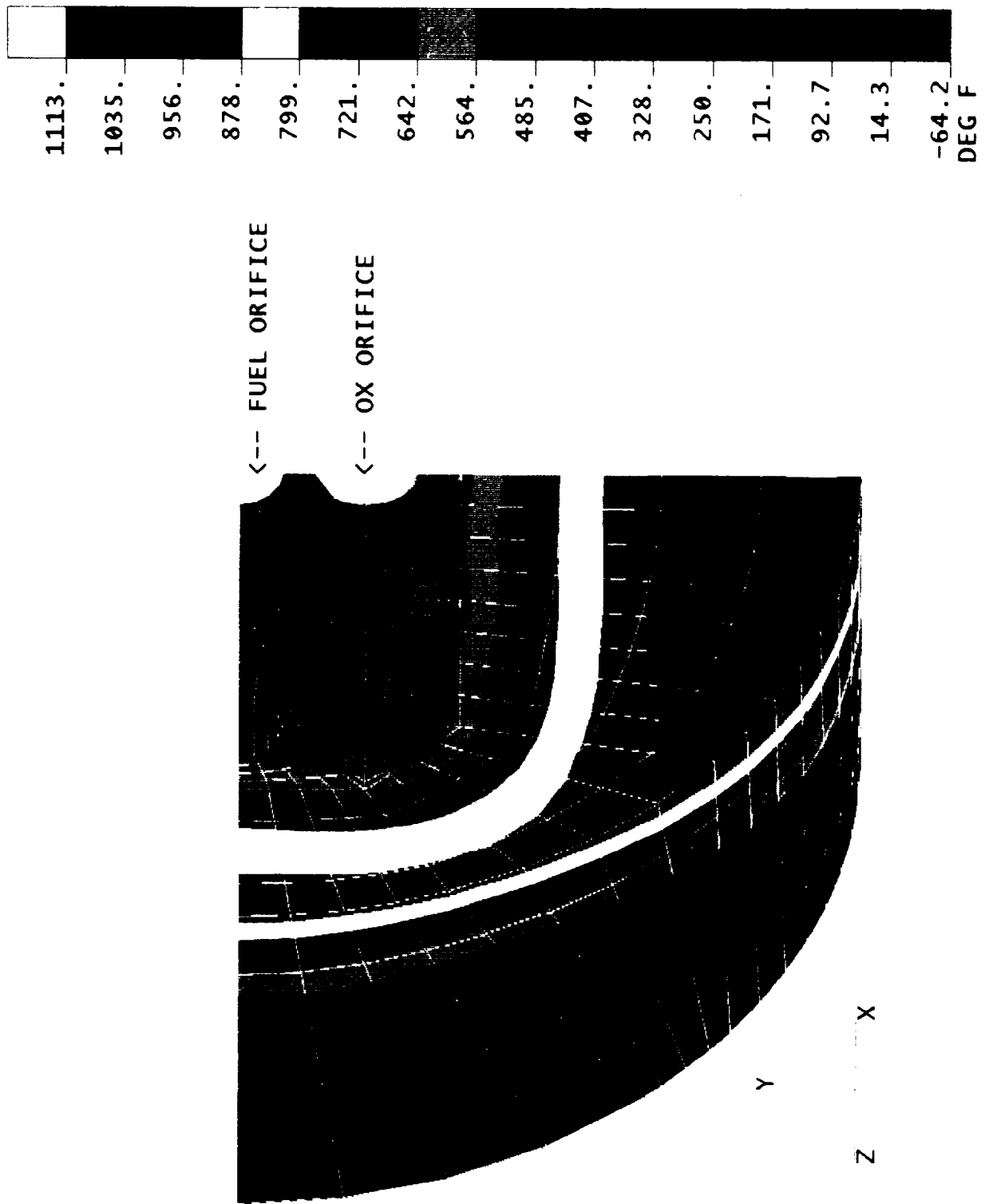


Figure 5.5.1 Module Temperatures Were Predicted Using Thermal Models

ORIGINAL PAGE
COLOR PHOTOGRAPH

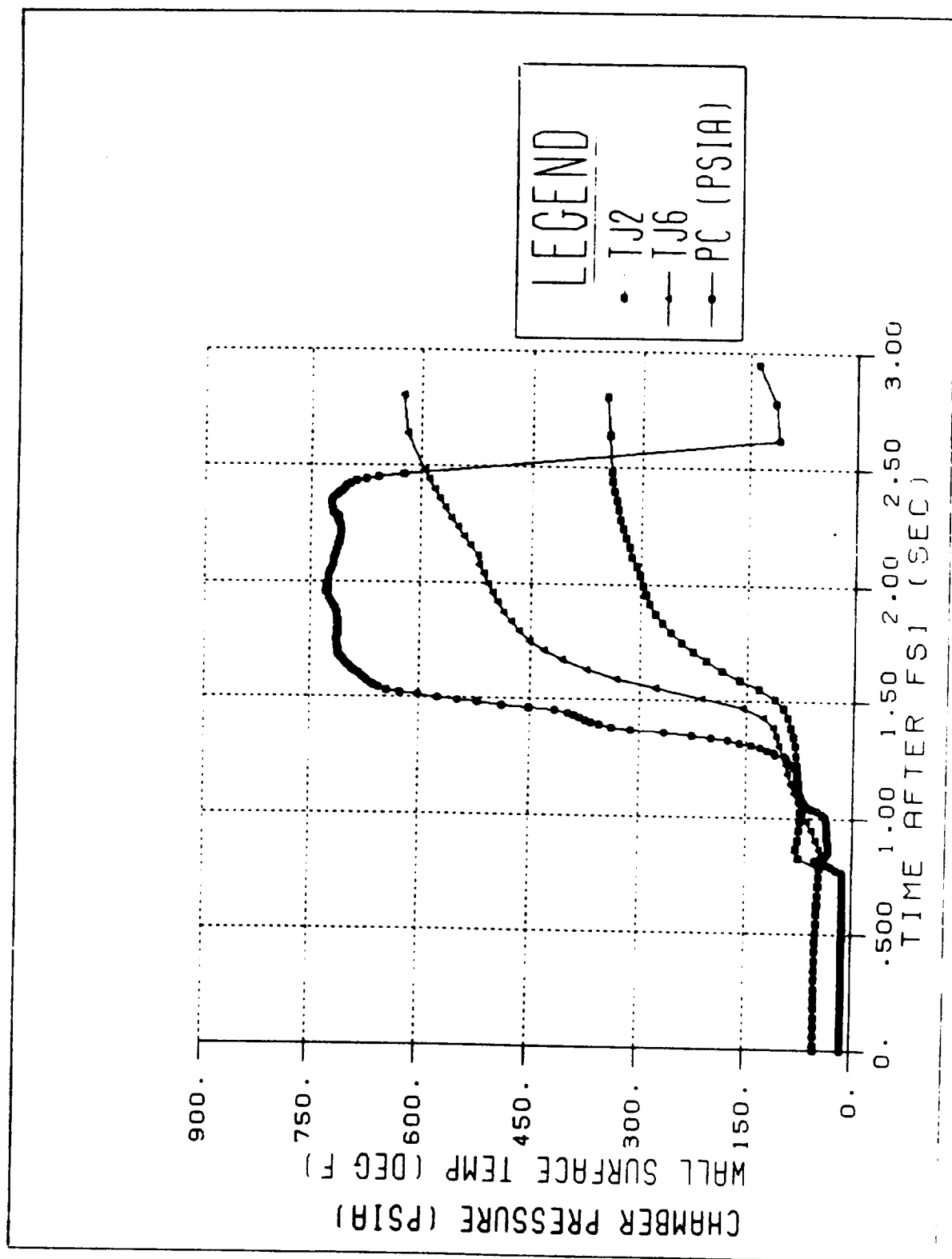


Figure 5.5.2 Module Temperatures Were Less Than Expected (Test 4)

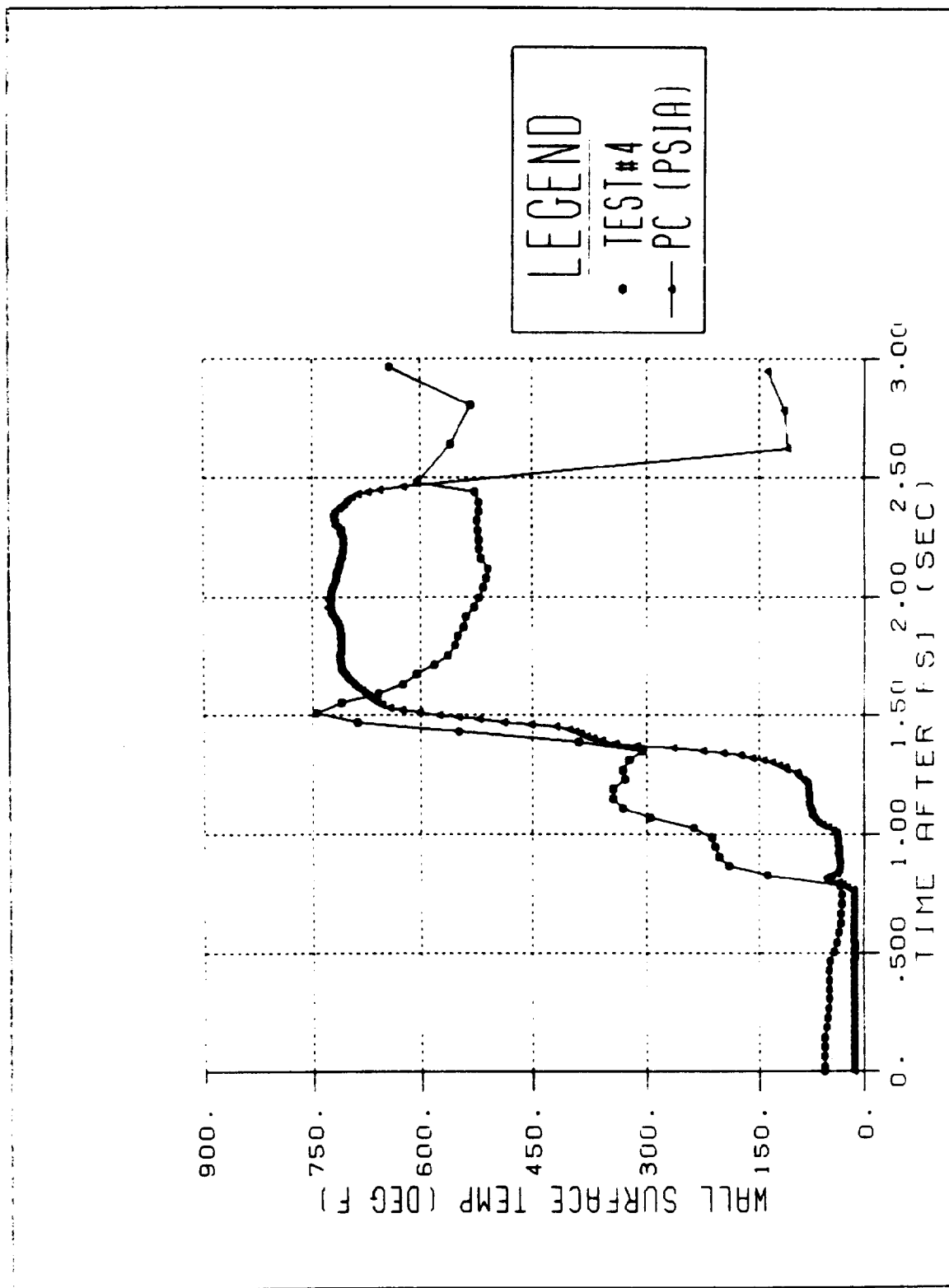


FIGURE E 5-3 Edge Temperature Where Loss Then Formed (T 14 J 11-1)

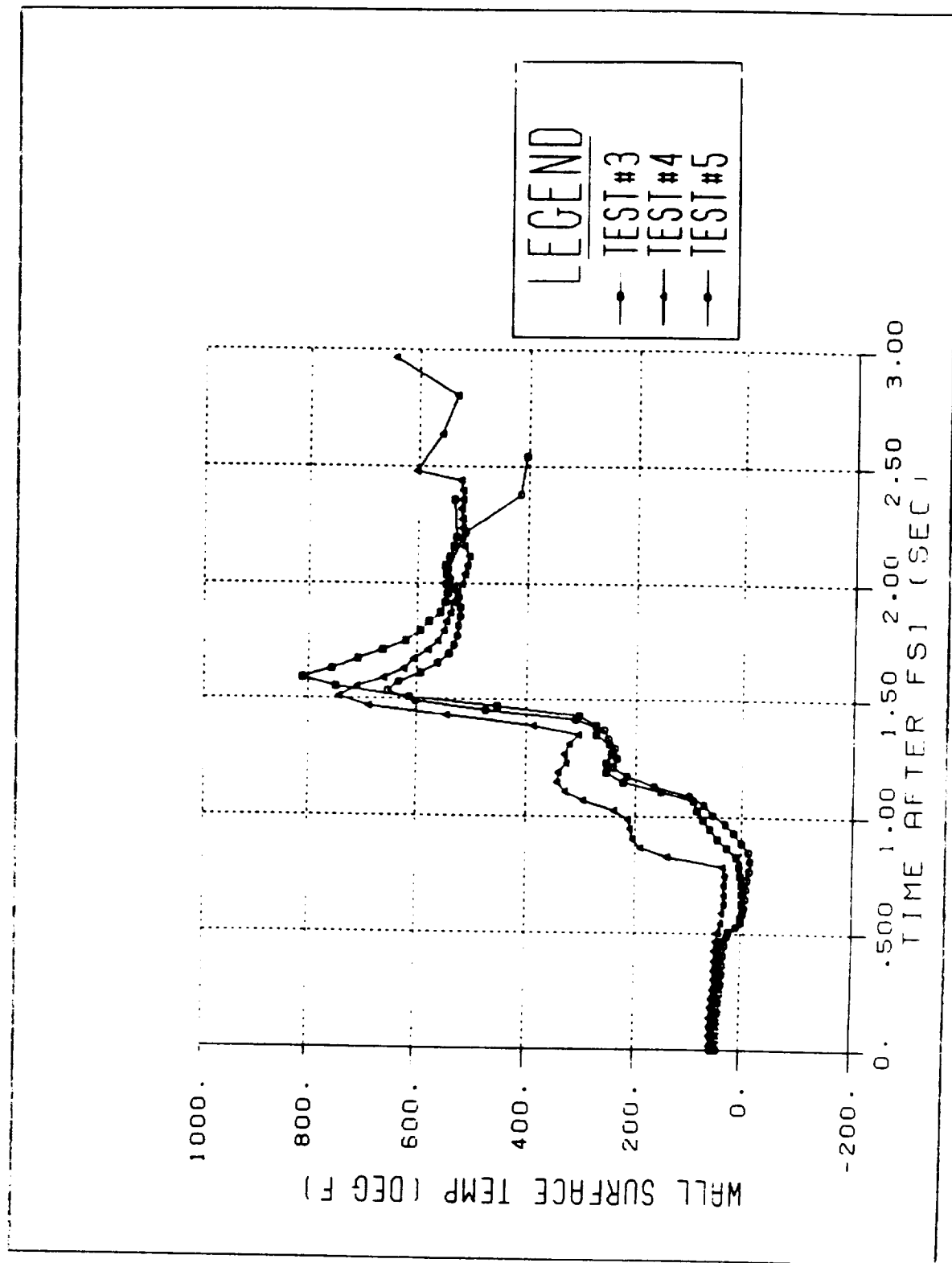


Figure 5.5.4 Face Temperature Measurements Show Cool Face Environment

TJ4 and TJ 5 during various tests. The data indicates that the region of the outer row of modules runs hotter than the region around the inner modules of the injector. This is attributed to radial winds caused by the three inner modules flowing past the void between the outer row of modules. The over shoot in the temperatures are due to mixture ratio variations occurring during the start transient due to the LO₂/TEA-TEB ignition. The fact that the temperatures plateau out suggests that gas recovery temperatures are very low (< 1200°F) in these regions. This accounts for the high test durability of the ablative face.

5.5.2.2 Combustion Chamber

Thermal predictions of wall temperature histories for the throat plane at different operating points were conducted assuming 16% fuel film cooling. The following table shows the results from an analysis to determine maximum gas side wall surface temperature resulting from a .15 second long start transient followed by a .3 sec. steady state burn.

	Predicted Steady-State Wall Temperature	
	<u>Pc = 720 psia</u>	<u>Pc = 660 psia</u>
MR = 2.62	1685°F	1601°F
MR = 2.91	1890°F	1707°F
MR = 3.20	2058°F	1983°F

These predictions were found to be optimistic. Axial wall temperature profiles did not follow expected trends, which are characterized by gradually increasing wall temperatures with a sharp peak at the throat plane followed by a gradual drop off in the nozzle. It was not unusual to see a lower wall temperature in the convergent section than in the barrel section. Figure 5.5.5 shows the axial wall temperature profile for 0.8 sec. of steady Pc at 22% fuel film cooling at nominal operating conditions. The data shows that the region between the modules ran 400°F hotter than the region in line with the modules. This can be explained by the combustion analysis predictions previously presented in section 5.3. Figures 5.5.6 and 5.5.7 show the temperature histories of the chamber thermocouples for a 0.9 second duration test at steady state nominal Pc and 22% fuel film cooling.

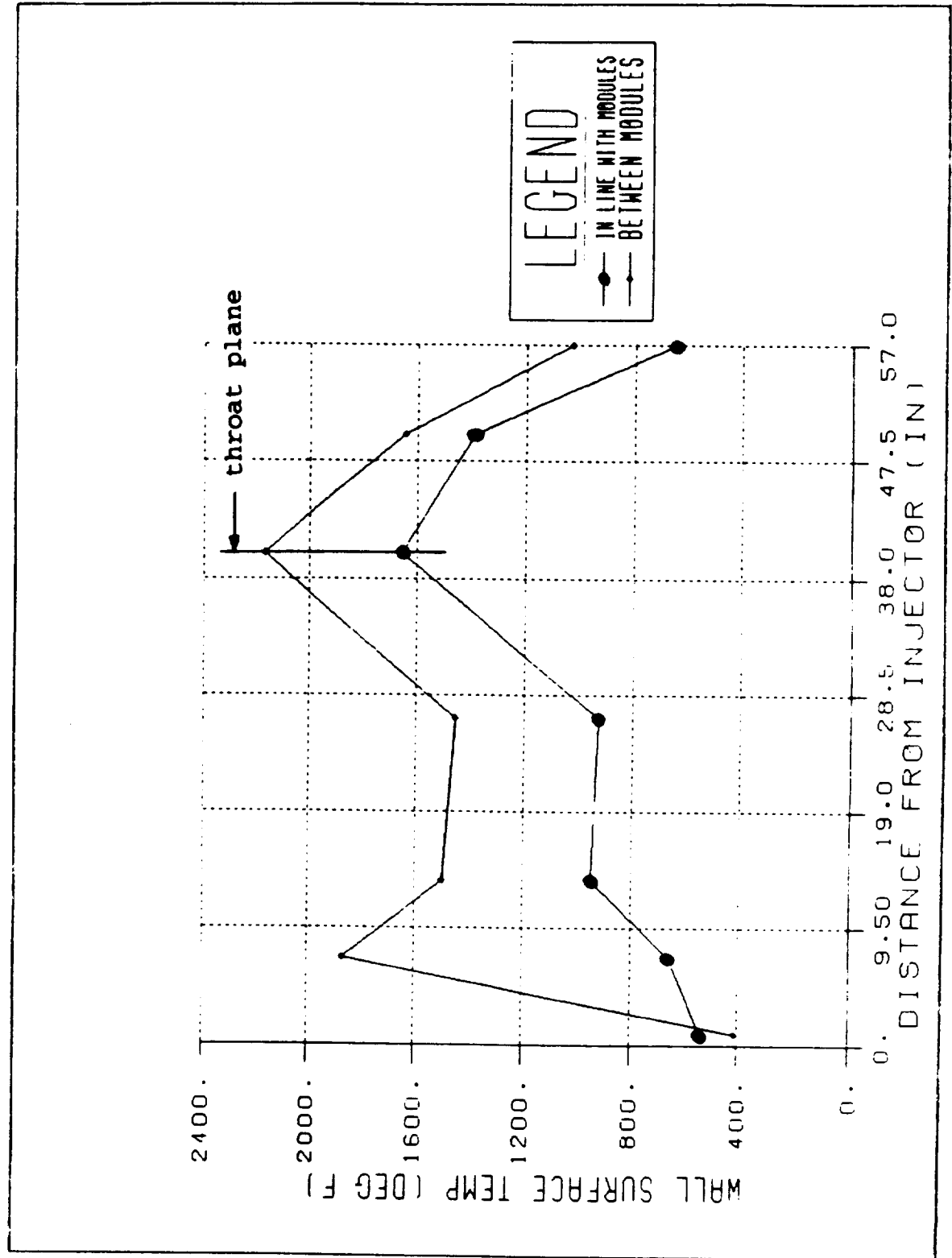


Figure 5.5.5 Chamber Wall Temperatures Vary With Module Position

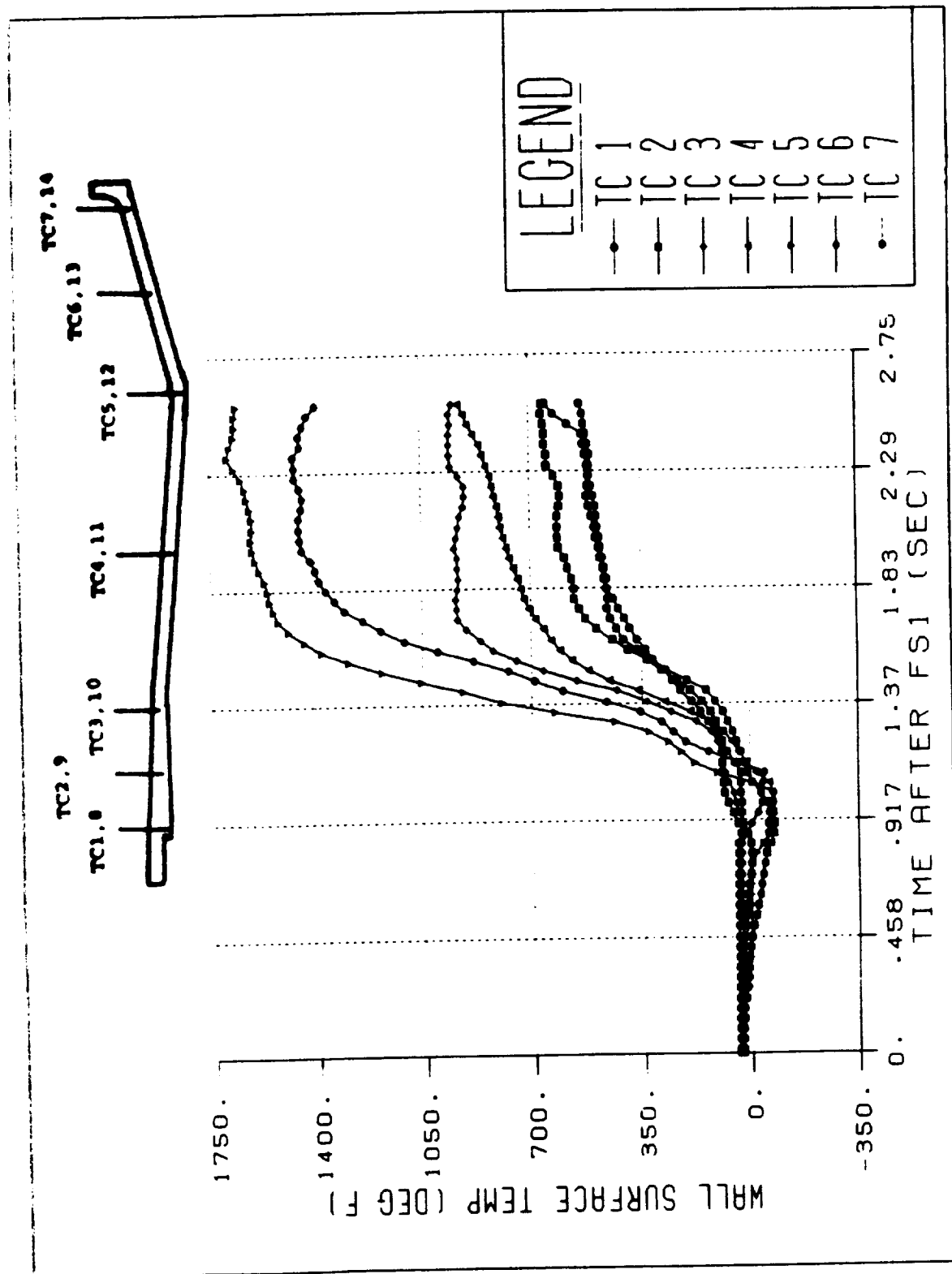


Figure 5.5.6 Temperature Profile Inline with Modules

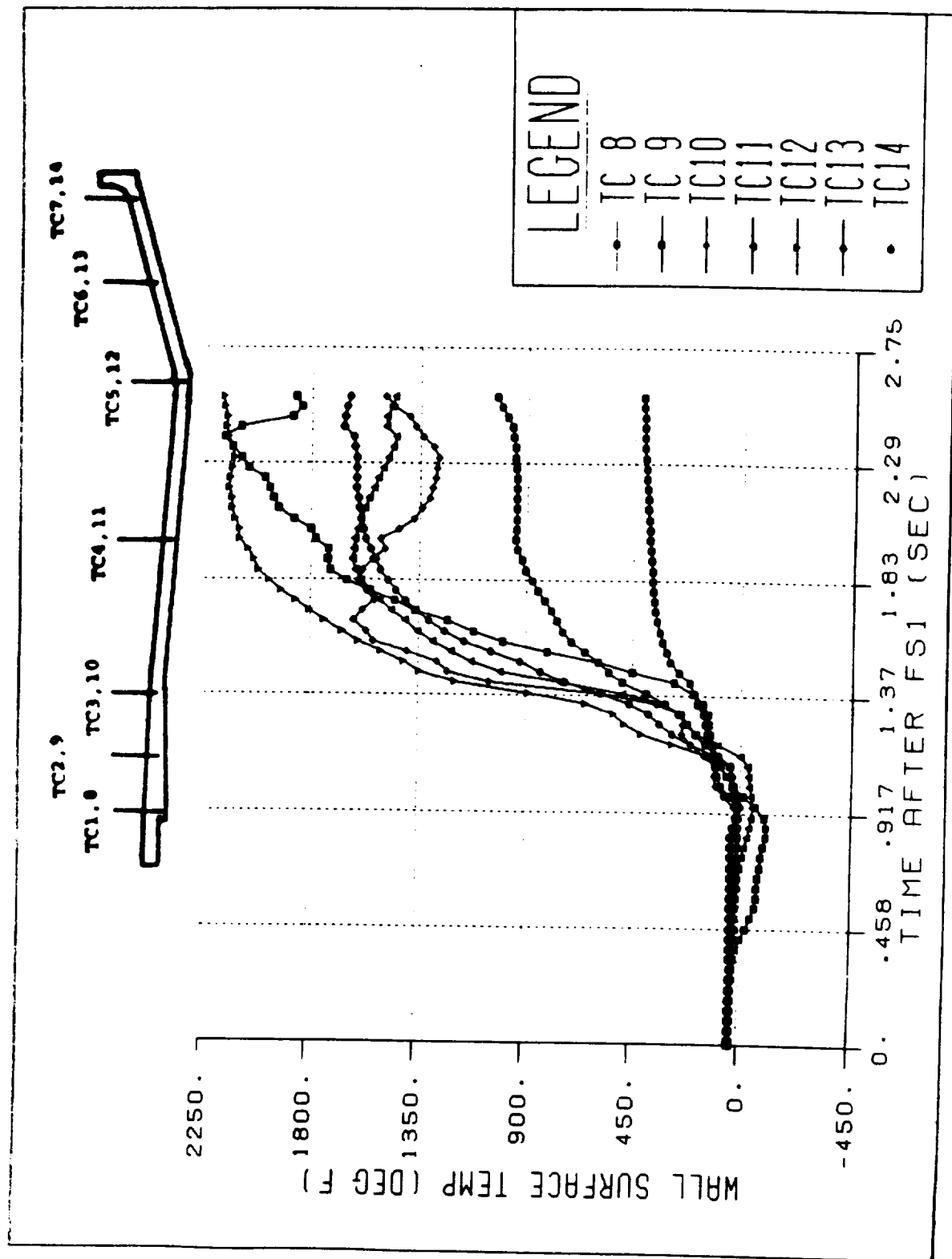


Figure 5.5.7 Temperature Profile Between Modules

The RP1 is less volatile than the LO₂ and thus the vaporized mixture ratio near the forward end of the combustor are oxidizer rich. These oxidizer rich combustion gases produce especially strong radially outward winds from the three inner modules between the outer modules. This was shown by TJ4 > TJ5 and TJ6 > TJ2. Furthermore, accuracy of pre test combustion analysis predictions were validated by the axial Pc profile correlation which required no post test adjustment to either atomization distance or mean atomized drop size predictions. These oxidizer rich combustion gases between the outer row modules partially consumed the FFC causing an overshoot in TC9 temperature before increasing core fuel vaporization rate reduces mean gas temperature again at TC10 and TC11. In future design applications less FFC will be required in line with the modules than in between the modules.

Although the 2200°F maximum wall temperature at TC12 may appear excessive for a CRES heat sink chamber, all of the measured temperatures are excessively cooled for the planned fullscale ablative silica phenolic chamber application which can withstand up to 4000°R adiabatic wall temperatures with negligible erosion. Test data indicate that the maximum amount of fuel film cooling required for this engine size to accommodate a silica phenolic lined chamber is 22%. As the sub-scale chamber is scaled up to full scale, film cooling percentage will decrease (to approximately 10-13%) for the same film cooling entrainment rates. Since a smaller percentage of the total fuel flow will make up the film cooling flow, engine performance will be increased.

5.6 HARDWARE DURABILITY

5.6.1 Injector Face

A concern at the start of testing was the durability of the ablative faceplate and the copper modules. Face temperatures were predicted to be very high with a low element density injector pattern, and the response to these high temperatures, especially during a possible combustion instability, were of concern. This unique injector configuration, with its modular design and large (0.241 inch) orifices, made predictions of combustion recirculation difficult due to an inadequate data base.

The functional performance of the copper modules was excellent. The modules showed absolutely no deterioration after the first 13 tests which included several forced instabilities. Test 14 was a high Pc (1030 psia) test and of longer duration

(1 sec). This test resulted in some copper loss about .060 inch deep at the outer edges of the module face on the outer modules only as shown in Figure 5.6.1. The copper melting appeared to be inhibited after it had progressed to within about 1/4 inch of the orifice, demonstrating the self cooling effects of the LOX and fuel flows. The modules showed no additional erosion until the next high Pc test, Test 30, which resulted in additional copper loss at the outer edges, but no additional melting near the orifices. The higher Pc tests have significantly higher heat flux than the nominal design condition. All of the module orifices remained round and hydraulically unaffected by the erosion.

The ablative faceplate also performed well. Even though the longest test was about 1 second, the ablation rate was less than expected.

The original faceplate was replaced after Test 6 due to a failure mode unrelated to face durability. A sealing void between the back of the faceplate and the manifold mounting surface is suspected to have allowed seepage of residual RP-1 from the previous test's shutdown transient. Ignition of the next test probably resulted in a detonation which fractured the faceplate along a high stress concentration plane occurring at the attachment point. The faceplate was replaced with a new unit, making sure a positive seal was accomplished between the faceplate and the injector body. This faceplate endured the remaining 26 tests without incident. After these tests, with a combined duration of about 15 seconds, the ablative material had recessed approximately 0.25 inch at the maximum point, which occurred adjacent to the eroded copper module edge. Faceplate erosion near intact module edges was less than 0.13 inch. Figure 5.6.1 shows the faceplate at the conclusion of testing. Post test inspection of the ablative material (forcibly removed for analysis) showed a char layer of only .030 inch. This indicates a lower than expected ablation rate, however, predictions are difficult using data from short duration tests. More precise ablation data could be obtained with longer duration testing.

The FFC injection ring experienced some overheating and metal loss between the injection orifices during the two high Pc tests described above. The orifices were able to self-cool themselves, as with the modules, and were hydraulically and functionally unaffected by the surrounding erosion. The FFC ring is also shown in figure 5.6.1 at the conclusion of testing. The areas of erosion and self-cooling can be clearly seen.

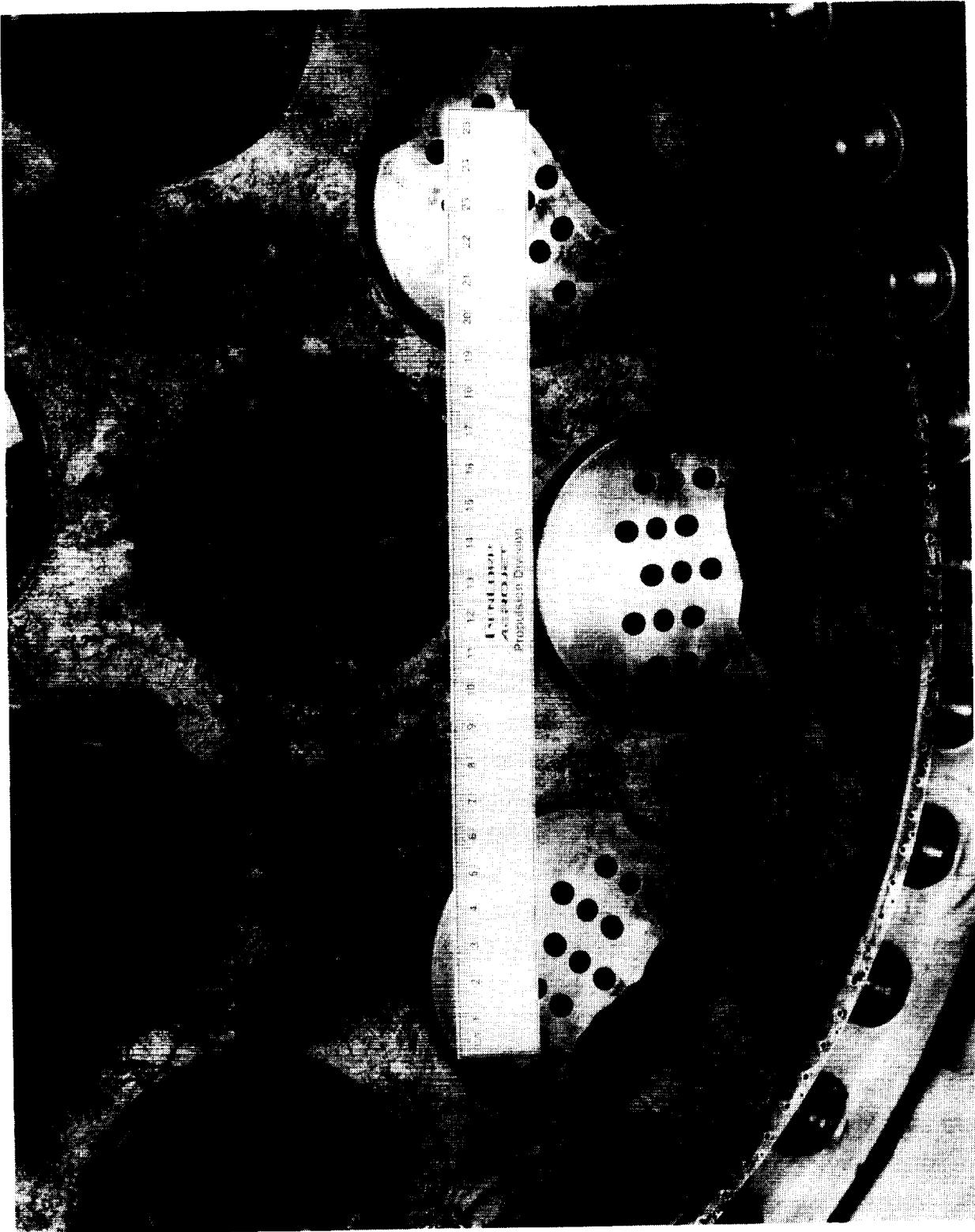


Figure 5.6.1 Some Module Erosion Occured After High Pc Tests

ORIGINAL PAGE
BLACK AND WHITE PHOTOGRAPH

5.6.2 Chamber

The chamber performed well throughout the test program with some erosion , approximately 0.5 inch of the 1.65 inches wall, due to overheating at the surface. The CRES "heat-sink" design was expected to absorb the heat from combustion, and local erosion at the wall was anticipated. The chamber was designed so that the majority of the steel structure would remain at room temperature even if the wall experienced local melting.

During the initial Block II testing, premature engine shutdown was signaled when chamber wall temperatures exceeded their 1700°F kill limits. Wall temperatures were higher and occurred sooner than predicted. Erosion and molten flow of the steel in three distinct areas was also noticed. The erosion of the wall, although not structurally threatening, was of concern at this early stage in the testing. By adjusting the temperature kill limits as high as 2100°F, the tests could be extended to durations of 0.2 to 0.5 seconds. These steady-state durations were still long enough to obtain satisfactory thermal data, due to the length of the shutdown transient (≈ 0.3 sec). Block II testing was completed successfully through Test 8.

Inspection of the chamber after Test 8 revealed the probable cause for the high wall temperatures. Impingement of the fuel film cooling (FFC) streams was not as intended, as shown in Figure 5.6.2. FFC flow intended for the chamber wall was actually impinging 50% into the acoustic cavity. This condition was confirmed by very low cavity gas temperatures (500°F vs. the 1100°F expected) measured by cavity thermocouples. Misimpingement of the FFC is postulated to be a result of stronger radial combustion winds than expected.

The chamber was modified by chamferring the leading edge 0.070 inch by 1.5 inches, as shown in Figure 5.6.2 . This was done before the stability series for two reasons; redirecting the FFC flow down the chamber wall would allow longer durations and better thermal data and, reducing the excess fuel in the acoustic cavity would provide more valid cavity sound speed data for the full scale design conditions. The chamber was modified on the test stand by grinding and , although not as precise as a lathe-turned cut, was adequate to improve cooling with the minimum cost/schedule impact. Subsequent tests showed significantly lower wall temperatures, and resulting test duration increases, even at higher P_c 's and MR's. Some overheating of the wall still

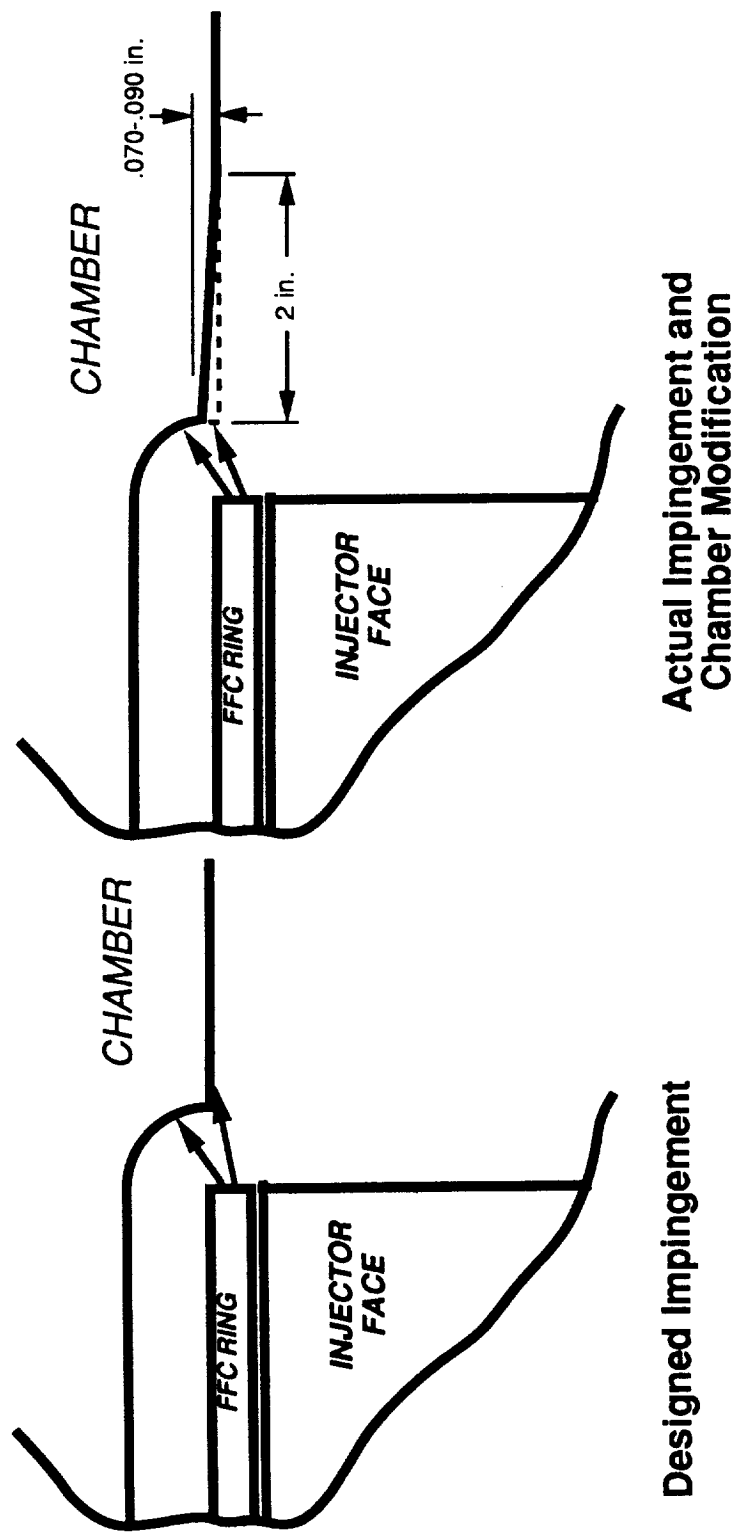


Figure 5.6.2 The Chamber was Modified to Correct FFC Impingement Point

occurred at high MR and low FFC rates, but chamber erosion was limited to approximately 0.5 inch after 32 tests. Unfortunately, the initial erosion created a roughened surface that could have easily tripped the boundary layer and had a significant effect on the wall heating during later tests. An attempt was made to smooth this roughened surface, but because of the hardness of the remelted steel and the large surface area involved, the time required was prohibitive. The chamber would probably have cooled better if the initial damage had not occurred.

In addition to the FFC flow issue, the erosion pattern on the chamber was indicative of an injection non-uniformity. The presence of three distinct erosion areas, or "streaks", indicated that oxygen-rich combustion gas was impinging on the chamber wall, causing secondary combustion with the FFC flow as shown in figure 5.6.3. This non-uniformity appeared to be a result of interaction between 3 grouped modules and may be aggravated by radial winds. This interaction of developed injection fans is difficult to predict, and will require cold-flow characterization and possibly CFD techniques to analyze and resolve. Since this condition could not be corrected on the existing hardware, overall FFC rate was increased, wall temperatures were monitored closely and testing continued.

There were no other problems experienced with the chamber or the resonator rings. All instrumentation ports and flanges remained leak-free throughout testing. Bomb port openings, especially the tangential port, experienced some erosion at the sharp edge into the chamber, but this erosion did not affect the installation or performance of the bombs.

5.6.3 Other Components

All other components performed flawlessly throughout testing. Bomb hardware, which had been proven on previous programs, caused no difficulties. The proof plates, adapters and instrumentation components performed without incident.

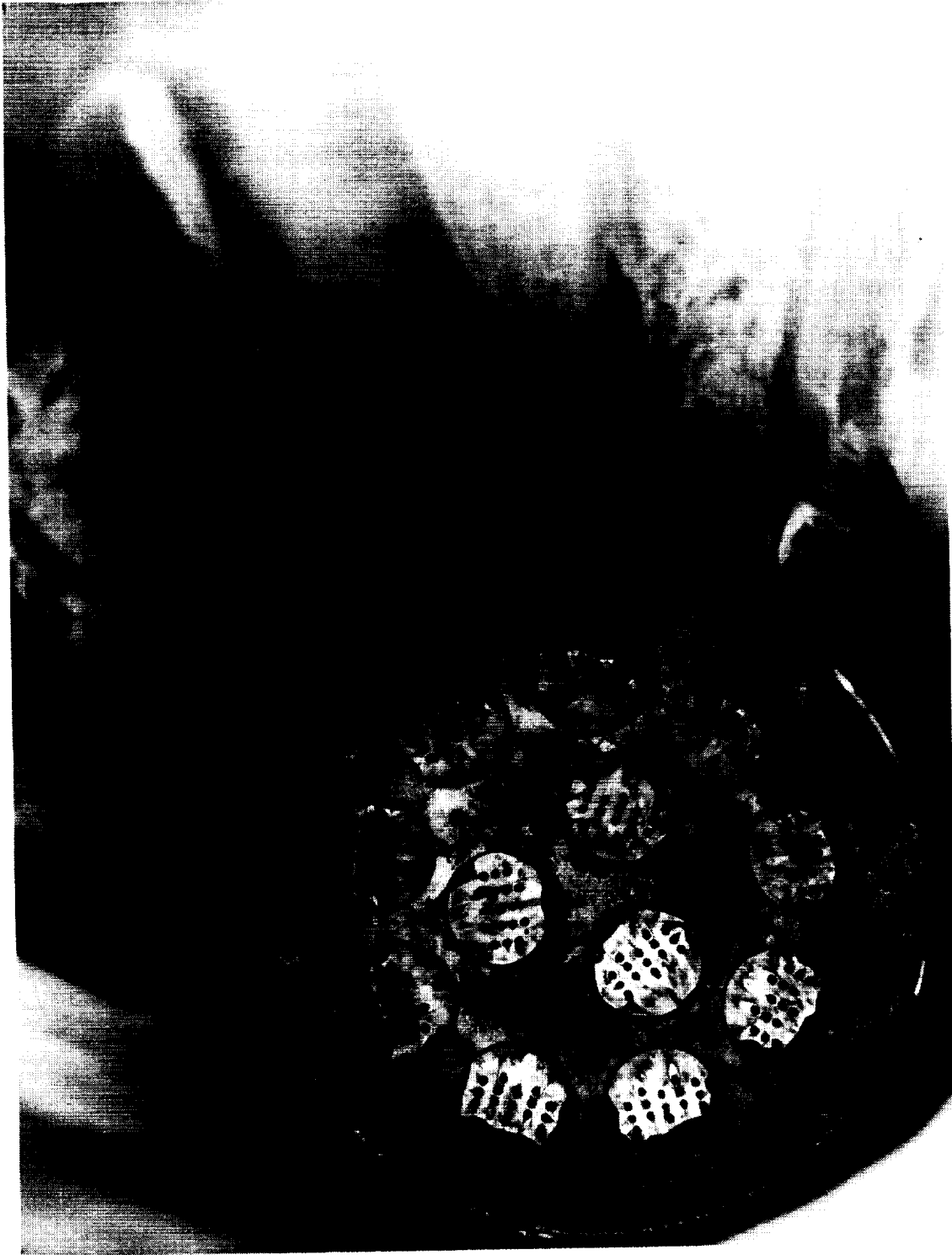


Figure 5.6.3 Chamber Indicated Erosion Areas at the Completion of Testing

ORIGINAL PHOTOGRAPH
BLACK AND WHITE PHOTOGRAPH

6.0 APPLICABILITY TO FULLSCALE

6.1 SUBSCALE TESTING RESULTS AND CONCLUSIONS

The goal of this program was to develop the technology for pressure fed engines by resolving several design issues through subscale testing. This testing was very successful in resolving many of these design issues with test data. The most critical of the design issues and their resolution are described below.

6.1.1 Fullscale Design will Require Only Simple Damping Devices for Stable Operation

The most important issue requiring resolution was the stability question. Demonstrated stability is an essential step in the development of a new engine technology. Our plan was to demonstrate stability on a subscale level which could be correlated to the fullscale engine using Aerojets proven scaling techniques.

The subscale engine was stable at all operating points tested. Artificial perturbation of the combustion drove some instabilities, all in the 1T (first tangential) mode. The development of a bituned acoustic cavity successfully damped the instabilities, and the engine was dynamically stable near the nominal operating point at the conclusion of testing.

This result indicates that stable operation in the fullscale configuration will be achievable and will require only acoustic cavity damping for the 1T mode. This elimination of the need for higher-order mode damping (baffles, etc.) will significantly reduce complexity and cost of the fullscale design.

6.1.2 Ablative Chamber / Nozzle will Meet Design Requirements

The fullscale design employs an ablative lined chamber and nozzle for economy and performance. The ablative material chosen was silica phenolic due to its low cost and past success in LOX/RP engines in short duration applications. Verification of its suitability for the flight application (approximately 150 seconds duration) was required.

Measurement of the gas-side temperatures during subscale testing was performed to predict fullscale temperatures during a long duration burn.



REPORT DOCUMENTATION PAGE

1. Report No. KGG-29		2. Government Accession No.		3. Recipient's Catalog No.	
4. Title And Subtitle Pressure Fed Thrust Chamber Technology Program Final Report				5. Report Date 20 August 1992	
				6. Performing Organization Code	
7. Author(s) Colin Faulkner, Program Manager Glenn Dunn, Project Engineer				8. Performing Organization Report No.	
9. Performing Organization Name and Address Acrojet Propulsion Division P.O. Box 13222 Sacramento, CA 95813-6000				10. Work Unit No.	
				11. Contract or Grant No. NAS 8-37365	
12. Sponsoring Agency Name and Address National Aeronautics and Space Administration Washington, D.C. 20546 NASA MSFC, Huntsville				13. Type of Report and Period Covered Final Report	
				14. Sponsoring Agency Code	
15. Supplementary Notes					
16. Abstract <p>This is the final report for the Pressure Fed Technology Program. It details the design, fabrication and testing of subscale hardware which successfully characterized LOX/RP combustion for a low cost pressure fed design. The innovative modular injector design is described in detail as well as hot-fire test results which showed excellent performance.</p> <p>The program summary identifies critical LOX/RP design issues that have been resolved by this testing, and details the low risk development requirements for a low cost engine for future Expendable Launch Vehicles (ELVi).</p>					
17. Key Words (Suggested by Author(s)) Pressure Fed Stability Performance Injector Subscale Composite Structure Braided Construction				18. Distribution Statement Unclassified-Unlimited	
19. Security Classif. (of this report) Unclassified		20. Security Classif. (of this page) Unclassified		21. No. of pages 125	
				22. Price	